



University of Brasília – UnB
Faculty UnB Gama – FGA
Electronic Engineering

Automation and Instrumentation of a Workbench for Braking Tests

Author: João Victor Avancini Guimarães
Advisor: Evandro Leonardo Silva Teixeira Ph.D.

Brasília, DF

2018



João Victor Avancini Guimarães

Automation and Instrumentation of a Workbench for Braking Tests

Thesis submitted to the course of undergraduate in Electronic Engineering at the University of Brasília, as a partial requirement to obtain a Bachelor's degree in Electronic Engineering.

University of Brasília – UnB

Faculty UnB Gama – FGA

Advisor: Evandro Leonardo Silva Teixeira Ph.D.

Brasília, DF

2018

João Victor Avancini Guimarães

Automation and Instrumentation of a Workbench for Braking Tests/ João
Victor Avancini Guimarães. – Brasília, DF, 2018-
118 p. : il. (some colors.) ; 30 cm.

Advisor: Evandro Leonardo Silva Teixeira Ph.D.

Graduation Thesis – University of Brasília – UnB
Faculty UnB Gama – FGA , 2018.

1. Electronic Instrumentation. 2. Braking Tests. I. Evandro Leonardo Silva
Teixeira Ph.D.. II. University of Brasilia. III. Faculty UnB Gama. IV. Automation
and Instrumentation of a Workbench for Braking Tests

CDU 02:141:005.6

João Victor Avancini Guimarães

Automation and Instrumentation of a Workbench for Braking Tests

Thesis submitted to the course of undergraduate in Electronic Engineering at the University of Brasília, as a partial requirement to obtain a Bachelor's degree in Electronic Engineering.

Thesis approved. Brasília, DF, 01st of july of 2018:

Evandro Leonardo Silva Teixeira
Ph.D.
Advisor

Wellington Avelino do Amaral Ph.D.
Invited Lecturer

Cueva Ph.D.
Invited Lecturer

Brasília, DF
2018

This work dedicated to all who seek knowledge and truth.

Acknowledgements

First of all I thank my parents Rita de Cassia and Carlos and my brothers Frederico, Pedro and Ana for all their efforts, dedication and support over the years.

To my uncles Maria Aparecida and Luís Henrique for the reception and support during my graduation.

To my supervisor Prof. Dr. Evandro Leonardo Silva Teixeira for his patience, support and teachings given throughout my stay at the University of Brasilia.

To my friends Mairon, Phelippe and Joel for companionship along the course.

To the teachers Julia Peterle, Casé Marques, Patrícia Lovatti, Aline Demuner, Graciela Ramos, Genildo Ronchi, Carmen Santos, Ricardo Fragelli, Adson Rocha, Eneida Valdes, Renato Lopes, Gerardo Pizo, Cristiano Miosso, Gilmar Beserra, André Penna, Fabiano Soarez, Gustavo Cueva, Richard Pearl, Josh Reynolds, Eleanor Baldwin, Steve Hegarty, Wellington Amaral, Marcelino Andrade, Sébastien Rondineau and other teachers that I had the privilege of knowing over the years.

*“Science, my lad, is made up of mistakes, but they are mistakes which it is useful to
make, because they lead little by little to the truth.”*
(Jules Verne, A Journey to the Center of the Earth)

Abstract

This paper aims to design the automation of a testbench for brake tests. There are already consolidated standards rules for brake system testing, this research project is focused with respect to *SAE J2522* regulation that addresses on brakes tests on passenger vehicles. The major focus of the project is to ensure a resilient solution for the testbench in order to make possible the acquisition of all relevant physical information and to automate the tests.

Key-words: Electronic Instrumentation. Brake Test. Automotive Systems Simulation.

List of Figures

Figura 1 – Schematic for disk brake systems (NICE, 2017)	29
Figura 2 – <i>Crankshaft Position Sensor</i> (REMAN, 2016)	32
Figura 3 – Magnetic Sensor Signal (PETROLHEAD GARAGE, 2014)	33
Figura 4 – Thermocouple characteristic voltage output (BOJORGE, 2014)	34
Figura 5 – Thermocouple Measurement (ECIL, 2016)	34
Figura 6 – Distension (INSTRUMENTS, 2016a)	35
Figura 7 – Wheatstone bridge (INSTRUMENTS, 2016b)	36
Figura 8 – Piezo Accelerometer (UK, 2016)	37
Figura 9 – Instrumentation Amplifier (DESCONHECIDO, 2016)	38
Figura 10 – INA 118 (INSTRUMENTS, 2000a)	39
Figura 11 – Typical Connections for ISP Programming (EQUINOX TECH, 2018) .	41
Figura 12 – Duty Cycle Examples (RZTRONICS, 2016)	42
Figura 13 – USB 2.0 Wires (UNKNOWN, 2017)	43
Figura 14 – What Differential Signaling Is All About (AUTODESK, 2017)	44
Figura 15 – ESD Test Waveform (LITTLELFUSE, 2015a)	45
Figura 16 – Campling action of a uni-directional TVS (RENESAS, 2016c)	46
Figura 17 – Campling action of a bi-directional TVS (RENESAS, 2016b)	46
Figura 18 – $V \times I$ characteristic of a uni-directional TVS (RENESAS, 2016e) . .	47
Figura 19 – $V \times I$ characteristic of a uni-directional TVS (RENESAS, 2016d) . .	47
Figura 20 – Project Problem Depuration (GUIMARAES, 2017c)	51
Figura 21 – Hardware Project Architecture (GUIMARAES, 2017a)	55
Figura 22 – <i>ATmega238PB</i> pinout (MICROCHIP, 2018)	56
Figura 23 – MCU Complete Complementary Circuit (GUIMARAES, 2018l)	57
Figura 24 – AD8495 Functional Block Diagram (DEVICES, 2011)	60
Figura 25 – RFI Circuit (GUIMARAES, 2018s)	61
Figura 26 – Overvoltage Detection Circuit (GUIMARAES, 2018m)	62
Figura 27 – Thermocouple Complete Circuit (GUIMARAES, 2018w)	63
Figura 28 – AD8223 Schematic (DEVICES, 2008)	64
Figura 29 – Conditioning Circuit for the Load Cell (GUIMARAES, 2018h)	65
Figura 30 – Load Cell Complete Circuit (GUIMARAES, 2018k)	66
Figura 31 – Tachometer with Adjustable Zero Speed Voltage Output, adapted from (TEXAS INSTRUMETS, 2018)	67
Figura 32 – Speed Acquisition Channel Circuit (GUIMARAES, 2018u)	69
Figura 33 – Speed Sensor Detection Channel Circuit (GUIMARAES, 2018v)	70
Figura 34 – 16-LFCSP (DEVICES, 2016)	71

Figura 35 – Adafruit ADXL335 - 5V ready (??)	71
Figura 36 – Accelerometer Signal Conditioning Circuit (GUIMARAES, 2018g)	72
Figura 37 – Accelerometer Sensor Detection Circuit (GUIMARAES, 2018f)	73
Figura 38 – Weg CFW-08 Frequency Inverter (WEG, 2017)	74
Figura 39 – Sallen-Key Active Low Pass Filter (TEXAS INSTRUMENTS, 1999)	76
Figura 40 – PWM to Speed Reference Circuit	78
Figura 41 – MCP2221A basic circuit (MICROCHIP, 2010)	79
Figura 42 – STF202-22T1G Internal Circuit (ONSEMI, 2012)	80
Figura 43 – USB/UART Converter Circuit (GUIMARAES, 2018y)	80
Figura 44 – PMOS low side driver (ELECTRONICS TUTORIALS, 2018)	81
Figura 45 – Digital Output Circuit (GUIMARAES, 2018j)	82
Figura 46 – Digital Input Circuit (GUIMARAES, 2018i)	82
Figura 47 – UART feedback LEDs driver (GUIMARAES, 2018x)	84
Figura 48 – Sensor Disconnection and Acquisition LED driver circuit (GUIMARAES, 2018t)	86
Figura 49 – Power Supplies Voltage LEDs Circuit (GUIMARAES, 2018r)	86
Figura 50 – 5V Power Supply Circuit (GUIMARAES, 2018e)	87
Figura 51 – 12V Power Supply Circuit(GUIMARAES, 2018b)	88
Figura 52 – Voltage Input Protection Circuit (GUIMARAES, 2018z)	88
Figura 53 – 10V voltage reference circuit (GUIMARAES, 2018a)	89
Figura 54 – 4V5 voltage reference circuit (GUIMARAES, 2018d)	90
Figura 55 – ADR510 Typical Operating Circuit (ANALOG DEVICES, 2018)	90
Figura 56 – 1V voltage reference circuit (GUIMARAES, 2018c)	91
Figura 57 – PCB Top 2D View (GUIMARAES, 2018p)	92
Figura 58 – PCB Bottom 2D View (GUIMARAES, 2018o)	93
Figura 59 – PCB 3D View (GUIMARAES, 2018n)	93
Figura 60 – PCB Top 3D View (GUIMARAES, 2018q)	94
Figura 61 – PCB Bottom 3D View	95
Figura 62 – Microcontroller Code Map (GUIMARAES, 2017b)	98

List of Tables

Table 1 – Thermocouples and their operation ranges	34
Table 2 – Blocks functionality	52

List of abbreviations and acronyms

SAE	Society of Automotive Engineers.
GUI	Graphical User Interface.
ABS	Anti-lock Braking System.
CKP	Crankshaft Position Sensor.
GPIO	General-Purpose Input/Output
SRAM	Static Random-Access Memory
EEPROM	Electrically Erasable Programmable Read-Only Memory
DIP28	Dual In-line Package 28pins
ISR	Interruption Service Routine
IC	Integrated Circuit
MCU	Microcontroller Unit
I ² C	Inter-Integrated Circuit
DAQ	Data Acquisition
PWM	Pulse Width Modulation.
N-MOSFET	N channel Metal-Oxide-Semiconductor Field-Effect Transistor.
LPF	Low-Pass Filter.
TVS	Transient Voltage Supressor
OPAMP	Operational Amplifier
USB	Universal Serial Bus
UART	Universal Asynchronous Receiver-Transmitter
ESD	Electrostatic Discharge
EMI	Electromagnetic Interference
PCB	Printed Circuit Board

RFI	Radio Frequency Interference
DAC	Digital-to-Analog Converter
ADC	Analog-to-Digital Converter
SNR	Signal-to-Noise-Ratio

List of symbols

Pa	Pascal: Unit used to measure pressure.
kPa	10^3 Pascal.
MPa	10^6 Pascal.
°C	Celsius Degree: Unit used to measure temperature.
kph	Kilometer per hour: Unit used to measure speed.
m	Meters: SI unit used to measure distance.
cm	10^{-2} Meters.
s	Seconds: SI unit for measuring time.
ms	10^{-3} Seconds.
hp	Horsepower: Unit used to measure power.
kB	KiloBytes: Used to measure memory size.
V	Volts: SI unit for measuring electrical potential.
mv	10^{-3} Volts.
Ω	Omega: SI unit for measuring electrical resistance.
A	Ampere: SI unit for measuring electrical current.
mA	10^{-3} Ampere.
g	Earth gravity acceleration ($9.8m/s^2$).

Summary

1	INTRODUCTION	25
1.1	Purpose of the project	27
1.2	Text Structure	27
2	LITERATURE REVIEW	29
2.1	Working principles of disk brake systems	29
2.2	The <i>SAE J2522</i> regulation	30
2.2.1	Monitored Parameters	31
2.3	First Solution Overview	31
2.3.1	Speed Measurement	31
2.3.2	Temperature Measurement	32
2.3.3	Brake Pressure Measurement	35
2.3.4	Vibration Measurement	36
2.3.5	Instrumentation Amplifier	37
2.3.5.1	Important features to consider in a amplifier	38
2.3.6	System Controlling	39
2.3.6.1	Microcontroller basic characteristics	40
2.3.6.2	Microcontroller ISP programming	40
2.3.7	Pulse Width Modulation	41
2.3.8	Data Communication	42
2.3.8.1	USB	43
2.3.9	Circuit Protection	44
2.3.9.1	Low Pass Filters	45
2.3.9.2	Transient Voltage Supression Diodes (TVS)	45
2.3.9.2.1	TVS diodes principle of operation	45
2.3.9.2.2	Selecting TVS Diodes	46
3	METHODOLOGY	49
3.1	Lieterature Review	49
3.2	Problem Description	49
3.3	Project Conception	49
3.4	Case Study	49
4	PROBLEM ANALYSIS AND PROJECT REQUIREMENTS	51
4.1	Problem Analysis	51
4.1.1	Brake System Simulator	51

4.1.2	Lower Layer Hardware	52
4.1.3	Higher Layer Hardware	52
4.1.4	Solution Overview	52
4.2	Monitored Parameters	53
4.3	Functional Requirements of the Testbench	53
4.4	Software Requirements	54
5	HARDWARE PROJECT	55
5.1	MCU	55
5.1.1	The chosen MCU	55
5.1.2	MCU circuit	56
5.1.2.1	MCU Communication Ports	56
5.1.2.2	MCU Power Ports	59
5.1.2.3	Crystal Oscillator Circuit	59
5.2	Temperature Acquisition Channel	59
5.2.1	Thermocouple Types and Characteristic Signal	59
5.2.2	Thermocouple Signal Conditioning	59
5.2.3	Input Protection and Filtering	60
5.2.4	Thermocouple Sensor Detection	62
5.2.5	Complete Circuit	63
5.3	Brake Pressure Acquisition Channel	63
5.3.1	Load Cell Signal	63
5.3.2	Load Cell Signal Conditioning	64
5.3.3	Load Cell Sensor Detection	66
5.3.4	Complete Circuit	66
5.4	Speed Acquisition Channel	66
5.4.1	CKP Signal Conditioning	66
5.4.1.1	LM2907 Basic Tachometer Circuit	67
5.4.1.2	LM2907 Designed Circuit	68
5.4.2	CKP Sensor Detection	70
5.5	Vibration Acquisition Channel	70
5.5.1	Accelerometer	70
5.5.2	Signal Conditioning Circuit	71
5.5.3	Sensor Detection Circuit	73
5.6	Speed Reference Output Channel	73
5.6.1	Speed Control	73
5.6.2	Filter characteristics definition	74
5.6.3	Sallen-Key Low Pass Active Filter	76
5.6.4	Complete Circuit	77
5.7	Hardware Interface Between Microcontroller and Computer	78

5.7.1	USB and UART	78
5.7.2	Conversion Circuit	78
5.7.3	Circuit Protection	79
5.7.4	Complete Circuit	79
5.8	Digital Interfaces	80
5.8.1	Digital Outputs	80
5.8.1.1	Low-side Driver	80
5.8.1.2	Digital Output Circuit	81
5.8.2	Digital Inputs	82
5.9	LED driver circuits	83
5.9.1	Serial Communication Leds	84
5.9.2	Sensor Disconnection and Acquisition Leds	85
5.9.2.1	Sensor Disconnection	85
5.9.2.2	Acquisition	85
5.9.2.3	Sensor Disconnection and Acquisition LED driver	85
5.9.3	Power Supplies Voltage LEDs	85
5.10	Voltage Supplies	86
5.10.1	Power Supplies	86
5.10.1.1	5V Supply	87
5.10.1.2	12V Supply	87
5.10.1.3	Voltage Input Protection	88
5.10.2	Voltage References	89
5.10.2.1	10V Reference	89
5.10.2.2	4V5 Reference	89
5.10.2.3	1V Reference	90
5.11	Printed Circuit Board	91
5.11.1	PCB Design	91
5.11.2	PCB Assembly	92
6	SOFTWARE PROJECT	97
6.1	Microcontroller Code	97
6.1.1	Microcontroller programming basics	97
6.1.2	Microcontroller Code Map	97
6.2	Computer Software	99
	REFERENCES	101

APPENDIX	111
APPENDIX A – FIRST APPENDIX	113
A.1 Micontroller Code	113

1 Introduction

With the advancement of technology, cars are leaving the factory each time with more power for more affordable prices. In 1995 the best-selling car in Brazil ([HERNANDES, 2017](#)), (*Volkswagen Gol Plus 1.0*), had 49.8hp of maximum power and brand-new would accelerate from nought to 100kph in 22.4 seconds ([CNW, 2017b](#)). On the other hand, the sales champion of 2015 , *Volkswagen Gol 1.0*, had 76hp of maximum power and could do the same task in 13.3 seconds ([CNW, 2017a](#)), almost half the time from the previous. Interisting fact is that even though the latter is 20 years younger, both cars have similar brake systems: disk brakes in the front wheels and drum ones in the back. This enhancement on vehicle accelerations naturally imply on higher top speeds, which should lead to a bigger concern in brake systems effectiveness.

During the development of any solution or enhancement on any technology or product, testing is fundamental (??). In the matter of brake systems, the fact stated on the previous sentence can also be considered true. On the process of developing more effective brake systems, it is important to perform brake tests.

Although brake tests are so importatant, performing this tests with full scale vehicles are obviously expensive and this somehow makes extensive testing unfeasible. Also the time required for each test might be a constrain. It is a possibility that maybe using a small scale test plataform would still make it possible to provide relevant and reliant information about quality and performance of brake systems with lower costs and reduced testing time. Small scale tests do not have the purpose of fully replacing full scale ones, but the savings in costs and time that they could provide can be used for mass testing, and this can already somehow show their utility and relevance ([GARDINALLI, 2005](#)).

Evaluating the brake efficiency of a vehicle as a whole, involves a lot of factors, a small scale test plataform will not provide results that could be used to fully address the quality of a car break system, instead, it is possible to focus the results on the performance of individual componentes of the system such as pads, disks and calipers ([HALDERMAN; MITCHELL, 2016](#)), and evaluating the performance of this components is a good start for evaluating the braking capacity of a brake system.

Governament and legal authorities have been creating strict regulations for manufacturers to follow in order to ensure that cars have a higher standard of safety. Braking tests have been regulated for some time. A international standard for brake testing is the regulation *SAE J2522* ([SAE, 2016](#)), it gives a the description of how break tests should be conducted for systems used in low weight passengers cars.

The brake system is a critical part of an automobile, thanks to this system it is possible to use the latter under safe conditions both in urban and rural areas. There are some ideal requirements that a brake system should be able to attend ([KAWAGUCHI, 2005](#)):

- Reduce the speed of a moving vehicle, increasing the deceleration of the same.
- Stop the vehicle completely.
- Maintain the vehicle speed, preventing unwanted acceleration in downhill paths.
- Keep the vehicle motionless while it is parked.

It is important to emphasize that these conditions are ideal, considering that in extremely hazardous or stressful situations the system might not operate properly and will not attend those previous requirements. Considering the importance of brake system the same need to have minimal breaking capacity so vehicles can be decelerated with greater efficiency.

Another point of view should also be considered during this analysis, the manufacturers point of view. More effective brake systems means more research and probably more expensive materials, generating more cost to manufacturers and consequently more cost to customers. Theoretically this would mean that manufacturers need to choose a trade-off between quality and cost. However, the point in which this trade-off is set is determined by government regulations. Moreover if there was no general regulations each car manufacturer would have a standard that they judge is sufficient. In Brazil, according to Resolution N.519 (??) from the National Traffic Council (*CONTRAN - Conselho Nacional de Trânsito*), the minimal requirements of performance of brake systems from any vehicle with 750kg or less should meet the following regulations from Brazilian Association of Technical Standards (*ABNT - Associação Brasileira de Normas Técnicas*): *NBR 10966-1, NBR 10966-2, NBR 10966-3, NBR 10966-4, NBR 10966-5, NBR 10966-6, NBR 10966-7* and *NBR 16068*. Most of these regulations are based in the European regulation ECE-13/05.

Considering the importance of regulatory standards, the need for brake tests becomes even more evident as it is mandatory to ensure that brake-systems will attend to regulations requirements. Only with extensive testing it is possible to ensure that a particular system will attend to all standards regarding its category of operation.

Making all these considerations, a *Break-Testbench* can be a useful device for the automotive industry and research. Considering that this device would be able to simulate a replica of real environments and situations that a brake system is submitted, this testbench could allow car manufacturers and brake system parts manufacturers to avoid expenses in

full scale tests as they would be able to test different parts of the system in a assisted and controlled environments.

1.1 Purpose of the project

The purpose of this work is to develop, implement and test a microcontrolled electronic instrument system for monitoring and controlling a small scale brake-testbench based on the information from the internationl regulation *SAE J2522* ([SAE, 2016](#)). The system will comprehend both software and hardware layers and should be able to perform brake tests and acquire physical data through sensors in order to judge brake systems components level of performance.

1.2 Text Structure

The rest of this paper was divided on chapters briefly explained bellow.

Chapter 2, Literature Review: This chapter will explore somo concepts and aspects of engineering and of brake tests that are considered fundamental to following parts of this paper.

Chapter 3, Methodology: This is the where the strategy for developing this paper and the engineering solutions it proposes are dicussed.

Chapter 4, Problem Analysis and Project Requirements: On this chapter the problem this project tries to solve will be defined in a specific way and the project requirements, both from hardware and software will be enumerated. Also, based on this requirements the parameters that the final solution will have to monitor in order to meet thoose requirements will be listed.

Chapter 5, Hardware Project: This chapter provides a detailed explanation of each of the hardware solutions that were either developed, integrated or implemented on this project.

Chapter 6, Software Project: This chapter is basically splitted in two parts, one for explaining the code from the bottom layer of the solution (low level hardware) and one for explaining the code from the upper layer (high level hardware).

2 Literature Review

2.1 Working principles of disk brake systems

This section will give a short explanation of how disk brakes work as the vast majority of cars and motorcycles nowadays are equipped with this technology instead of the outdated drum scheme.

In general terms, a disc break can be summarized as a type of brake that uses calipers to squeeze pairs of pads against a disc coupled to a shaft in order to create friction. This generated friction ought to retard the rotation of this shaft coupled to the disk. A moving car, or being more specific, a rotating shaft has a certain amount of kinetic energy, the brakes of a car are designed to convert this kinetic energy to heat (through friction) in order to decelerate the car ([LIMPERT, 1999](#)). Figure 1 shows a schematic for a typical disk break.

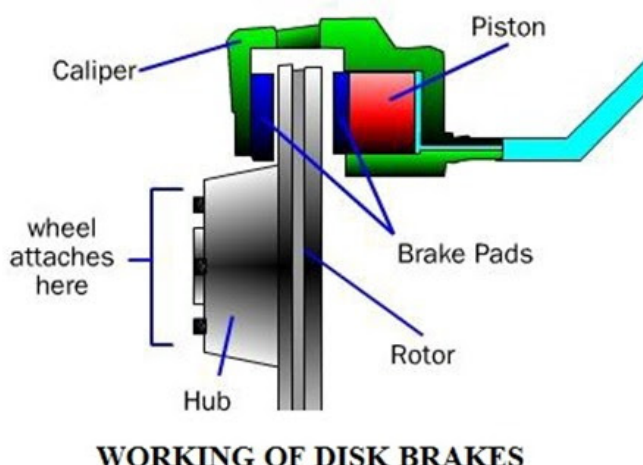


Figura 1 – Schematic for disk brake systems ([NICE, 2017](#))

As Figure 1 shows, some of the main components of a typical disk brake system and their respective functions are ([CARPARTS, 2018](#)):

- *Caliper*: Fits over the rotor like a clamp, houses the pads and pistons. This part does not tend to wear out quickly, usually, damages on this part are caused by using outworn pads or disks ([GOODYEAR, 2018](#)).
- *Pads*: There are two brake pads on each caliper, this is the part that is effectively in contact with the disk. Pads are used in order to prevent disk wear and caliper wear, this parts are made with specific materials that provide better performance, hence

more friction with less dissipated heat. Pads tend to wear out quickly in a vehicle and should be checked and replaced quite often.

- *Piston:* Most of brake discs have are activated through a hydraulic mechanism, when the break pedal is pressed the brake fluid goes to the piston and the piston squeezes the to brake pads against the disk.
- *Rotor:* The disk rotor is the main component of the system, it is directly connected to the wheel's shaft. The rotor wears with time, if break pads are replaced accordingly the rotor tends to last more than the pads. Usually a vehicle will undergo more than one brake pads replacement before having its disks replaced.

2.2 The *SAE J2522* regulation

SAE International was founded in 1905 and the acronym SAE stands for Society of Automotive Engineers. Nowadays their emphasis is on transports industries, such as automotive, aerospace and commecial vehicles. One of their main activity is providing parameters and regulations of quality and safety standards for the industry. One great example of their operation is the SAE has long provided standards for horsepower rating.

More related to this project is the *SAE J2522*, entitled *Dynamometer Global Brake Effectiveness*, at the beggining it already states the it's utility with the following:

“The SAE Brake Dynamometer Test Code Standards Committee considers this standar useful in supporting the technological efforts intended to improve motor vehicle braking systems overall performance and safety”

([SAE, 2003](#)). This regulation was developed to be used in conjecture with other test standards in other to address the friction of a certain material to check it's adequacy for a certain application. It is important to state that this paper is based on the *SAE J2522*, it is not a faithful application of the standard though. This paper is more concerned about the settings of the tests mentioned on the regulation rather than the formulas and criteria for a materials engineering analysis.

All the tests mentioned on the regulation can generalised on repetitive cycles of accelerating the rotor to a specified speed and appling brake force (may vary along the test) until the rotor reaches a lower limit of speed. On the regulation, sometimes the desacceleration ratio is also defined but not always. Initial temperature is also defined, some tests can only be perfomed if the brake parts are under a certain temperature.

2.2.1 Monitored Parameters

According to Regulation *SAE J2522* ([SAE, 2003](#)), in order to perform the brake tests specified it is mandatory to evaluate the following parameters:

- *Temperature of the brake pads:* It is important during the entire test to be fully aware of the temperature of the brake system, firstly by the safety factor (there is a maximum operating temperature for the system), also by the wear of the system that is tied to the temperature therein. Last but not least is the fact that knowing the temperature it is possible to carry out tests based on it, being possible to conduct tests in known temperature ranges.
- *Braking pressure:* The pressure to be measured is the pressure that the brake caliper is applying to the rotor over time, knowing the magnitude of this force means having control over how much the temperature increases according to braking and how much the rotor speed decreases as a function of braking.
- *Rotation Speed:* Without knowledge of rotor speed it would be impossible to determine whether the brake is being effective or how effective it is. Speed monitoring is the most critical parameter for system operation, without it there is no utility to the rest of the equipment.

Another interesting parameter to monitor that is not specified on Regulation *SAE J2522* is the vibration on the caliper, usually when the magnitude of this vibration is considerably high it usually indicates that this part is already worn out ([GOODYEAR, 2018](#)) and it may damage the rotor by bending it over time. Is is also relevant to mention that vibration is measured in terms of g ($9.8 \text{ m} \cdot \text{s}^2$).

2.3 First Solution Overview

At this section some of the electronic components and solutions that could be used in this project are going to be discussed in order to make paper more acknowledgeable.

2.3.1 Speed Measurement

As it was specified in in Item [2.2.1](#) from Section [2.2.1](#), monitoring the rotor speed is mandatory in order to perform brake tests. There are many different ways to measure speed in rotors and shafts. On the automotive environment this measurements are done using magnetic sensors ??.

The name used for the sensor in the automotive environment is Crankshaft Position Sensor (CKP), it has this name because most of the time this sensor is mounted

aligned with the crankshaft and is used to monitor both the speed and the position of the crankshaft. A typical CKP sensor is shown in Figure 2.



Figura 2 – Crankshaft Position Sensor (REMAN, 2016)

This sensor is widely used in the automotive industry to determine the speed (RPM) of cranks and gears in the engine. There are several types of CKP sensors, the most common are the variable reluctance type because they have low cost and good accuracy (SCHROEDER, 2002).

As the gear in question rotates each tooth of the gear aligns with the variable reluctance sensor, a magnetic flux in the sensor coil changes as the air gap between the sensor and the gear changes. This change in the magnetic field generates induces a voltage pulse at the sensor output. This type of sensors have an analog voltage output where amplitude and frequency vary proportionally to the speed of rotation of a gear, as Figure 3. With this type of sensor it is possible to extract data of linear velocity, angular velocity and angular position. However, only the angular velocity data (frequency) is important to be measured for brake tests specified by the regulation (SAE, 2003).

2.3.2 Temperature Measurement

In Section 2.1 it is explained that a brake system is designed to convert the kinetic energy from a rotor to thermal energy (heat). Whereas, considering this fact it is possible to address that the performance of a break system is therefore directly related to the variation of temperature during the braking act. Moreover, as it was explained in Item 2.2.1 from Section 2.2.1 Regulation SAE J2522 (SAE, 2003) especifies that it is mandatory to measure temperature in order to perform the tests it describes.

There are many different temperature sensors such as: Thermocouples, RTD (Resistance Temperature Detector) and Thermistors. Regulation SAE J2522 (SAE, 2003) states that temperature measurements for performing specified brake tests should be done with a Thermocouple. According to (NEWTON, 2016) brake pads from production passenger cars operate at the temperature range from 100°C to 650°C and according to

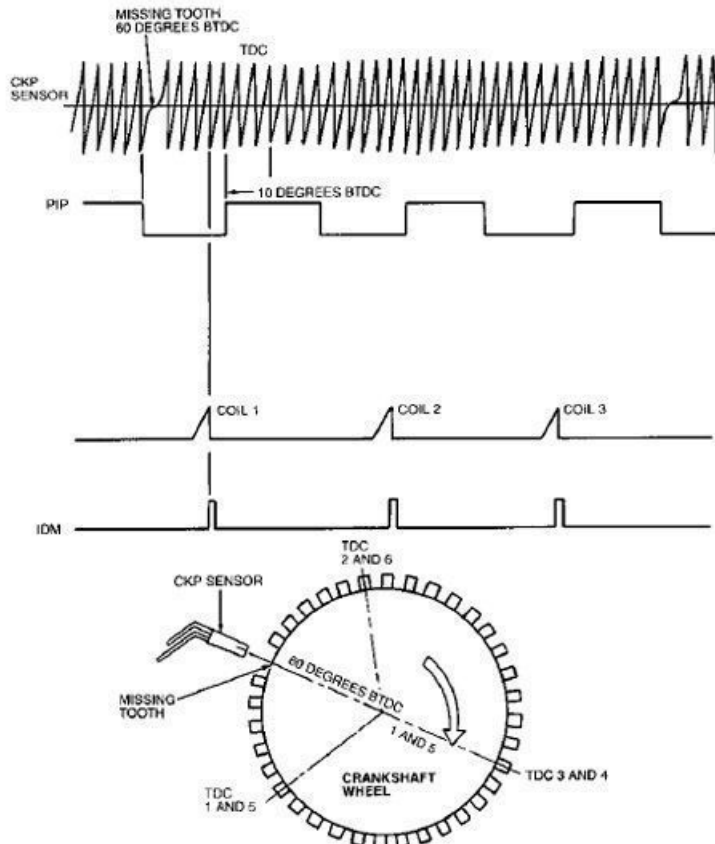


Figura 3 – Magnetic Sensor Signal ([PETROLHEAD GARAGE, 2014](#))

(GUMS, 2018), from the most common temperature sensors the thermocouple is by far the one with the widest temperature range (-270°C to 1820°C).

Since the 19th century it is known that the junction between two different metals submitted to a heat flow generates a electromotive force. A thermocouple is a device that has this junction of two different metals and has a known voltage generated output proportional to the heat transfer on the junction. In theory any combination of two different metals could be used, but there are standardized combinations that produces more stable and predictable voltage outputs (POLLOCK, 1991). This relation between heat transfer and voltage is known not to be linear as Figure 4 shows (E,J,K,T,R,S and B are designators for normalized thermocouples junction types).

Thermocouple actually have two junctions, a hot junction (the one that is submitted to heat transfers) and a cold junction (also called reference junction). What the thermocouple really measures is the difference between the temperature of this two junctions, this means that in a hypothetical situation which the hot junction is submitted to a 100°C and the cold junction is submitted to a environmental temperature of 25°C, after thermal equilibrium is reached the thermocouple voltage will be proportional to a temperature of 75°C. Hence the thermocouple will only produce a "real"output voltage when the cold junction is submitted to a 0°C (in some calibrations procedures the cold

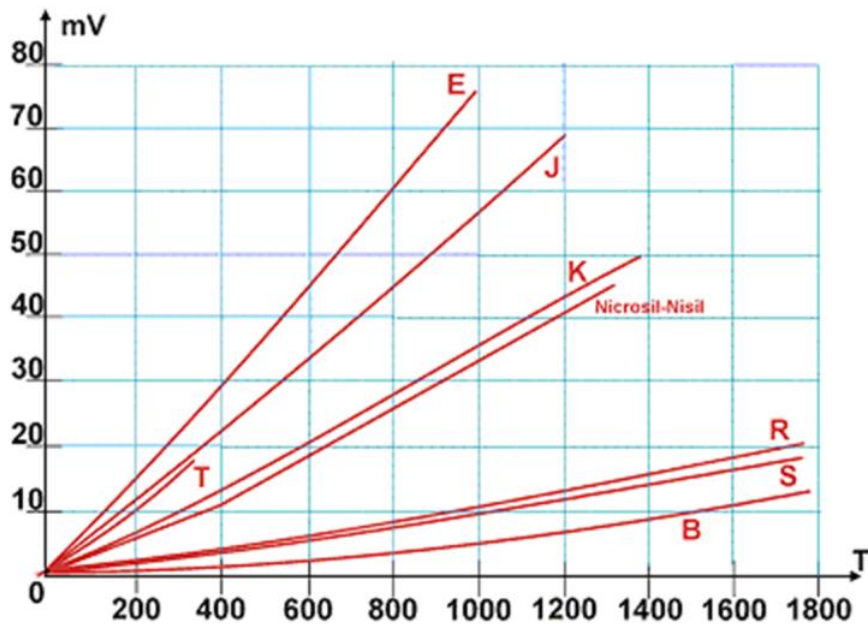


Figura 4 – Thermocouple characteristic voltage output (BOJORGE, 2014)

junction is actually submitted to 0°C) (KINZIE; RUBIN, 1973).

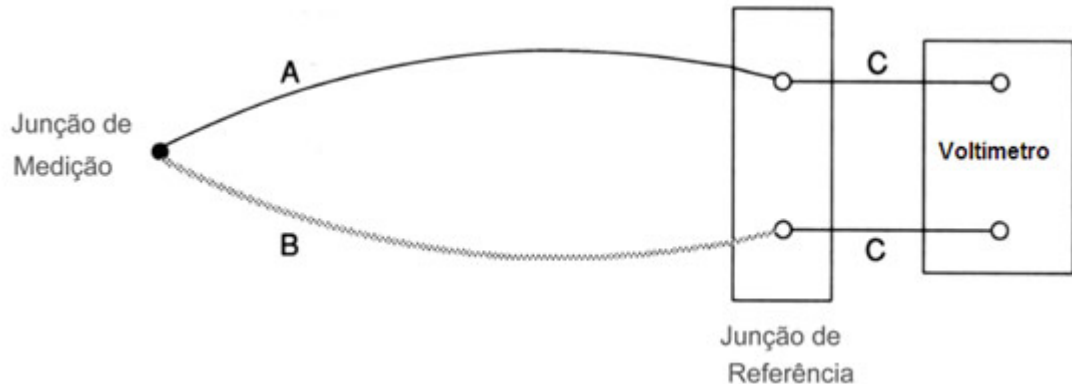


Figura 5 – Thermocouple Measurement (ECIL, 2016)

There is a big variety of thermocouples available, table 1 shows the most common thermocouples and their temperature range.

Table 1 – Thermocouples and their operation ranges

<i>Thermocouple Type</i>	<i>Range of Operation (°C)</i>
J	0 a 750
K	-200 a 1250
E	-200 a 900
T	-250 a 350

2.3.3 Brake Pressure Measurement

Brake pressure can be interpreted as the force that the brake system applies to the disc in a distributed way along the area of the pads. Considering this, in order to find out the break pressure the force applied to the calipers must be measured.

There are different types of force transducers (devices that converts a signal from one physical form to a corresponding signal having a different physical form (PALLA; WEBSTER et al., 2012)) and they are used with instrumentation of varying complexity. The load cell is the most common type ??, and according to (DILLON; GRIFFEN; WEIHS, 1989) the main advantages and disadvantages of Load Cells are:

- *Accuracy*: usually less than 0.1%.
- *Rigid in Construction*: it is extremely resistant to impact and to any mechanical stress.
- *Calibration*: load cells are usually already calibrated by manufacturers and vendors.

The main disadvantage of the Load Cell is its size and weight, which is not a issue for a testbench.

The load cell is a transducer formed by strain gauges. Those are devices which their electrical resistance varies proportionally to their distension. Distension is a quantification of the deformation of a body, it can also be defined as a fractional change of the body of a body. Distension may be negative (compression) or positive (traction).

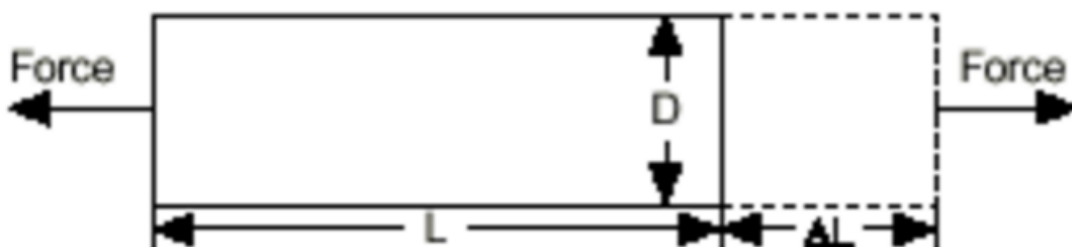


Figura 6 – Distension (INSTRUMENTS, 2016a)

Generally, the length variation in a strain gauge is very small and this makes them very susceptible to measurement errors. As a result, the use of a Wheatstone bridge is very common, it is formed by four resistive arms and an excitation voltage applied to the bridge (WINDOW; HOLISTER et al., 1982).

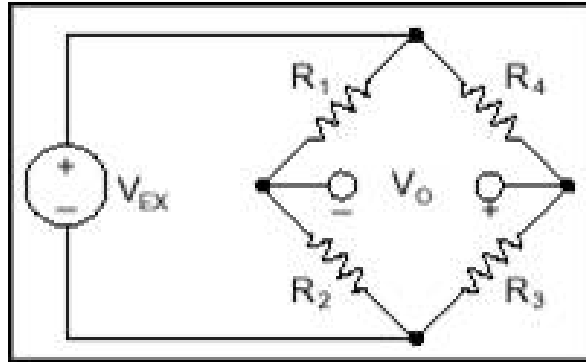


Figura 7 – Wheatstone bridge ([INSTRUMENTS, 2016b](#))

The voltage output V_O can be obtained from the Equation 2.1, V_O the load cell signal output is a differential pair signal.

$$V_O = \frac{R_3}{R_3 + R_4} - \frac{R_2}{R_1 + R_2} \quad (2.1)$$

2.3.4 Vibration Measurement

Even though measuring vibration is not mandatory in order to perform break tests, it can provide useful data in order to address the wear of the caliper of a disc break, and as excessive vibration can stress the rotor enough to cause it to bend (as explained in Section 2.2.1).

A body is said to vibrate when it describes an oscillatory movement around a reference point ([FERNANDES, 2000](#)). For the measurement of vibration in machines it is more common the measurement of the acceleration as a function of g ($9.8m/s^2$). The same is measured as a function of g as a function of Einstein's Principle of Equivalence, where the acceleration of a reference data is not distinguishable from the gravitational action on it ([JR, 1968](#)).

Accelerometers are sensors that measure acceleration itself, that is, the acceleration that the sensor itself is subjected to. Accelerometers are widely used in the automotive industry, initially only in the Air Bag system and currently even for vehicle stability control.

Currently the most common accelerometers are those based on the piezoelectric effect, this effect discreves the variation of electrostatic force or electric voltage in a material when subjected to a force.

By measuring this variation of electrostatic force or electrical voltage it is possible to determine the acceleration that the sensor has undergone. In Figure 8 we can observe that there is a mass in the piezoelectric material, so when the sensor is submitted to

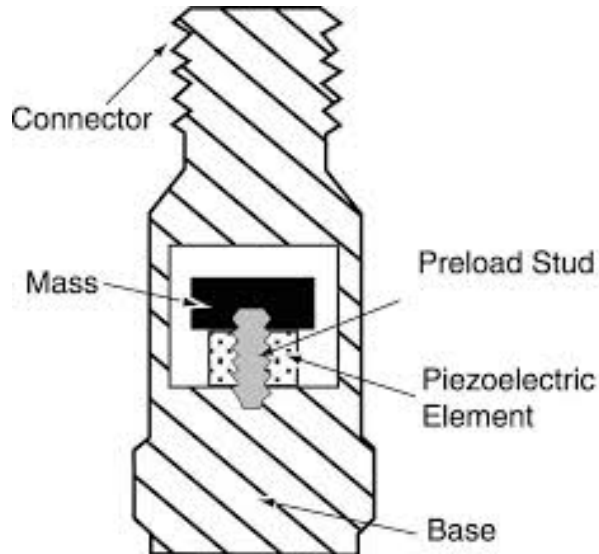


Figura 8 – Piezo Accelerometer (UK, 2016)

some movement, based on the principle of inertia the mass will exert a force of traction or compression which will generate a voltage variation at the sensor output (PATRICK, 2007).

2.3.5 Instrumentation Amplifier

In general, sensors and transducers have very low voltage output levels (specially passive transducers), and therefore an amplification is fundamental. The most commonly used amplifier circuit in instrumentation engineering is the common joint differential amplifier more commonly referred as *Instrumentation Amplifier* (Figure 9), which is very stable and significantly reduces the output signal noise (WAIT; HUELSMAN; KORN, 1975).

The instrumentation amplifier has two stages, the first stage consists in amplifying both inputs of a sensor, with the gain of this amplification stage controlled by R_{gain} in Figure 9. The second stage consists in taking the difference of the two input signals. If the differentiation happens before the amplification, noise may be so big in the input signals that some signal information might be lost. In the instrumentation amplifier noise and signal is amplified on the first stage, considering that the noise is similar in both inputs the differential stage will take out the noise and only output the difference between both inputs. One advantage of this amplifier is that it has high input impedances, that means it will not drain significant current from the signal, i.e., it will not interfere with the measure (THOMSEN et al., 2003). Another advantage is that the gain of this amplifier can be adjusted with just one resistor (METTINGVANRIJN; PEPPER; GRIMBERGEN, 1994).

The gain of the instrumentation amplifier is given by the following 2.3.5 (COUNTS;

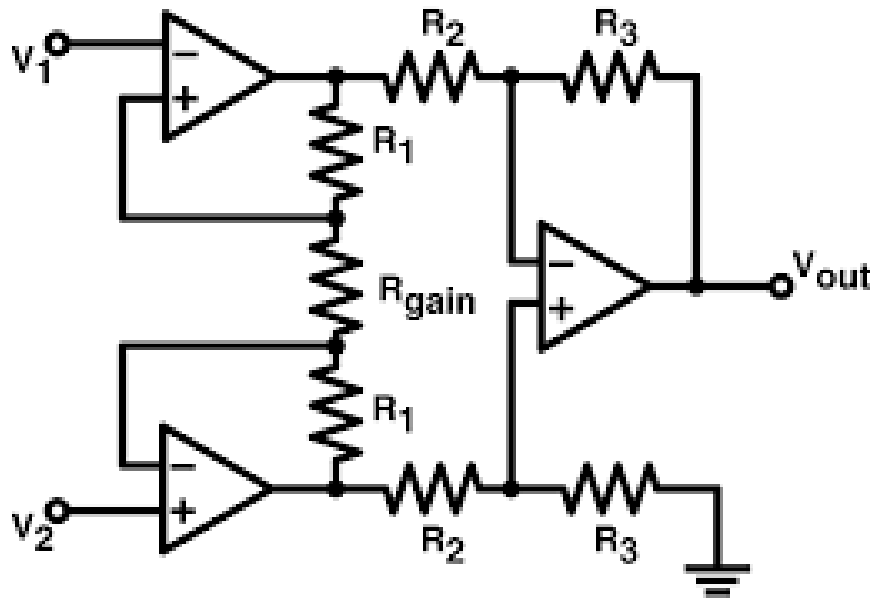


Figura 9 – Instrumentation Amplifier ([DESCONHECIDO, 2016](#))

[KITCHEN, 2006](#)).

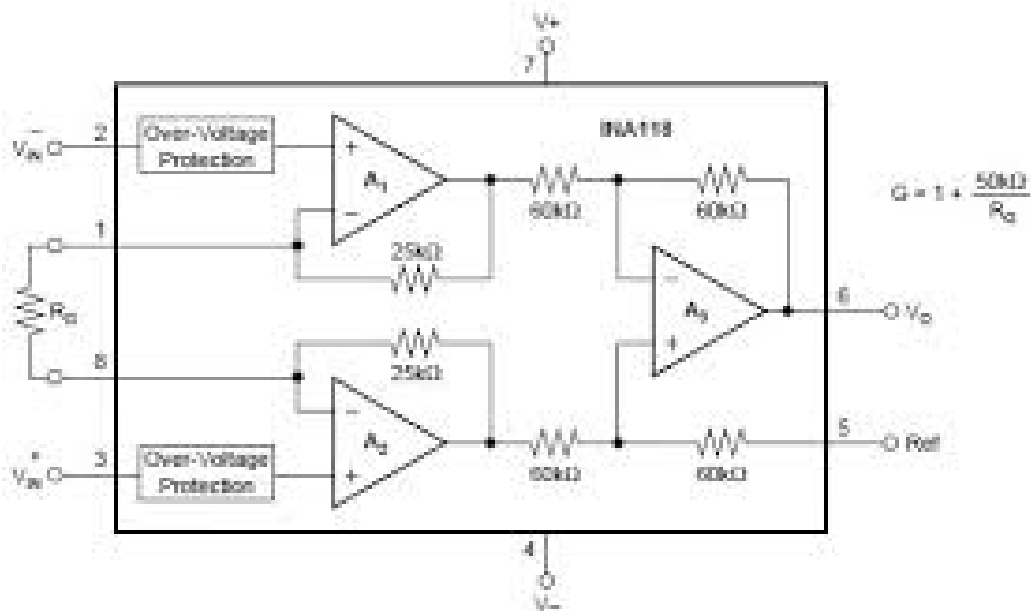
$$V_{out} = (V_2 - V_1) \cdot \left(1 + \frac{2 \cdot R}{R_{gain}}\right) \quad (2.2)$$

Something interesting to notice is that if we take out the R_{gain} (open load), the gain of the amplifier is equal to one. Besides this advantageous behavior of the instrumentation amplifier, it is quite hard to make it work with seven resistors and three operation amplifiers because of components imprecision. Hence, it is more practical to work with ICs that ensure the symmetry of between those components. As an example, there is the Texas Instruments INA118 ([INSTRUMENTS, 2000b](#)), which is one of many encapsulated solutions for the instrumentation amplifier, the schematic of this component is shown in Figure 10.

2.3.5.1 Important features to consider in a amplifier

There are some important factors when choosing a OPAMP in a certain application, according to ([INC.\(NORWOOD, 2011\)](#)), some of the important features to know in a amplifier are:

- *Common-Mode Voltage Range (CMVR)*: Allowable input voltage range at both inputs before clipping or excessive nonlinearity.
- *Common-Mode Rejection Ratio (CMRR)*: The ratio of common-mode voltage range (CMVR) to the change in the input offset voltage over this range, expressed in dB.

Figura 10 – INA 118 ([INSTRUMENTS, 2000a](#))

- *Gain Bandwidth Product (GBW)*: The product of open-loop and bandwidth at a specific frequency.
- *Input Bias Current (I_B)*: The current at the input terminals.
- *Operating Supply Voltage Range*: The supply voltage range that can be applied to an amplifier for which it operates within specifications. Many applications implement op amp circuits with balanced dual supplies, while other applications for energy conservation or other reasons, use single-supply.
- *Supply Current*: The current required from the supply voltage to operate the amplifier with no load.

2.3.6 System Controlling

In order to automate break tests a system block that should be able to interface both sensor signals and user commands to the system is needed. Summarizing, this block should be responsible to handle the interface between the electric signals and higher level user instructions.

At the design of this block of the solution a important thing should be considered, data acquisition. According to ([NATIONAL INSTRUMENTS, 2018](#)) DAQ (Data Acquisition) can be defined as the process of measuring an electric or physical phenomenon, such as voltage, current, temperature, pressure or sound. There is a type of device that is able to perform data acquisition and system control, the microcontroller.

2.3.6.1 Microcontroller basic characteristics

A microcontroller is a compact computer on a single integrated circuit chip, in most cases a microcontroller (also referred by the acronym MCU) includes a processor, volatile and non-volatile memory, input/output ports and other peripherals. The great thing about the microcontrollers is their low cost, many small appliances that do not require a powerful hardware are only economically viable because of those devices. The components a microcontroller has may vary, it is a responsibility of the project designer to decide the microcontroller that has the best fit (technically and economically) for the project.

Microcontrollers differ from microprocessors only in one thing, MCUs can be used standalone while microprocessors need other peripherals to be used. By reducing the size and cost compared to a design that uses a separate microprocessor, memory, and input/output devices, microcontrollers make it economical to digitally control even more devices and processes. “A microprocessor can be considered the heart of a computer system, whereas a microcontroller can be considered the heart of an embedded system”([ROUSE, 2012](#)).

A great thing about microcontrollers is that they can provide real-time response to events, so for instrumentation they are crucial. With them it is possible to acquire signals with good sampling rates without loss of relevant information. It is common in electronic instrumentation to use MCUs to handle the events that have real-time constraints and use more sophisticated hardware solutions to manage and process the acquired data later ([BARTZ; ZHAKSILIKOV; OGAMI, 2004](#)).

2.3.6.2 Microcontroller ISP programming

In-system programming (ISP), also called in-circuit serial programming (ICSP), is a technique where a programmable device is programmed after the device is placed in a circuit board ([MICROCHIP TECHNOLOGY INC., 2003](#)) rather than before placing the circuit in the board.

There are many different standards protocols for ISP, most of them variants from the Joint Test Action Group (JTAG) protocol ([OSHANA, 2002](#)). An example of devices using ISP is the AVR line of micro-controller by Microchip such as the ATmega328PB MCU ([MICROCHIP, 2018](#)). According to ([EQUINOX TECH,](#)), important ISP definitions are:

- **ISP Programmer:** This is a device which is capable of producing the required logic and power signals to in-system program the **Target Microcontroller**.
- **Target Microcontroller:** This is the MCU which is to be in-system programmed.

- **Target System:** The Target System is the physical PCB which contains the MCU to be in-system programmed.
- **ISP Header:** The programmer must interface to the correct pins of the target device, systems that have ISP programmers usually have a standard connector to ensure the connection is done the right way between the programmer and the MCU.

Figure 11 show the typical connection for most AVR ISP systems

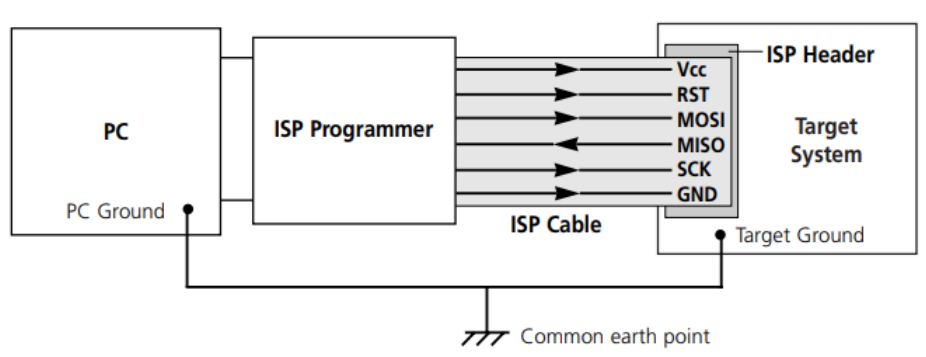


Figura 11 – Typical Connections for ISP Programming ([EQUINOX TECH, 2018](#))

According to ([EQUINOX TECH,](#)), the signals from the 6-pin headers are:

- **VCC:** Programmer Vcc Connection.
- **MOSI:** Programmer MOSI signal (SPI Data Out).
- **MISO:** Programmer MISO signal (SPI Data In).
- **RESET:** Programmer RESET Control Line.
- **GND:** Programmer Ground Connection.
- **SCK:** Programmer Serial Clock Signal.

2.3.7 Pulse Width Modulation

Pulse Width Modulation (PWM), is a way of modulation for encoding information on a pulse train signal. There are many ways of encoding and extracting this message in and out of the PWM signal and this type of modulation can be used for a wide variety of applications such as controlling the charge delivered to a load and transmitting information ([STANDARD, 1996](#)). PWM signals have a fixed high and a fixed low voltage level, there are two parameters that can be varied on a PWM signal: oscillation frequency and duty cycle. Figure 12 shows how the duty cycle affects a PWM signal.

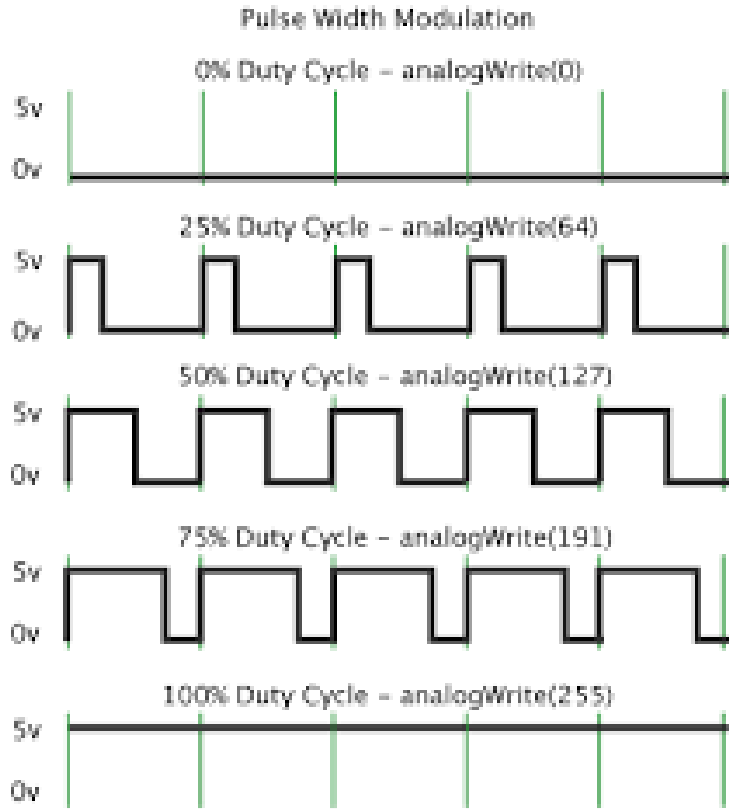


Figura 12 – Duty Cycle Examples ([RZTRONICS, 2016](#))

Duty cycle can be defined mathematically by the Equation 2.3 ([JAMES, 2001](#)), where $D\%$ is the duty cycle in percentage, PW is the pulse width (pulse active time) and T is the wave period.

$$D_{(\%)} = \frac{PW}{T} \quad (2.3)$$

One useful way of using a PWM duty cycle variation is by encoding a analog voltage level proportional into it's percentage ([HOLMES; LIPO, 2003](#)), meaning that 100% duty cycle would represent maximum voltage amplitude and 0% the minimum voltage. This means it is possible to extract a analog voltage level by taking a PWM average level ([ALTER, 2008](#)), this is a practical way for designing digital to analog converters.

2.3.8 Data Communication

Performing data acquisition is the core endeavour of this project, but after data is acquired by the lower level hardware the next step is to convert and export this data to a upper layer of the system. For example, lets say that a DAQ system to acquire temperature has a thermocouple, a conditioning circuit and a MCU with an ADC. The acquired temperature measurement stored on the MCU volatile memmory is completely useless unless it is exported to another plataform that will perform the HIM (Human-

Machine-Interface). In short terms, according to (GONZALEZ, 2015), HIM includes any device or software that allows you to interact with a machine.

In order to export this data it is important to choose a communication interface. Nowadays, computers and mobile devices are available with a wide array of ports and USB (universal serial bus) is the most common laptop and desktop connector by far (PILTCHE, 2017).

2.3.8.1 USB

Universal Serial Bus, more commonly known as USB, is a industry standard created to define cables, connectors and protocols for connection, communication and power supply between computers and their peripheral devices (GARFINKEL, 1995).

There are many specifications in the USB standard, one of than being the USB 1.0. It states that USB cables and connectors must have four wires: a pair of power wires (V_{BUS} and GND) a two wires for differential serial data signals, like Figure 13.

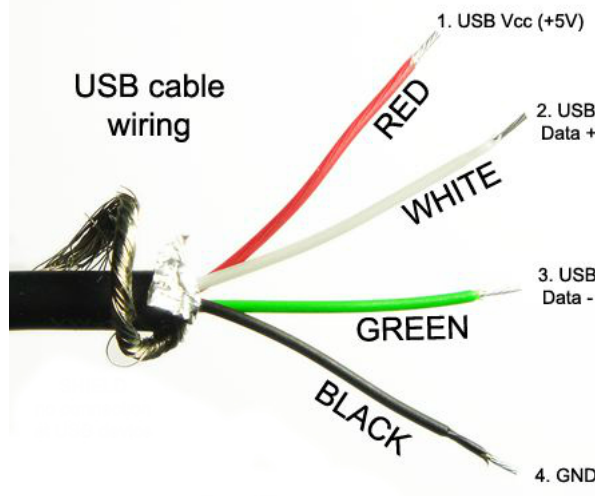


Figura 13 – USB 2.0 Wires (UNKNOWN, 2017)

USB 1.0 specifies data rates of 1.5 Mbit/s (Low-Bandwidth, is mostly used for Human Input Devices (HID) such as keyboards, mouses, joysticks and often the buttons on higher speed devices such as printers or scanners) and 12 Mbit/s (Full-Bandwidth) (SPECIFICATION-REV,).

Differential signaling employs to complementary voltage signals to transmit one information signal, while one wire carries the signal the other carries the inverted signal (KINNAIRD, 2012) as Figure 14.

Two of the many advantages on differential signaling stated by (PINKLE, 2016) are:

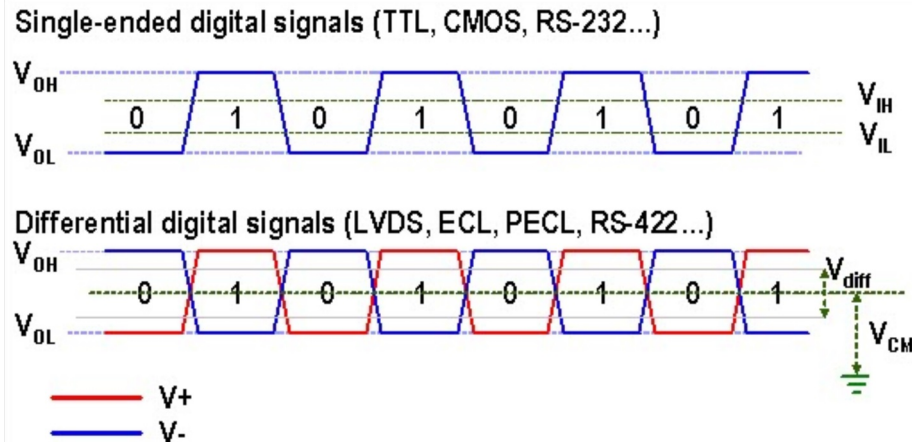


Figura 14 – What Differential Signaling Is All About ([AUTODESK, 2017](#))

- Resistance to EMI: Any interference on the signal will probably affect both signals the same way, so as the receiver responds to the difference between both signals, the receiver will reduce the amplitude of the interference.
- Lower-Voltage Operation: Because of their improved resistance to noise, differential signals can use lower voltages and still maintain adequate SNR. Also, the SNR of differential signaling is automatically increased by a factor of two relative to an equivalent single-ended implementation, because the dynamic range at the differential receiver is twice as high as the dynamic range of each signal within the differential pair.

2.3.9 Circuit Protection

A important feature of any electronic product/appliance is the immunity against undesired inputs. In DAQ systems this is a relevant issue, the inputs of this systems must be protected from possible damage that may be caused by unintentional/accidental high voltage inputs, surges, etc ([MATHIVANAN, 2007](#)).

According to ([LITTLELFUSE, 2015b](#)), Voltage Transients are defined as short duration surges of electrical energy and are the result of the sudden release of energy previously stored or induced by other means. There are many things that can cause voltage transients (commonly referred just by transients) and those can be divided in two groups:

- Repeatable Transients: Usually caused by the operation of inductive loads such as motors, generators and switching circuits.
- Random Transients: Uncorrelated transients generated by exclusive events such as lightning, ESD and unpredictable events.

In order to enhance energy efficiency, devices are now operating at lower voltages ([SOUZA et al., 2017](#)). With the miniaturization of electronic components, those have become even more sensitive to electrical stress ([LITTLELFUSE, 2015b](#)).

In automotive environment, many of the supporting electrical components of the vehicle can generate transients, specially from inductive load switching. When the inductive load is switched off, the collapsing magnetic field is converted into electrical energy that turns into a transient ([LITTLELFUSE, 2015b](#)).

2.3.9.1 Low Pass Filters

According to ([LITTLELFUSE, 2015b](#)), a ESD pulse (fastest common transient pulse) has an overall duration period of less than 100ns (50% of the peak value) and a rising time that lasts less than 1.2 μ s. Figure 15 shows an example of a ESD Test Waveform.

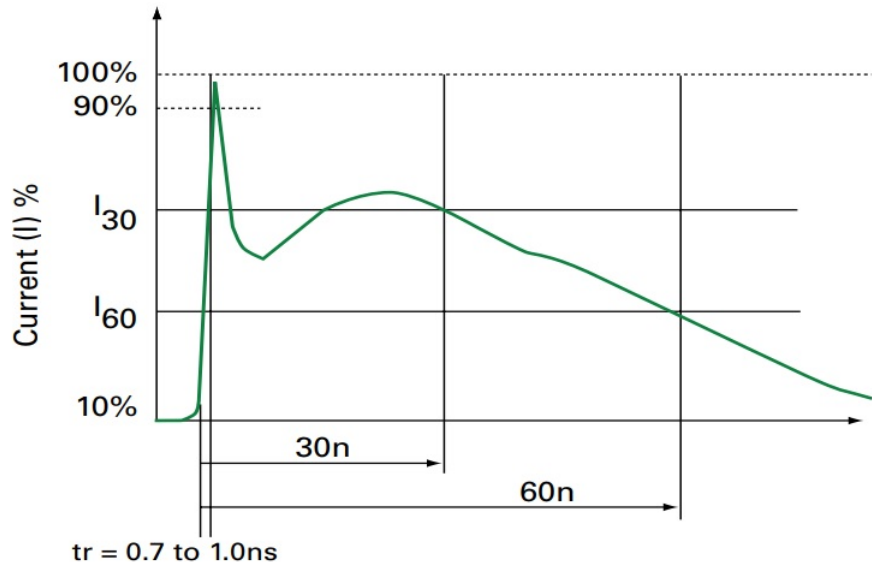


Figura 15 – ESD Test Waveform ([LITTLELFUSE, 2015a](#))

Considering that a signal has a frequency that is lower than the frequency of the transient it is vulnerable to, using a low pass filter to provide suitable attenuation for that transient and still letting the signal frequency on the passband, it is possible to protect that part of the circuit against this particular transient ??.

2.3.9.2 Transient Voltage Suppression Diodes (TVS)

2.3.9.2.1 TVS diodes principle of operation

Transient Voltage Suppression Diodes or TVS Diodes are nowadays the most popular choice for protection components in circuit due to their fast response, low clamping voltage and longevity. Under normal operation TVS diodes are high-impedance devices,

interacting as a open circuit to the protected component, during a transient event the TVS diode junction provides a low-impedance path for the transient current (RENESAS, 2016a).

There are both uni-directional and bi-directional, the first has a operation curve similar as the one from a Zener diode, during positive transients the device limits the input voltage to it's clamping voltage and during negative transients the spike is clamped to the diode drop. On the other hand, bi-directional TVS diodes are always reverse biased during both negative and positive transients. Figures 16 and 17 show respectively the action of a uni-directional TVS and a bi-directional TVS during transient events.

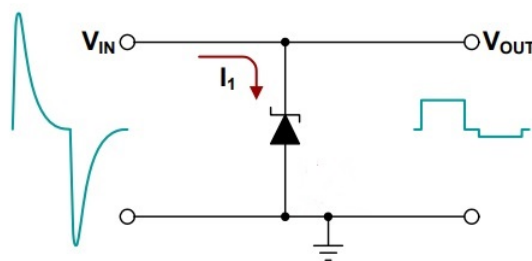


Figura 16 – Campling action of a uni-directional TVS (RENESAS, 2016c)

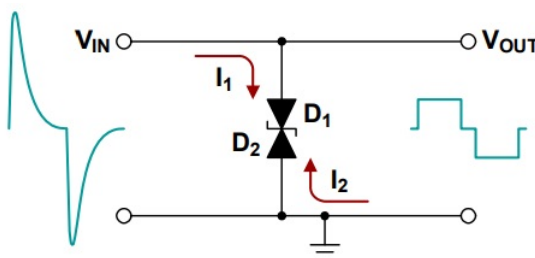


Figura 17 – Campling action of a bi-directional TVS (RENESAS, 2016b)

The *Voltage X Current* curve of both uni-directional and bi-directional TVS diodes can be seen repectively on Figures 18 and 19.

2.3.9.2.2 Selecting TVS Diodes

According to (WALTERS, 2016), the following parameters of TVS devices are important to consider in order to choose one for protecting a particular circuit net:

- V_C (Campling Voltage): the voltage limit that the TVS will allow on the point of intended protection. This voltage should be slightly lower than the point of intended protection absolute maximum voltage rating.
- V_{WM} (Rated Standoff Voltage): this is the maximum voltage in which the TVS still works as a high-impedance device. Therefore, the first step when selecting a TVS

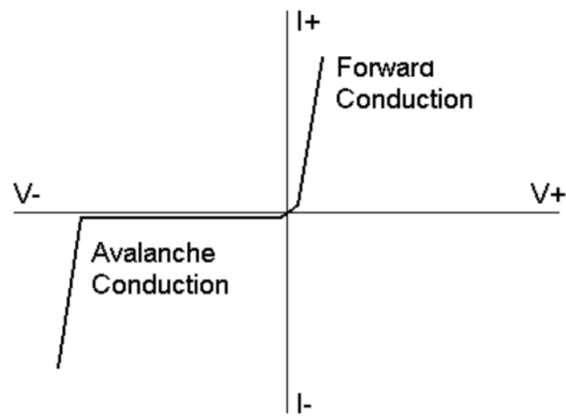


Figura 18 – $V \times I$ characteristic of a uni-directional TVS (RENESAS, 2016e)

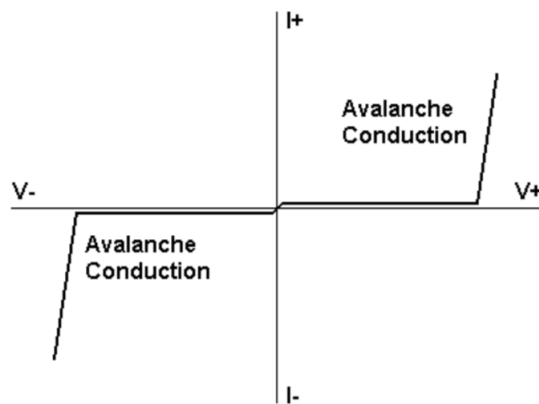


Figura 19 – $V \times I$ characteristic of a uni-directional TVS (RENESAS, 2016d)

device is to know the peak voltage at the point of intended protection during normal operation and then select a TVS device with a appropriate V_{WM} .

- P_{PP} (Peak Pulse Power): in order to ensure the durability of the TVS device, the maximum power it needs to dissipate should be known. This P_{PP} is calculated by multiplying the TVS device V_C (Clamping Voltage) and the I_{PP} (Peak Impulse Current, peak current for the transient event).

3 Methodology

In order to achieve the goals of this project the endeavours were divided into three

3.1 Literature Review

This stage can be considered the most important of the whole project because it layers the foundations for development of all that follows. This stage comprehended the knowledge needed in all further stages and steps of the project, even on the further stages of development it was necessary to review some of the information acquired on this part in order to achieve best results. On the Literature Review stage, concepts, components and other necessary information to make the foundations for the project were addressed. For instance it will be on this stage that the brake tests parameters and requirements will be analysed in order to choose the proper solutions for this project.

3.2 Problem Description

This particular stage consisted on the depuration of the problem in question, leading to a study of the requirements that were necessary to ensure in order to develop and execute the project.

3.3 Project Conception

After a deep problem analysis it was possible to address a more detailed solution description, in this stage the general solution was splitted in many smaller ones that were defined according to the requirements of the previous stage. All this solutions were focused in functionality, this is a project of electronic instrumentation, so the goal was not to develop electrical/electronic solutions from the beginning, it was evaluating the requirements and finding a group of components/solutions that combined in a particular and unique way could lead to this project achieving its goals.

3.4 Case Study

After the particular and smaller solutions are developed, tested and considered functional, the general solution of this project will be tested as a whole thing. This being doing a brake test that is capable of proving the functionality and usability of the developed technology.

4 Problem Analysis and Project Requirements

4.1 Problem Analysis

As mentioned in Section 1.1 this project aims on developing a functional brake test bench. Based on the *SAE J2522* (SAE, 2016) and considering some instrumentation engineering concepts the project solution can be divided in the structure showed in Figure 20.

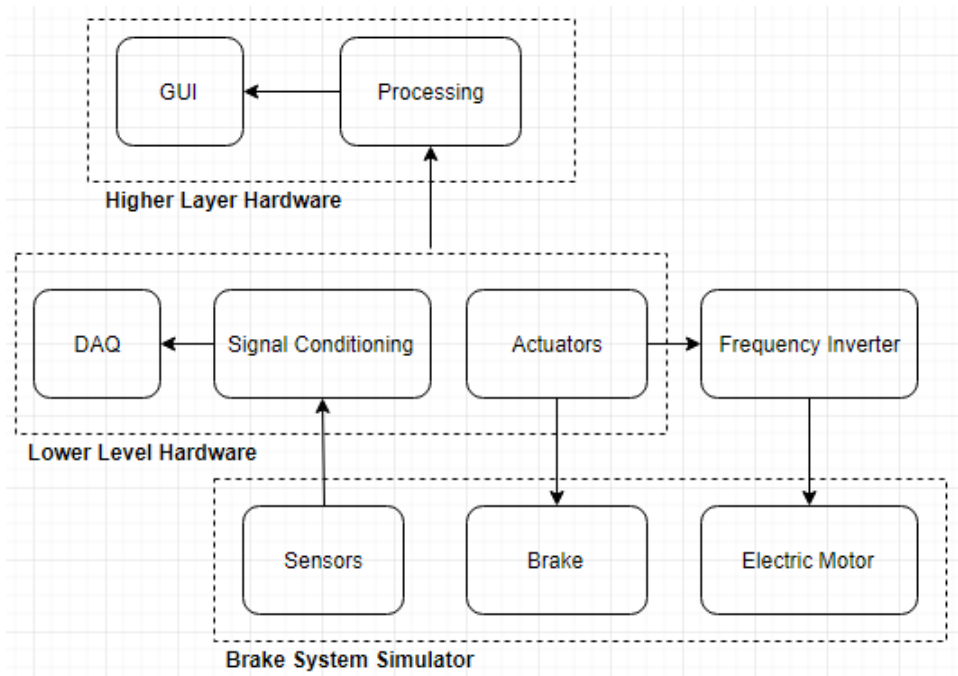


Figura 20 – Project Problem Depuration ([GUIMARAES, 2017c](#))

The explanation of the structure of Figure 20 will be explained in Sections 4.1.1 to 4.1.4.

4.1.1 Brake System Simulator

The *Brake System Simulator* block as the name says comprehends the hardware responsible for simulating the environment of a brake system, the two basic components are the *Brake* component itself (in this case being a disc brake system) and a *Electric Motor* to accelerate the rotor in order to simulate the speed a vehicle wheel might be submitted. A *Sensors* block was also added, without acquiring a physical/mechanical quantities such as temperature and pressure, a brake test would be useless because no

possible technical analysis could be done afterwards. The *Sensors* block was placed inside the *Brake System Simulator* block because the sensors and transducers will be placed around the components of this major block.

4.1.2 Lower Layer Hardware

This layer of hardware will make the translation from physical/mechanical quantities to computer data, *i.e.*, converting physical/mechanical quantities to voltage and then to bytes of information and also on the opposite way (bytes to voltage and voltage to physical/mechanical quantities). *Sensors* signals are not always ready to read, as mentioned in Section ??, Instrumentation Engineering also involves doing *Signal Conditioning* to adapt sensor signals. The *DAQ* block was inserted in order to demonstrate that there is the need for a solution to capture the sensors signals. *Actuators* block are responsible to adapt the commands from upper layers to control the hardware. The *Frequency Inverter* is already a more specific detail of the solution, but it was included here because most electric motors work with triphasic power and this device is fundamental to control them.

4.1.3 Higher Layer Hardware

This layer of hardware although represented in a quite simple way in Figure 20 will probably involve the most dense code. This is because this layer needs to do all the heavy data processing, *i.e.*, converting and dealing with the information that flows through all the structure. The *GUI* block is the one responsible for acquiring and displaying computer information in a human-friendly format.

4.1.4 Solution Overview

Table 2 shows the basic function of each block on Figure 20.

Table 2 – Blocks functionality

Block	Function
<i>Sensors</i>	Convert physical quantities to electrical signals
<i>Signal Conditioning</i>	Adapt sensors electrical signals to best suit DAQ
<i>DAQ</i>	Converts electrical signals to computes bytes
<i>Actuators</i>	Convert voltage levels to physical/mechanical quantities
<i>Frequency Inverter</i>	Controls a triphasic motor speed
<i>Processing</i>	Control and process data flow
<i>GUI</i>	Displays/acquire information in a human-friendly format

4.2 Monitored Parameters

As mentioned before this paper will be based in the *SAE J2522* regulations, this regulation says that to evaluate the efficiency of a brake system it is mandatory to monitor temperature on the brake pads, the pressure applied on the disk and the speed of the rotor throughout all the process. Monitoring the vibration is not mandatory but has some advantages.

- *Temperature of brake pads:* During all test it is mandatory to have full knowledge of the temperature of the break pads, firstly because of security reasons (there is upper limit for temperatura in any system) and also because of the wear of parts that is related to temperature.
- *Pressure applied on the disks:* Knowing the magnitude of this force means being able to relate the pressure applied and the deceleration, knowing how the pressure applied increases the temperature of the pads and evaluate how this promotes wear of the parts.
- *Rotation speed:* Without knowing how the speed of the rotor varies over time it would be impossible to determine the acceleration and deceleration rates among many other issues.
- *Vibration:* As mentioned before this is not mandatory but rather interesting, measuring vibration makes it possible to determine how the extensive use can wear out the parts and reduce stiffness among other properties. Also it is natural that the system will vibrate during braking, minimal vibration or too much vibration can indicate a fault that on the future could damage the system.

4.3 Functional Requirements of the Testbench

According to the specification of the *SAE J2522* and according to parameters considered to be important, some requirements for the testbench were defined.

1. Measure a braking pressure up to 16 MPa.
2. Apply a braking pressure of at least 300 kPa.
3. Measure temperatures up to 600 °C
4. Measure temperatures with a minimal resolution of 7.5 °C.
5. Accelerate the rotor to a speed up to 200 kph.
6. System must have a sampling period of 50ms.

7. The system hardware must be able to operate under temperatures up to 40°C.
8. System must have two acquisition channels for temperature.
9. System must have at least two channels for braking pressure acquisition.
10. System must have a channel for vibration acquisition.
11. System must have at least two digital outputs to control relays.
12. System must have a channel for acquiring speed.
13. The system must work with real time acquisition.
14. The system must be able to detect when the sensors from the acquisition channels are disconnected.

4.4 Software Requirements

1. System must have a sampling rate of 50 ms.
2. System must be able to monitor six analog channels at once.
3. System must be able to control the digital outputs and one analog output during acquisition without losing the real time constraint.
4. The data acquired does not need to be shown to user in real time.
5. The software layer must be able to record the data of the test.
6. The software highest layer must have a friendly GUI, advanced electronic and simple programmable knowledge cannot be a requirement to operate the software.
7. Calibration of the sensors data must be easy to modify on the software.
8. Software must be multiplatform.

5 Hardware Project

Based on the matters analysed on the previous sections of this paper a hardware architecture was defined and it displayed on the following Figure 21.

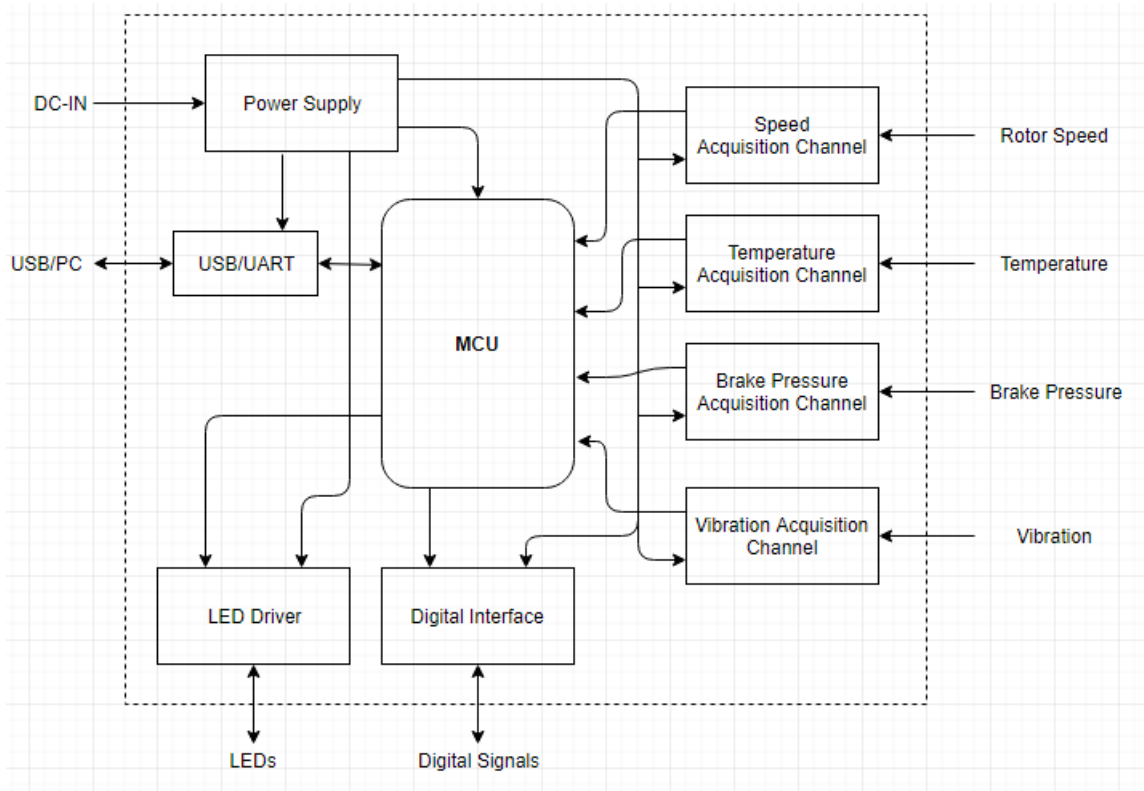


Figura 21 – Hardware Project Architecture ([GUIMARAES, 2017a](#))

5.1 MCU

5.1.1 The chosen MCU

The chosen microcontroller for the system is the *ATMEGA328PB* manufactured by *Microchip*. It has 32 Kb of flash memory, 1 Kb of *EEPROM* (Electrically Erasable Programmable Read-Only Memory), 2Kb of *SRAM* (Static Random Access Memory), 27 GPIOs, 32 general purpose registers, five flexible timer/counters, two USARTs, 8-channel 10bit ADC ([MICROCHIP, 2018](#)).

This microcontroller is widely used in academic environment (specially after the Arduino project started, when microcontroller programming became much more feasible and reachable), and is famous for being easy and reliable to use. The *ATmega328p* has eight ADC inputs with a resolution of 10 bits and more 27 GPIO ports. This microcontroller

also has a UART (explained in Section ??). It is really versatile and more important it meets this project requirements, listed in Section 4.3. This microcontroller will be used with a five volts supply, giving digital inputs and outputs a standard high logic level of five volts and low logic level of zero volts. The Figure 22 shows the pinout of this device.

Figure 5-1 32 TQFP Pinout ATmega328PB

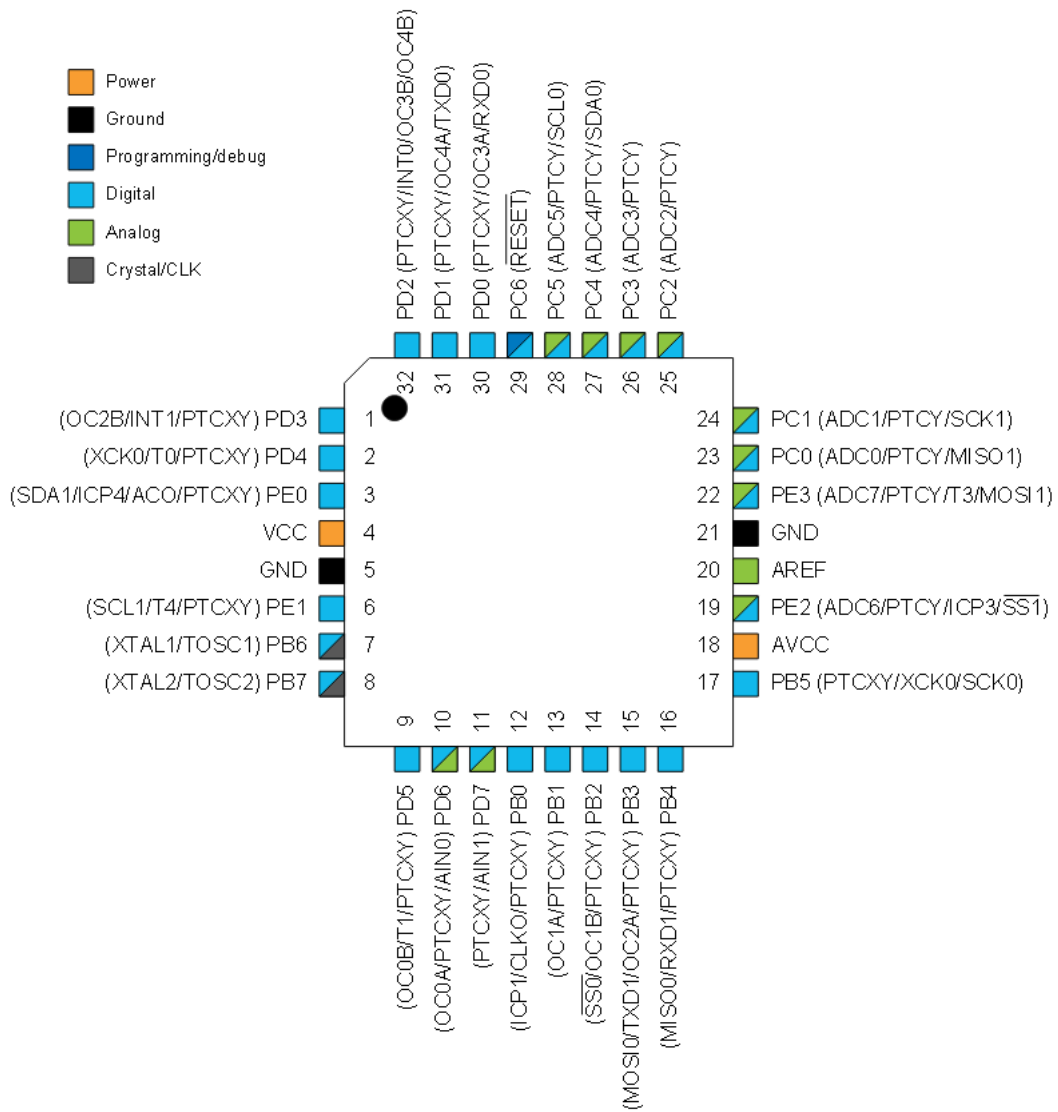


Figura 22 – ATmega238PB pinout ([MICROCHIP, 2018](#))

5.1.2 MCU circuit

Figure 23 shows the complete complementary circuit for the MCU.

5.1.2.1 MCU Communication Ports

The ports in yellow and the RST ports are the MCU communication connections with other circuit modules, they are described as it follows.

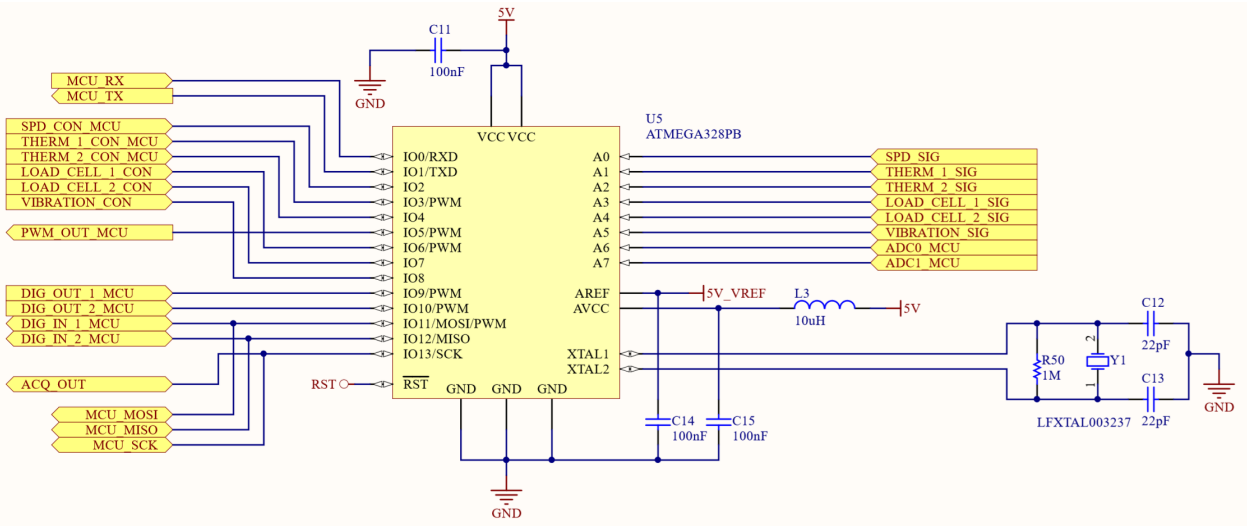


Figura 23 – MCU Complete Complementary Circuit ([GUIMARAES, 2018l](#))

- *MCU_RX (input)*: This port is used for receiving the serial data from the USB/U-ART circuit, as it was explained in Section 5.7.4.
- *MCU_TX (output)*: This port is used for transmitting the serial data to the USB/U-ART circuit, as it was explained in Section 5.7.4.
- *SPD_CON_MCU (input)*: A signal coming from the speed acquisition channel (Section 5.4.2) that indicates whether the sensor is connected or not.
- *THERM_1_CON_MCU (input)*: A signal coming from the first temperature acquisition channel (Section 5.2.4) that indicates whether the sensor is connected or not.
- *LOAD_CELL_1_MCU (input)*: A signal coming from the first brake pressure acquisition channel (Section 5.3.3) that indicates whether the sensor is connected or not.
- *LOAD_CELL_2_MCU (input)*: A signal coming from the second brake pressure acquisition channel (Section 5.3.3) that indicates whether the sensor is connected or not.
- *VIBRATION_CON (input)*: A signal coming from the vibration acquisition channel (Section 5.5.3) that indicates whether the sensor is connected or not.
- *PWM_OUT_MCU (output)*: This is a PWM signal that goes from the MCU to the DAC circuit in order to control the electric engine speed (Section 5.6.4).

- *DIG_OUT_1 MCU (output)*: First digital external output used in the circuit (Section 5.8.1).
- *DIG_OUT_2 MCU (output)*: Second digital external output used in the circuit (Section 5.8.1).
- *DIG_IN_1 MCU (input)*: First digital external input used in the circuit (Section 5.8.2).
- *DIG_IN_2 MCU (input)*: Second digital external input used in the circuit (Section 5.8.2).
- *ACQ_OUT (output)*: Used to control a LED that blinks when signal acquisition is taking place (Section ??).
- *MCU_MOSI*: Used for ISP programming (Section 2.3.6.2).
- *MCU_MISO*: Used for ISP programming (Section 2.3.6.2).
- *MCU_SCK*: Used for ISP programming (Section 2.3.6.2).
- *SPD_SIG (input)*: Analog input for the speed signal (Section 5.4.1).
- *THERM_1_SIG (input)*: Analog input for the first temperature signal (Section 5.2.2).
- *THERM_2_SIG (input)*: Analog input for the second temperature signal (Section 5.2.2).
- *LOAD_CELL_1_SIG (input)*: Analog input for the first brake pressure signal (Section 5.3.2).
- *LOAD_CELL_2_SIG (input)*: Analog input for the second brake pressure signal (Section 5.3.2).
- *VIBRATION_SIG (input)*: Analog input for the vibration intensity signal (Section 5.5.2).
- *ADC0 MCU (input)*: This port is not used and an internal MCU pull-up resistor is used.
- *ADC1 MCU (input)*: This port is not used and an internal MCU pull-up resistor is used.
- *RST (input)*: This is the reset connection for the MCU, used to reset the MCU using ISP programming.

5.1.2.2 MCU Power Ports

The MCU power ports are described as follows, each power port function was taken from the components datasheet ([MICROCHIP, 2018](#)). All voltage supplies have a 100nF decoupling capacitor also recommended by the MCU datasheet.

- *VCC*: This is the main voltage supply port for the MCU, as mentioned in Section [5.1.1](#) the MCU will be powered up with a 5V supply. More details of this supply line in Section [5.10.1.1](#).
- *GND*: This is the ground reference for the MCU.
- *AREF*: This is the analog voltage reference for the ADC, as good as it's voltage reference ([ANDREWS, 2015](#)). The net $5V_VREF$ is internally connected to the MCU precision reference.
- *AVCC*: This is the ADC power supply, the inductor was used to filter unwanted noise, and the usage of this inductor was based on the Arduino Uno Rev3 Schematic ([ARDUINO, 2010](#)).

5.1.2.3 Crystal Oscillator Circuit

The MCU datasheet indicates the use of an external oscillation crystal, the additional components to the crystal were based on the Arduino Uno Rev3 ([ARDUINO, 2010](#)).

5.2 Temperature Acquisition Channel

5.2.1 Thermocouple Types and Characteristic Signal

For this project it was defined that thermocouples of type K (formed by the junction of two metal leagues: Alumel and Cromel) would be used in this project. This is because this specific type of thermocouple has a wide range of operation (-200°C - 1200 °C), so according to the requirements they are never too close from the boundary values, a thermocouple of type T or even a type J would not be suitable. Other appealing factor is that this type of thermocouple is quite common so getting eventual replacements would be easier, in comparison with type E thermocouples.

5.2.2 Thermocouple Signal Conditioning

As mentioned in sub-section [2.3.2](#), besides amplification and linearization, the thermocouple signal also needs its cold junction temperature difference compensation. There is an integrated solution from *Analog Device* called AD8495, this IC functional diagram is displayed on Figure [24](#).

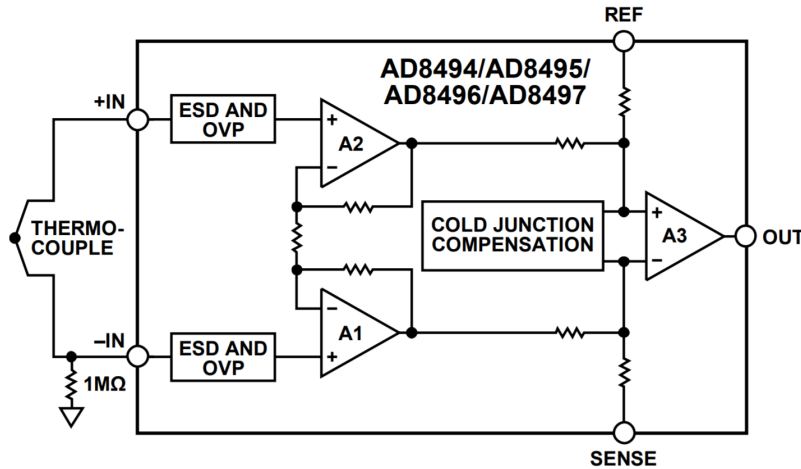


Figura 24 – AD8495 Functional Block Diagram ([DEVICES, 2011](#))

This IC produces a linearized output with a fixed gain of $5\text{mV}^{\circ}\text{C}$, it is a quite practical solution as it can be powered with single-supply voltage source and it's output saturates to the power supply voltage if the thermocouple is disconnected ([ANALOG DEVICES, 2010](#)).

5.2.3 Input Protection and Filtering

Although this IC already has overvoltage and ESD protection, thermocouples tips can pick a load of unwanted noise and transients. Hence, additional protection and external filtering is also recommended by ([DUFF; TOWEY, 2010](#)). First thing to do is to add current-limiting series resistors, the drawback is doing that is that resistors in the circuit net increases the overall noise. This type of noise is called Johnson-Nyquist Thermal Noise or more commonly just by Johnson Noise, thermal agitation of electrons in a resistor gives rise to random fluctuations in the voltage across its terminals ([ROMERO, 2000](#)). Moreover, it can be calculated using the following Equation 5.1 where K is the Boltzamann's constant $1.38 \cdot 10^{-23}$, R is the resistance in ohms (Ω) and T the temperature in kelvin (300K at room temperature) ([BRYANT et al., 2000](#)).

$$\text{Noise}(nV\sqrt{\text{Hz}}) = \sqrt{4 \cdot K \cdot R \cdot T \cdot 10^9} \quad (5.1)$$

Because the protection circuit includes two equal resistors, whose noise is uncorrelated, that is, the two noise sources are independent of each other—the above result must be multiplied by the square root of 2 (the root sum square of the two noise voltages) and it is considered as a general rule design to tolerate additional Johnson Noise from 10 to 30% to the amplifier IC ([BRYANT et al., 2000](#)). ([DUFF; TOWEY, 2010](#)) suggests using current-limiting resistors of $10k\Omega$, according to the AD8495 datasheet ([ANALOG DEVICES, 2010](#)), the chosen amplifier (AD8495) has a voltage noise density of $32\text{nV}\sqrt{\text{Hz}}$.

Combining this resistors noise with the amplifier noise will produce a overall noise of $36.85\text{nV}\sqrt{\text{Hz}}$, which is just 13% above the amplifier's own noise. Additional protection can be achieved using (TVS) to protect the inputs from differential input overvoltage, considering a bidirectional TVS with a 10V breakdown voltage, the device will theoretically limit the differential voltage between 10V and -10V, the AD8495 has overvoltage protection from -25V to 20V when powered with 5V, so this will successfully protect the amplifier inputs.

With the overloads protection done, another important feature to do is to filter unwanted signals in the inputs to avoid them to be amplified later, this is done by filtering Radio Frequency Interference (RFI), signal lines (specially for low level signals) are quite susceptible to RF interference ([COUNTS; KITCHEN, 2006](#)). Interference that occurs on both lines are usually reduced by the amplifiers own CMRR (check Section [2.3.5.1](#)), but only on a limited bandwidth, also the in-amp rectifier cannot filter differential RF interference. The choosen amplifier (AD8495) has a -3dB bandwidth at 25kHz, ([DUFF; TOWEY, 2010](#)) suggests setting a common-mode cutoff filter frequency at 16kHz (in order to guarantee the input signal within the 25kHz bandwidth). The standard circuit for the RFI filter is displayed on Figure [25](#), resistors R and capacitors C_C are used to filter common-mode interference. Capacitor C_D is connected across the bridge output to reduce any common-mode rejection errors due to the components mismatch, that way filtering any differential interference. C_D is usually choosen to be ten times larger than C_C ([ANALOG DEVICES, 2010](#)).

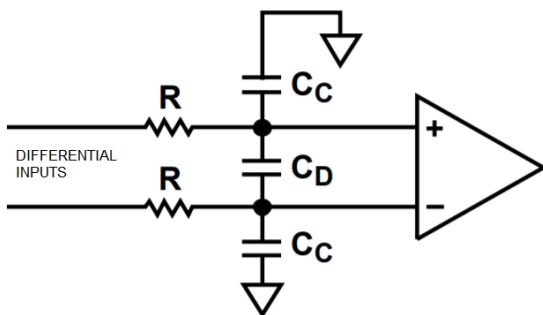


Figura 25 – RFI Circuit ([GUIMARAES, 2018s](#))

The -3dB common-mode bandwidth of this filter from Figure [25](#) is given by Equation [5.2](#) ([COUNTS; KITCHEN, 2006](#)).

$$BW_{CM} = \frac{1}{2 \cdot \pi \cdot R \cdot C_C} \quad (5.2)$$

The -3dB differential bandwidth of this filter from Figure [25](#) is given by Equation

5.3 (COUNTS; KITCHEN, 2006).

$$BW_{DIFF} = \frac{1}{2 \cdot \pi \cdot R \cdot (2 \cdot C_C + C_d)} \quad (5.3)$$

Using the values for the current limiting resistors ($10\text{k}\Omega$), Equation 5.2 and the suggested cutoff frequency of 16kHz (DUFF; TOWEY, 2010), it is possible to calculate a value of 1nF for C_C . Choosing a C_D value ten times larger than C_c implies on using a C_D value of 10nF , that used on Equation 5.3 will produce a differential interference filter cutoff frequency of 1.3kHz .

5.2.4 Thermocouple Sensor Detection

A important feature of any acquisition system is to detect when a sensor is disconnected from the the acquisition system input (O'MAHONY; GELFAND; MERRICK, 2011), because a signal acquisition circuit without the signal source will generate outputs that are uncorrelated to what the system was designed to measure/sense on the outside world. The AD8495 has a quite useful feature (ANALOG DEVICES, 2010), it offers open thermocouple detection, the inputs of the AD8495 are PNP type transistors, which means that the bias current always flows out of the inputs. This way, the input bias current drives any unconnected output high, which saturates the output to the maximum possible reading, being in this case 1000°C or 5V (considering the fixed $5\text{mV}^\circ\text{C}$ gain). In Section 4.3, it was defined that the system must measure temperatures up to 600°C , with the fixed gain of 5mV° this means an output voltage of 3V . The so called *Thermocouple Sensor Detection* must be able to detect whenever the output exceeds 3V . In order to do that, the circuit displayed in Figure 26 was designed.

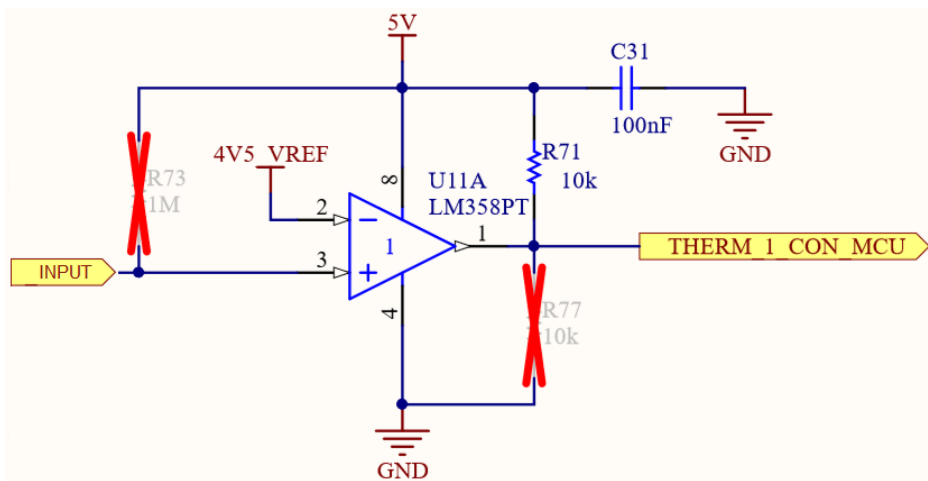


Figura 26 – Overvoltage Detection Circuit (GUIMARAES, 2018m)

U11 is a OPAMP working as a comparator, whenever the thermocouple signal is higher than the $4V5_VREF$ the OPAMP output will saturate to the 5V (the supply

voltage applied to the OPAMP). The net $4V5_VREF$ will be further explained in Section 5.10.2.2, whereas it is a constant voltage produced on the Power Supplies circuit block. The resistor $R71$ is a pull-up resistor used to guarantee that signal will go to high-logic level in case the voltage in the inputs is not present. The capacitor $C31$ is just a decoupling capacitor for the OPAMP power supply.

5.2.5 Complete Circuit

The thermocouple complete circuit is displayed on Figure 27.

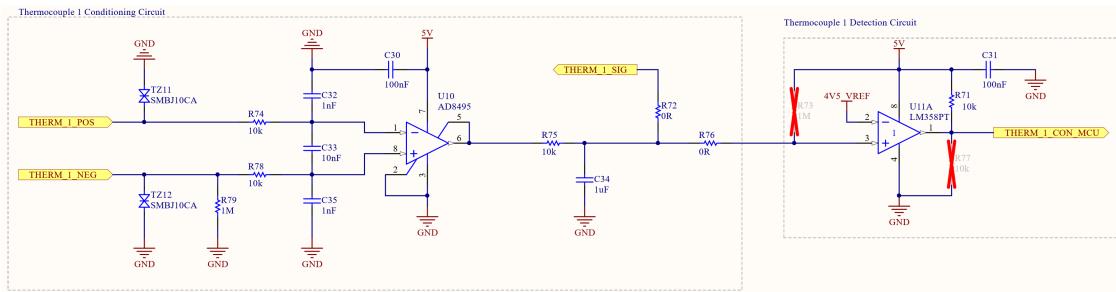


Figura 27 – Thermocouple Complete Circuit (GUIMARAES, 2018w)

As mentioned in Subsection 5.2.2, a TVS was added on each of the thermocouple signal lines, the SMBJ10CA (LITTELFUSE, 2017) was chosen because it has a maximum clamping voltage of 17V/-17V, which will guarantee that the voltage levels will not surpass the 20V/-25V limits of the AD8495. $R79$ is a resistor that is recommended by the amplifier's IC to enable sensor detection functionality. The pair composed of $R84$ and $C39$ is a LFP with a central frequency of 16Hz, used to filter any further noise including the 50/60Hz noise from AC power lines that the thermocouple wires may catch. $R81$ and $R85$ were included in case a individual circuit block test is required, both are 0R resistors (jumpers).

5.3 Brake Pressure Acquisition Channel

5.3.1 Load Cell Signal

A very influential parameter in a braking system is the pressure that the brake exerts on the rotor. Pressure is a magnitude measured in Pascal and can be expressed by the force ratio by the area. There are some sensors based on the piezoelectric effect, but the most accurate way to measure force is by using load cells.

Load cells have very low output levels, of the level of 2mV/V , and therefore an amplification is fundamental. It is not necessary to know the nature of the strain gauges when a load cell is being calibrated since generally the manufacturers provide a calibration curve based on the signals V_O and V_{EX} of the Figure 7, it is worth noting that these signals

can not have the same reference, otherwise it will not be possible to excite the wheatstone bridge correctly.

The most common way to amplify the signal of a load cell is using a instrumentation amplifier. Although it is a widely used configuration, assembling this amplifier using three different operational amplifiers and seven resistors as in Figure 9 may make it inaccurate due to manufacturing imperfections of the components. Another factor that greatly influences the output signal of a load cell is the excitation voltage of its wheatstone bridge, if it varies too much the output will vary greatly as well, which will hamper its calibration.

5.3.2 Load Cell Signal Conditioning

In order to solve these two problems there is a solution widely used in the market which is the *AD8223* from Analog Devices ([DEVICES, 2008](#)), this IC is an integrated single supply instrumentation amplifier that delivers rail-to-rail output swing. Other good feature of this amplifier is that as it has a great CMRR (*Common-Mode Rejection Ratio* check Section 2.3.5.1) of 80dB, making it very much suitable for condionting differential pair signals (such as the one from the Load Cell as Subsection 2.3.3 mentions), more information of CMRR in Subsection 2.3.5.1. The only external component needed is a resistor R_G , as shown in Figure 28. This resistor will determine the gain (G) for the amplification according to the Equation 5.4.

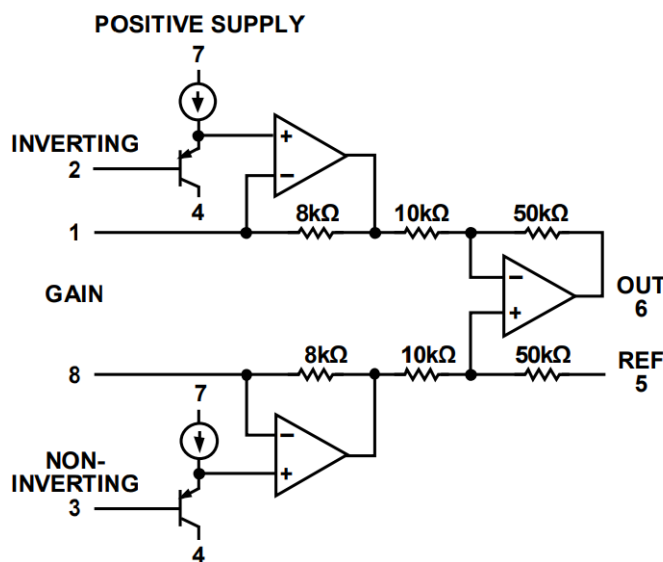


Figura 28 – AD8223 Schematic ([DEVICES, 2008](#))

$$R_G = \frac{80k\Omega}{G - 5} \quad (5.4)$$

Taking into account the sensitivity of 2mV/V , this means that if the cell is excited with 10V , its output will vary from 0 to 20mV . The precision of the excitation voltage will naturally affect the performance of the sensor, Section 5.10.2.1 will explain how a precise 10V voltage reference will be achieved.

Since the analog input of the chosen microcontroller (*Atmega328*) is 0 to 5V , we may need to amplify the cell output signal by a factor of 250 in order to use the most number of bits from the MCU's ADC. Using Equation 5.4, to obtain a gain of amplification ratio of the ideal R_G would be 326Ω , a resistor of this value and minimal tolerance (1%) is not commercially available, the closest one is 332Ω . This resistor will generate a gain of 246 and cause the IC output to range from about 0V to 4.92V , using 98.4% of the resolution of the microcontroller input.

Figure 29 shows the schematic of the load cell conditioning circuit with the AD8223.

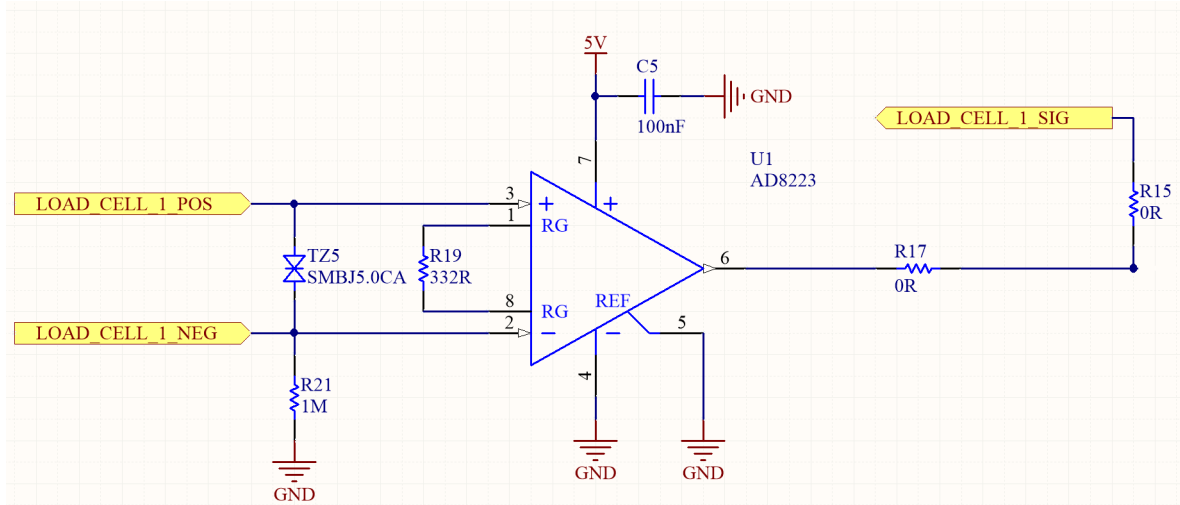


Figura 29 – Conditioning Circuit for the Load Cell (GUIMARAES, 2018h)

It is basically the amplifier with the gain resistor plus five different types of components:

- **TVS Diode:** AD8223 datasheet says that the differential input voltage must not be greater than the supply voltage (DEVICES, 2008), hence, as the supply is 5V , a 5V TVS was added.
- **Decoupling Capacitor:** A decoupling capacitor is recommended by the component's datasheet (DEVICES, 2008).
- **Resistor R21:** Used to guarantee that if the sensor is disconnected the inverted input will be shunted to GND as according to Figure 28 the PNP transistors in the non-inverted input will saturate the output to the supply voltage (*this feature is used for detecting when the sensor is disconnected, further explained in Subsection: 5.3.3*).

- **R17 and R15:** These jumpers are used just if the need to test circuit blocks separately.

5.3.3 Load Cell Sensor Detection

As was explained in Subsection 5.3.2, with R21 the circuit will saturate the output to the supply voltage when the load cell sensor is disconnected. The circuit to detect this voltage saturation is exact the same from the one used previously on the thermocouple circuit, the circuit schematic and functional explanation can be found in Subsection 5.2.4.

5.3.4 Complete Circuit

The thermocouple complete circuit is displayed on Figure 30.

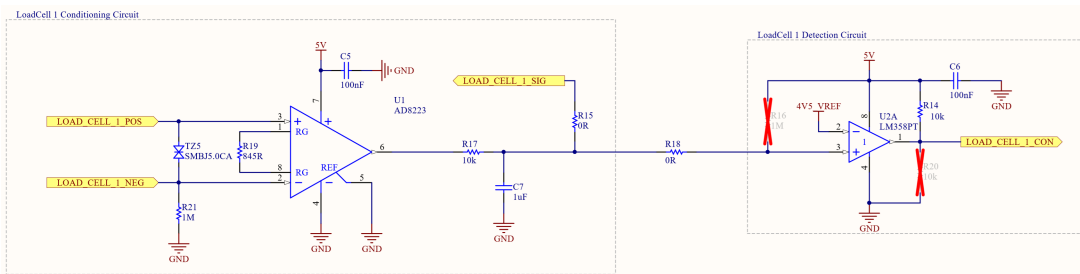


Figura 30 – Load Cell Complete Circuit (GUIMARAES, 2018k)

The pair composed of R17 and C7 is a LFP with a central frequency of 16Hz, used to filter any further noise including the 50/60Hz noise from AC power lines that the thermocouple wires may catch. R15 and R18 were included in case an individual circuit block test is required, both are 0R resistors (jumpers). R20 is just a pull-down to guarantee that the MCU input port will not fluctuate.

5.4 Speed Acquisition Channel

5.4.1 CKP Signal Conditioning

As mentioned in Section 2.3.1, a CKP sensor has an analog signal with variable amplitude. For this project the only important parameter to extract from the sensor output signal in order to obtain the wheel speed is its frequency (angular velocity). The most practical way to obtain this data is to use a tachometer interface circuit, for this project the LM2907 from *Texas Instruments* (TEXAS INSTRUMENTS, 2000) will be used. LM2907 is a *frequency-to-voltage* converter with a ground-referenced tachometer input with $\pm 28V$ maximum voltage, making it versatile for many different sensor models.

5.4.1.1 LM2907 Basic Tachometer Circuit

The conditioning circuit for this project was based on the *Tachometer with Adjustable Zero Speed Voltage Output* on Figure 31 suggested by LM2907 datasheet ([TEXAS INSTRUMENTS, 2000](#)).

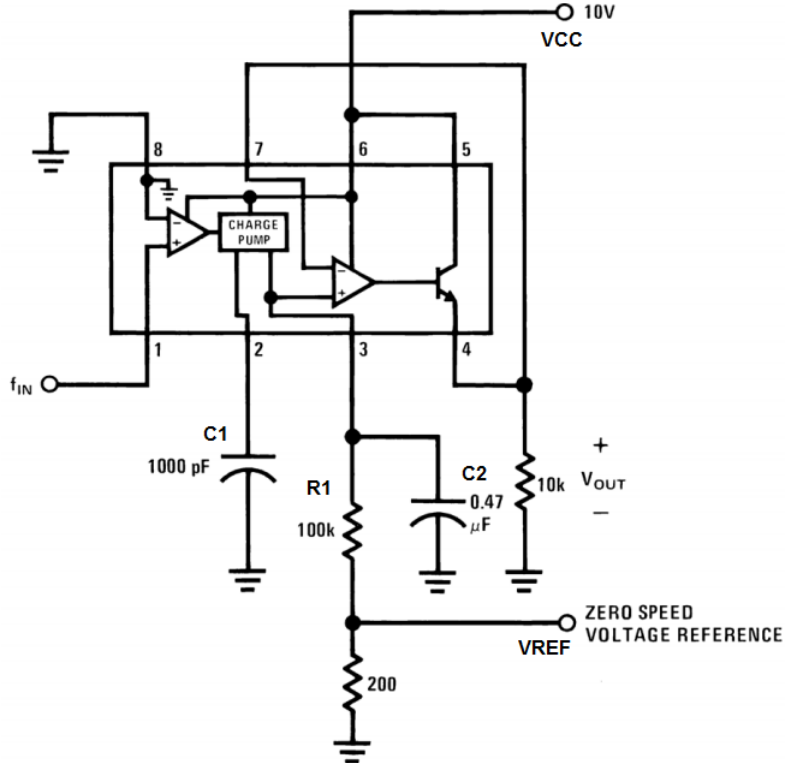


Figura 31 – Tachometer with Adjustable Zero Speed Voltage Output, adapted from ([TEXAS INSTRUMENTS, 2018](#))

According to the datasheet ([\(TEXAS INSTRUMENTS, 2000\)](#)), in order to configure the gain of the frequency-to-voltage converter, C₁, R₁ and C₂ must be configured in respect to the following design requirements.

- **C₁:** This capacitor is charged and discharged every cycle by a 180μA typical current source. C₁ must not be sized lower than 500-pF due to its role in internal compensation.
- **R₁:** Higher of R₁ values increase the output voltage for a given frequency, but too large will degrade the output's linearity. Because the current pulses are a fixed magnitude of 180 μA typical, R₁ must be big enough to produce the maximum desired output voltage at maximum input frequency. At maximum input frequency the pulse train duty cycle is 100%, therefore the average current is 180 μA and $R_1 = V_{out}(max) / 180 \mu A$.

- **C2:** This capacitor filters the ripple produced by the current pulses sourced by the charge pump. Large values reduce the output voltage ripple but increase the output's response time to changes in input frequency.

The output voltage (V_O) can be calculated using Equation 5.5, V_{CC} is the supply voltage and f_{IN} the input frequency.

$$V_O = V_{REF} + (V_{CC} \cdot f_{IN} \cdot C1 \cdot R1) \quad (5.5)$$

As said in Item 5.4.1.1, C2 controls the voltage ripple on the output(V_{RIPPLE}), this ripple is given by Equation 5.6. According to the datasheet, I_2 has a typical value of 180uA.

$$V_{RIPPLE} = \frac{V_{CC}}{2} \cdot \frac{C1}{C2} \cdot \left(1 - \frac{V_{CC} \cdot f_{IN} \cdot C1}{I_2}\right) \quad (5.6)$$

Finally, the last thing to consider is the maximum attainable input frequency, determined by V_{CC} , C1 and I_2 (180uA) in Equation 5.7.

$$f_{MAX} = \frac{I_2}{C1 \cdot V_{CC}} \quad (5.7)$$

5.4.1.2 LM2907 Designed Circuit

The first parameter to be calculated is the maximum frequency, functional requirement from Item 5 in Section sec:functionalRequirements says the the system should be able to reach 200kph. Hence, to know the relation between frequency and speed on a wheel it's important to know the wheel's diameter. According to (TODAS..., 2018), the smallest commercial tyre size in terms of diameter in Brazil is the standard 165/70R13 which has a diameter (D) of 561.2mm and the one with the biggest diameter (D) is the standard 265/50R20 having 773mm. Using Equation 5.8 to calculate the overall length of the wheel gives a approximately length of 1.762m for the smaller tyre and a approximately length of 2.428m for the bigger one.

$$C = \pi \cdot D \quad (5.8)$$

A speed of 200kph equals approximately 55.5556m/s, using this value of speed divided by the calculated values of length, we have maximum frequencies of approximately 31.52Hz (for the smaller tyre standard) and 22.88Hz (for the bigger tyre standard). Applying the greater value of frequency, a supply voltage of 5V (check Section 5.1.1) on Equation 5.7 (remembering that $I_2=180\mu A$) gives a approximately value of $C1=1\mu F$.

Using this calculated value of C_1 ($1\mu F$), with the maximum frequency (31.52Hz), the V_{CC} value (5V), the desired offset voltage V_{REF} (1V) and the maximum output voltage V_O (5V) on Equation 5.5 gives a R_1 value of $25.381k\omega$, the closest commercial value is of $24k\omega$, using this value gives a maximum output voltage in respect to the maximum input frequency of approximately 4.78V.

In Section 5.1.1, it is said that the chosen microcontroller's ADC has a resolution of 10-bit. A analog reference of 5V with 10-bit resolution gives a voltage resolution of 4.88mV. Hence, the calculated voltage ripple of the frequency-to-voltage converter must be less than the ADC resolution. Using values of V_{RIPPLE} , C_1 , R_1 , f_{IN} and V_{CC} in Equation 5.6 gives a C_2 value of approximately $63.75\mu F$, the closest commercial value is $68\mu F$.

Figure 32 shows the designed circuit for the speed acquisition channel.

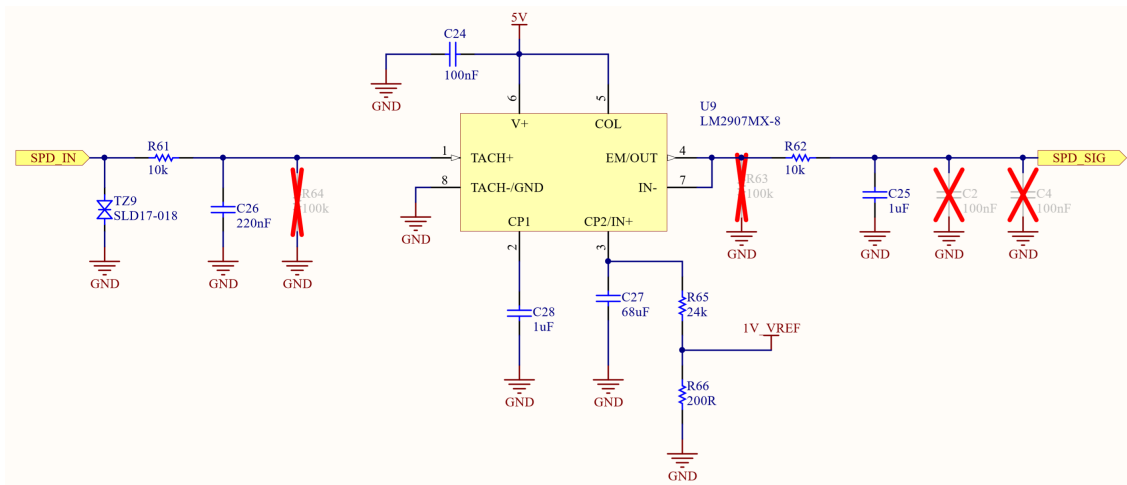


Figura 32 – Speed Acquisition Channel Circuit (GUIMARAES, 2018u)

In addition to the components from the circuit *Tachometer with Adjustable Zero Speed Voltage Output* on Figure 31, the following features have been added:

- **TVS Diode:** In order to protect the the IC's input the SLD17-018 TVS diode from *Littelfuse* was added. This diode has a maximum clamping voltage of 27.6V, the maximum input voltage is $\pm 28V$, thus the TVS will protect the input from overvoltages.
- **LPF at the input:** As the maximum frequency was determined to be 31.52Hz, it is possible to filter all the upper frequencies in order to avoid any noise to enter the circuit. R34 and C26 form a LPF with a cutoff frequency of approximately 160Hz, this cutoff frequency was chosen because at 31.52Hz (maximum input frequency), the attenuation is quite close to 0dB (-0.15dB) and shall not affect the input signal.
- **LPF at the output:** R62 and C25 form a LPF to that is used to filter any external post-conversion noise, it has a approximate frequency of 16Hz.

5.4.2 CKP Sensor Detection

The detection circuit consists basically of a filtered digital input, a extra cable from the CKP power supply line will need to be wired in order to detect when the board sensor is connected. Naturally, when this cable is disconnected this extra wire input will have zero volts.

Figure 33 shows the detection circuit for the CKP sensor.

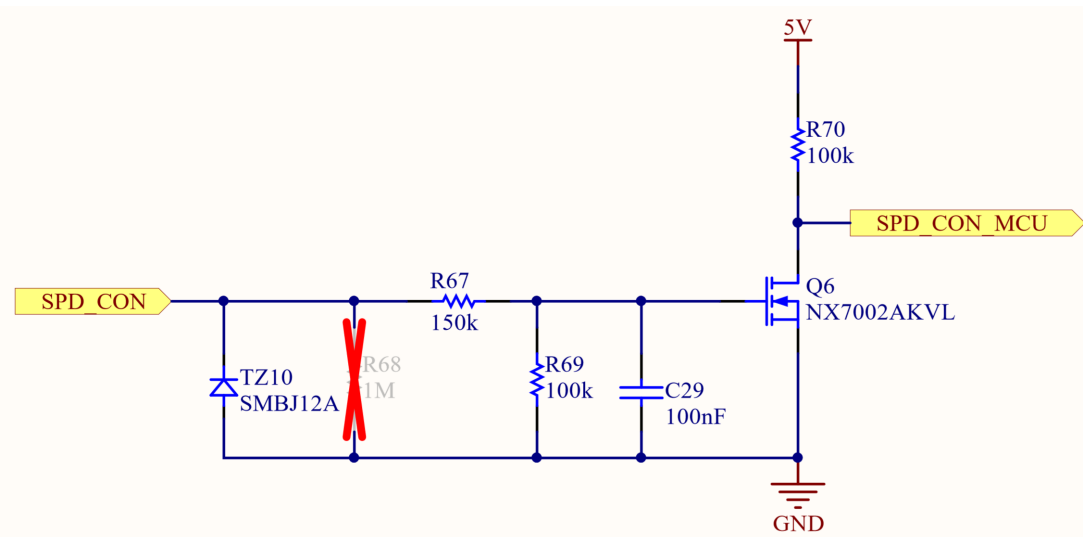


Figura 33 – Speed Sensor Detection Channel Circuit ([GUIMARAES, 2018v](#))

TZ10 is TVS diode to protect the input from overvoltages. Resistors R67 and R69 form a voltage divider that will transform the 12V input signal to a 5V level signal. Resistor R67 and C29 form a LPF with cutoff frequency of 10.66Hz, this filter is used to attenuate unwanted noise from the input.

5.5 Vibration Acquisition Channel

5.5.1 Accelerometer

As mentioned in Section 2.3.4, acceleration is measured in g. The chosen accelerometer for this project was the *ADXL335* from *Analog Devices* ([DEVICES, 2010](#)). The main characteristics of this sensor are:

- It has 3 axis sensing (easy to install).
- Low power operation ($350\mu\text{A}$).
- 10,000 g shock survival.
- 1V8-3V3 Single-supply operation.

- ±3g measurements.

When powered up with 3V3 the sensor has a linear voltage output of 0V for -3g and 3V3 for 3g. This sensor is ideal for this project, the only issue is the installation. The sensor comes in a 16-LFCSP IC (Figure 34), and this IC needs to be installed where acceleration is intended to be measured, so a additional board is necessary to install it.

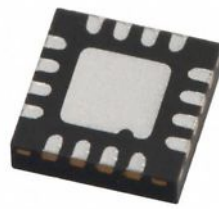


Figura 34 – 16-LFCSP ([DEVICES, 2016](#))

The are already embdded solutions that can solve this issue, such as the *Adafruit ADXL335 - 5V ready* ([ADAFRUIT, 2016](#)). This small (75mm x 75mm) board (Figure 35) has the ADXL335 with the capacitors recommended by the datasheet, with a 3V3 voltage regulator so the board can be powererd up with 5V and with the mounting holes to fix the board in any surface, making it ideal for this project.

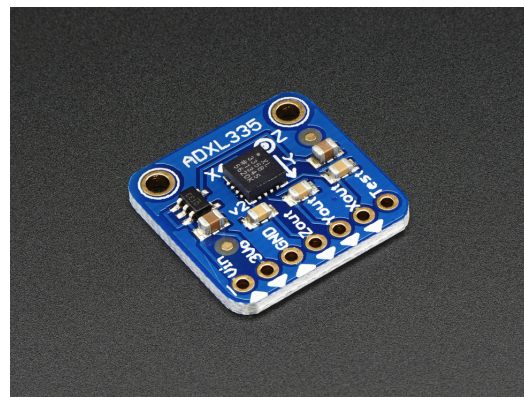


Figura 35 – Adafruit ADXL335 - 5V ready (??)

5.5.2 Signal Conditioning Circuit

The ADXL335 datasheet ([DEVICES, 2010](#)) says that for a -3g measured acceleration the device output is of 0V and for +3g measurement it is 3V3 voltage. As said in Section 5.1.1, the choosen MCU for this project has a ADC with a 5V voltage reference, so in order to use the maximum number os bits from the ADC is it important to amplify

this 0-3V3 signal to a 0-5V signal, meaning we need a circuit with a amplification gain of 1.5x.

The sensor conditioning circuit is displayed on Figure 36.

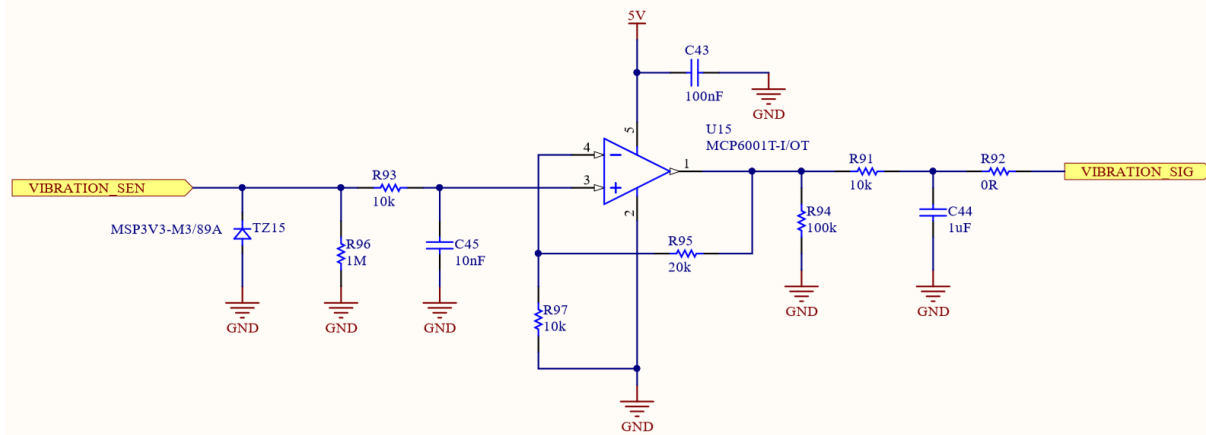


Figura 36 – Accelerometer Signal Conditioning Circuit ([GUIMARAES, 2018g](#))

The circuit is composed of three stages: protection, amplification and post-filtering.

- **First Stage (protection):** Composed of a TVS diode with a standoff voltage of 3V3 (same as the sensor maximum normal output voltage level, check Item [2.3.9.2.2](#) from Section [2.3.9.2.2](#)) and a LPF with a cutoff frequency of approximately 1.6kHz (enough to filter most ESD, check Section [2.3.9.1](#)).
- **Second Stage (amplification):** The second stage is composed by a simple non-inverting amplifier with a gain of 1.5x, to achieve this gain the resistors were choosing using Equation ?? from Section ?? . The choosen OPAMP is the *MCP6001* from *Microship* ([MICROCHIP, 2009](#)), it was choosen for this project because it optimized to work with single-supply, has rail-to-rail input/output and has wide-bandwidth operation.
- **Third Stage (post-filtering):** The third and final stage is composed just by a LPF filter to attenuate any post amplification noise and the 50/60Hz noise interference from the power line. It has a cutoff frequency of approximately 16Hz.

Resistor R92 is just a jumper that was included if this circuit block is intended to be tested separately from the rest of the circuit. Resistors R96 and R94 are external pull-downs and in theory should not be mounted, they were included in the layout just in case this pull-downs become needed and then a new PCB layout would not be necessary. Capacitor C43 is just a decoupling capacitor for the amplifier supply recommended by the component datasheet ([MICROCHIP, 2009](#)).

5.5.3 Sensor Detection Circuit

As mentioned in Section 5.5.1, the chosen solution for the accelerometer (*Adafruit ADXL335 - 5V ready*) has a integrated 3V3 voltage regulator. In Figure 35 it is possible to see that the 3V3 voltage output from the voltage regulator has a connection point on the board. Hence, if a wire is connected to this point and to the main circuit board, whenever this point does not have 3V3 voltage the sensor is disconnected. Moreover, the detection circuit just need to detect when the net is in 0V or 3V3.

The detection circuit can be seen in Figure 37, TZ16 is TVS diode with a stand-off voltage (Item 2.3.9.2.2 from Section 2.3.9.2.2) of 3V3 used to protect the circuit net without interfering with it's signal. Resistor R99 is pull-down resistor, used to guarantee that the mosfet will be not conduct current when there is no input, sensor disconnected, and the voltage on the *VIBRATION_CON* net will go to 5V. R98 and C46 form a first order LPF with a cutoff frequency of approximately 16Hz, and as a sensor disconnection process is not that fast it will filter any interference and also the noise from the 50/60Hz power lines. Finally there is R100, this is a pull-up resistor that will hold the voltage on the output to 5V when the mosfet is not polarized, sensor disconnected.

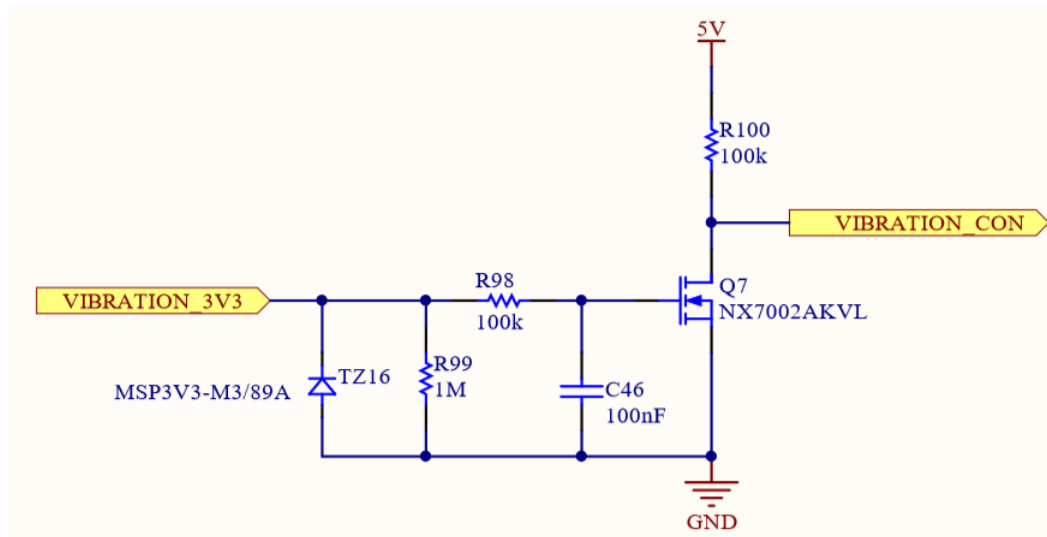


Figura 37 – Accelerometer Sensor Detection Circuit (GUIMARAES, 2018f)

5.6 Speed Reference Output Channel

5.6.1 Speed Control

For the braketests, somethings as important as measuring the speed of the rotor is controlling it, as mentioned in Subsection 4.1.2. The rotor speed can be controlled in two ways:

- First way is the deceleration of the rotor with the aid of the brake system using the brake pads.
- Second way of controlling it by accelerating the rotor with the aid of the electric engine.

The electric engine used is a alternate current three-phase type, it in order to control it's speed a frequency inverter was used. The frequency inverter has many different controlling interfaces that lead to manipulating the three-phase electric system in order to control the engine's rotary speed.

In this project the frequency inverter used was the *Weg CFW-08* ([WEG, 2009](#)), one way of controlling the speed of the rotor using this device is by using it's analog input, it can be configured as a notch to ten volts input that has a linear proportion to the output frequency that goes to the engine, that way the problem to figure out in this solution is how to implement a analog output from a microcontroller that only has digital outputs.



Figura 38 – Weg CFW-08 Frequency Inverter ([WEG, 2017](#))

5.6.2 Filter characteristics definition

Fortunately the microcontroller has pre-configured PWM (*Pulse Width Modulation*), as explained in Subsection [2.3.7](#), a PWM signal can encode a analog voltage value proportional to it's duty cycle, and this is usually done with the aid of a low pass filter that will extract this analog voltage from the PWM signal. As said in the previous paragraph the frequency inverter used in this project is the *Weg CFW-08*, and it's analog input has a zero to ten voltage input with eight bits of resolution. We can calculate the minimal

voltage difference that will change the output frequency of the device using Voltage, in which ΔV is the minimal voltage difference, V_{max} is the maximum voltage and "n" is the number of bits of the input resolution.

$$\Delta V = \frac{V_{max}}{2^n} \quad (5.9)$$

As mentioned in Section 5.1, the chosen MCU has a five volts high logic level, this voltage level will need amplification in order to best suit the zero to ten volts input from the frequency inverter. According to (ALTER, 2008), converting a PWM signal to a analog voltage generates a constant voltage ripple. It was decided to amplify this voltage prior to filtering because this way the voltage ripple generated from the filtering stage will not be amplified. Using a OPAMP and two resistors it is possible to convert a five volts amplitude square wave (PWM wave) to a 10V amplitude wave by giving a gain of two to the input signal. Using Equation ?? from Sub-section ??, it is possible to achieve the desired gain of two using both R_f and R_g of $10k\Omega$ as Figure ?? shows how to.

The maximum ripple is the ΔV from Equation 5.9. Equation 5.10 (METIVIER, 2013) gives the necessary $\frac{dB}{decade}$ attenuation to guarantee a PWM converted signal desired ripple.

$$A_{dB} = 20 \cdot \log \left(\frac{V_{RIPPLE}}{V_{PWM}} \right) \quad (5.10)$$

As the V_{PWM} will already be applied prior to filtering, $V_{PWM} = V_{max}$, this will produce the following Equation 5.11.

$$A_{dB} = -20 \cdot n \cdot \log (2) \quad (5.11)$$

And Equation 5.12 (METIVIER, 2013), is used to calculate the maximum needed cutoff frequency for the further to be designed LPF (*Low-Pass-Filter*) in order to convert the PWM signal to a analog voltage. This cutoff frequency can not be too much smaller than the one calculated otherwise this will have negative consequences to the output signal (KEIM, 2016). The slope value is the filter slope and for first order filters and second order filters this slope value is equal respectively to 20dB/decade and 40dB/decade (METIVIER, 2013).

$$f_c = f_{PWM} \cdot 10^{-\frac{A_{dB}}{Slope}} \quad (5.12)$$

It is possible to combine all this equations into one single equation to calculate

the needed cutoff frequency, is this done in Equation 5.13.

$$\begin{aligned}
 f_c &= f_{PWM} \cdot 10^{-\frac{A_{dB}}{Slope}} \\
 f_c &= f_{PWM} \cdot 10^{-\frac{-20 \cdot n \cdot \log(2)}{Slope}} \\
 f_c &= f_{PWM} \cdot 10^{\log\left(2^{\frac{20 \cdot n}{Slope}}\right)} \\
 \text{Knowing :} \\
 x \cdot \log(A) &= \log(A^x) \\
 10^{\log(A)} &= A \\
 \text{So :} \\
 f_c &= f_{PWM} \cdot 2^{\frac{20 \cdot n}{Slope}}
 \end{aligned} \tag{5.13}$$

As shown in Appendix A.1, the PWM frequency was defined so $f_{PWM} = 62.5\text{kHz}$, also $n = 8$ and as according to (METIVIER, 2013), a second order LPF is better for converting a PWM signal to voltage and it has by default $Slope = -40\text{dB/decade}$, using Equation 5.13 it is possible to calculate a maximum cutoff frequency of 3906.25Hz.

5.6.3 Sallen-Key Low Pass Active Filter

The Sallen-Key LPF setup is probably one of the best second order filters architectures available (DORF; SVOBODA, 2014), this setup is displayed on Figure 39.

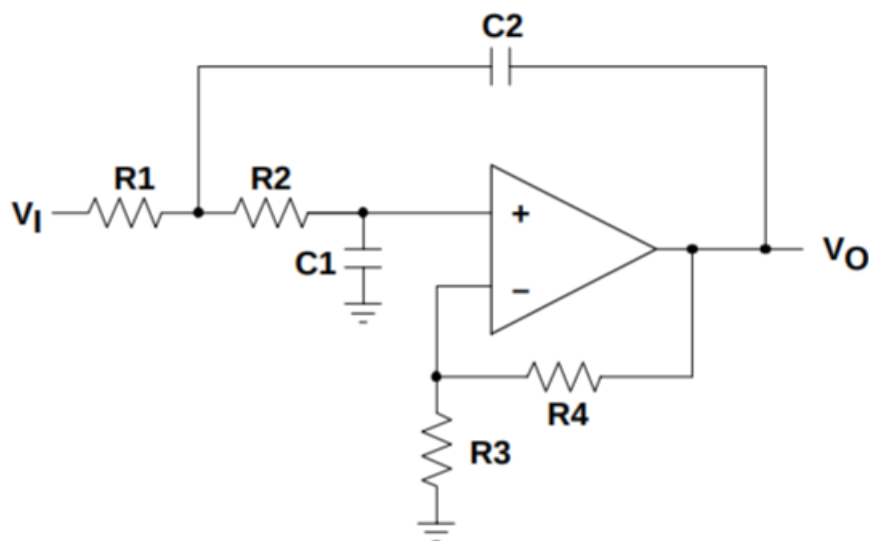


Figura 39 – Sallen-Key Active Low Pass Filter (TEXAS INSTRUMENTS, 1999)

According to (TEXAS INSTRUMENTS, 1999), this filter setup has a cutoff frequency defined by Equation 5.14, quality factor (Q) defined by Equation 5.15, gain (k)

defined by Equation 5.16 and cutoff frequency given by Equation 5.17.

$$H(s) = \frac{k}{s^2 \cdot (R_1 \cdot R_2 \cdot C_1 \cdot C_2) + s \cdot (R_1 \cdot C_1 + R_2 \cdot C_1 + R_1 \cdot C_2 \cdot (1 - k)) + 1} \quad (5.14)$$

$$Q = \frac{\sqrt{R_1 \cdot R_2 \cdot C_1 \cdot C_2}}{R_1 \cdot C_1 + R_2 \cdot C_1 + R_1 \cdot C_2 \cdot (1 - k)} \quad (5.15)$$

$$k = 1 + \frac{R_3}{R_4} \quad (5.16)$$

$$f_c = \frac{1}{2 \cdot \pi \sqrt{R_1 \cdot R_2 \cdot C_1 \cdot C_2}} \quad (5.17)$$

A useful design strategy is to set $R_1 = m \cdot R$, $R_2 = R$, $C_1 = C$ and $C_2 = n \cdot C$. Replacing this values in Equation 5.15 gives a new Equation 5.18.

$$Q = \frac{\sqrt{m \cdot n}}{m + 1 - m \cdot n} \quad (5.18)$$

The quality factor of a Sallen-Key filter is influenced by the gain (k) and defines the dB gain on the cutoff frequency, ideally this factor should be closer as possible to $\frac{\sqrt{2}}{2}$???. Setting an arbitrary value of $m = 2$, the ideal value of $Q = \frac{\sqrt{2}}{2}$ and using Equation 5.18 it is possible to calculate a $n = 0,6771$. It is possible to simplify Equation 5.17 using the same method used to simplify Equation 5.15 to 5.18. Using this method will produce Equation 5.19 that will be used to determine the $R \cdot C$ constant that will be later used to define the resistors and capacitor values of our filter.

$$R \cdot C = \frac{1}{2 \cdot \pi f_c \cdot \sqrt{m \cdot n}} \quad (5.19)$$

Using the previously calculated values for m , n , f_c and Equation 5.19 will give us a $R \cdot C = 3.50115 \cdot 10^{-5}$. Setting an arbitrary value of $R = 10 \cdot 10^3$ will lead to $C = 3.5 \cdot 10^{-9}$. Using the relations: $R_1 = m \cdot R$, $R_2 = R$, $C_1 = C$ and $C_2 = n \cdot C$ and the commercial resistors and capacitors values from (BURGESS, 2015), will produce the following values: $R_1 = 22k\Omega$, $R_2 = 10k\Omega$, $C_1 = 3900pF$ and $C_2 = 2700pF$. If these values are used in Equations 5.15 and 5.17, we will have a quality factor of 0.7359 and a cutoff frequency of 3306.6986kHz, both which are close from the ideal ones.

5.6.4 Complete Circuit

Based on all the previously calculations and on (TEXAS INSTRUMENTS, 1999), the final circuit will be the one in Figure 40. R60 was added to reference the input to

ground and R58 was added to limit the amount of current that can flow from the MCU and the DAC circuit. R55 was added to prevent undesired currents to flow from the circuit output to the OPAMP, R59 is used to reference the output to GND and TZ8 is a TVS used to prevent any ESD or voltage spikes ([LEPKOWSKI; LEPKOWSKI, 2006](#)) to enter the board from the *Speed Reference Output Channel*.

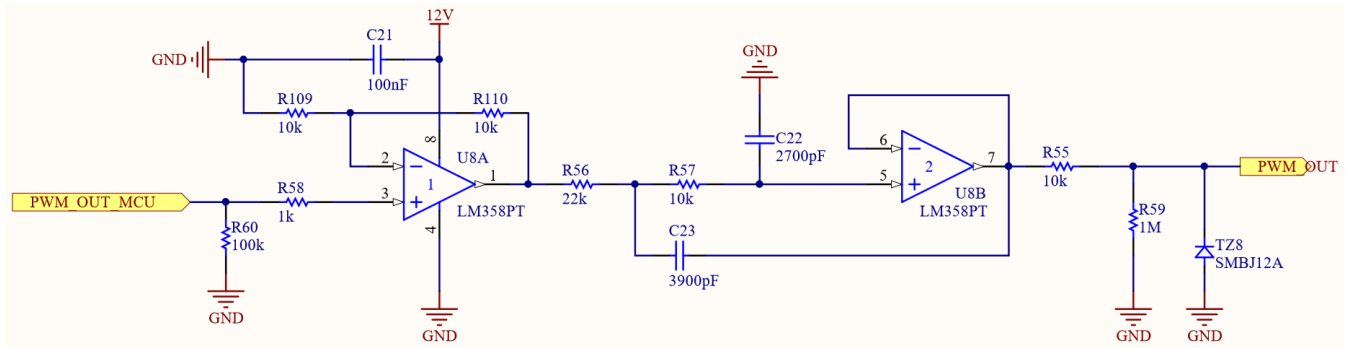


Figura 40 – PWM to Speed Reference Circuit

5.7 Hardware Interface Between Microcontroller and Computer

5.7.1 USB and UART

Nowadays most computers do not have a serial port connector ([EETIMES, 2013](#)), the majority of communications with peripherals are done through USB ports. The chosen microcontroller for this project (as discussed on Section 5.1) does not have USB interface, only UART.

As it was explained in Sections 2.3.8.1 and ??, USB communication protocol is half-duplex, UART protocol is full-duplex though. While USB is composed of a differential pair of data wires, UART has one wire for receiving and another one for transmitting information.

In order to make this project compatible with most of modern computers, there is the need to have a USB to UART converter circuit.

5.7.2 Conversion Circuit

The issue discussed in the previous section is not a new thing, so there are loads of integrated solutions to solve this issue ([RESEARCH, 2008](#)). The chosen one was the Microchip's MCP2221A ([MICROCHIP, 2016](#)), this is a USB to UART/I²C converter chip, it emulates a virtual serial port on the computer, making it possible to communicate with the microcontroller UART ports just using a pair of capacitors and a resistor as Figure 41 shows.

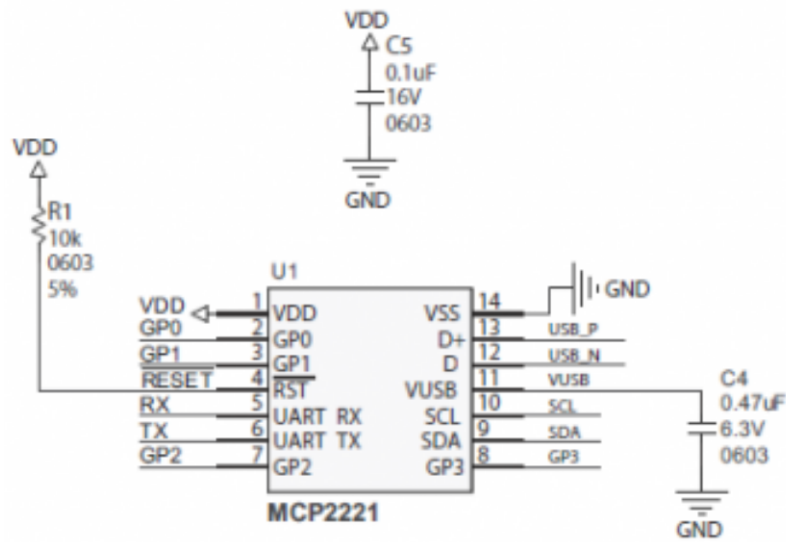


Figura 41 – MCP2221A basic circuit ([MICROCHIP, 2010](#))

This chip already contains a internal 3V3 LDO in order to convert the 5V TTL level to the 3V3 standard level for USB data lines. The voltage supply for this IC is being supplied by the voltage from the USB cable because there is no need to keep this IC turned on when the USB cable is not connected.

5.7.3 Circuit Protection

In order to ensure reliability on the circuit, ESD protection is needed, every connection between the circuit board and the outside world has the potential to pick unwanted noise and ESD, and USB is not excluded from that problem ([LITTLELFUSE, 2010](#)).

High-frequency noise could be filtered using low pass filters in both data lines using discrete passive components. Moreover, the data lines could be protected from ESD using discrete TVS. The number of discrete componentes needed to filter and protect the lines makes a discrete-component-solution unpractical, expensive and spacious. Nowadays there are unexpensive integrated solutions in order to save space on the PCB, one of them is the ON Semiconductor STF202-22T1G. This IC is a USB Filter with ESD protection, as the datasheet ([ON SEMICONDUCTOR, 2012](#)) says: "*This device is designed for applications requiring Line Termination, EMI filtering and ESD protection*", making it more than ideal for this project. The STF202-22T1G internal circuit can be seen on Figure 42.

5.7.4 Complete Circuit

For the final circuit the STF202-22T1G was connected before the MCP2221A in order to protect and filter the data lines. Moreover, two external resistors were added

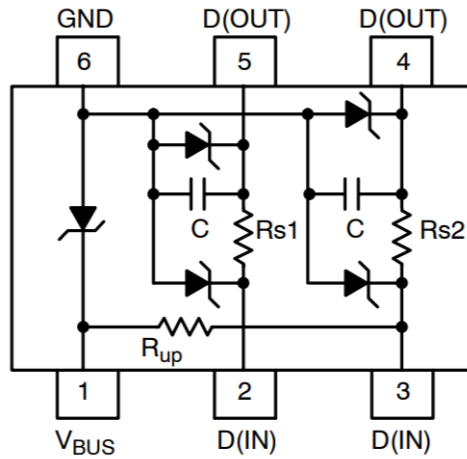


Figura 42 – STF202-22T1G Internal Circuit ([ONSEMI, 2012](#))

to the serial communication lines (based on the Arduino Rev3 Schematic ([ARDUINO, 2010](#))). Figure 43 contains the final circuit.

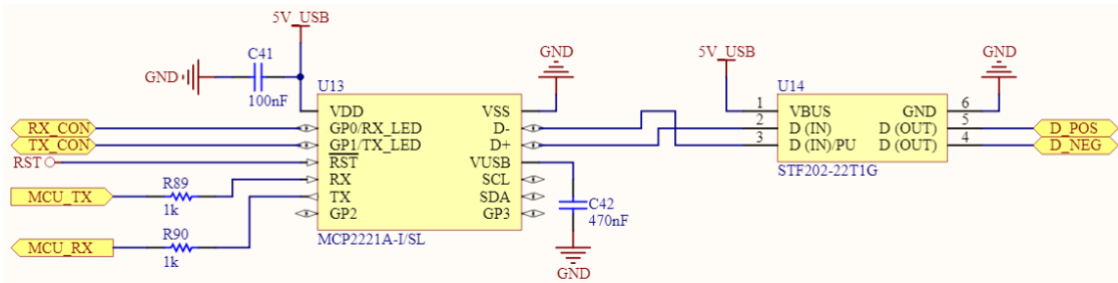


Figura 43 – USB/UART Converter Circuit ([GUIMARAES, 2018y](#))

The *TX CON* and *RX CON* lines are used in other to indicate when the MCP2221A chip is repectively transmitting or receiving data. This lines drain current when data is transmitted or received and are used to blink LEDs in other parts of the circuit board.

Both capacitors are decoupling capacitors for the 5V and 3V3 lines.

5.8 Digital Interfaces

All sensoring data was obtained using analog channels, some digital channels will be reserved on the board in order to provide another type of sensing and control.

5.8.1 Digital Outputs

5.8.1.1 Low-side Driver

Item 11 from Section 4.3 states that the system must have a digital output channel to control a relay (check section ??). According to ([SONGLE, 2018](#)), a standard 5V (MCU operating voltage, Section 5.1.1) relay will have a nominal current of 89.3mA, the

microcontroller's datasheet ([MICROCHIP, 2018](#)) says that the maximum DC current per I/O pin is 40mA though. Hence it is not possible to activate a relay connected directly to a MCU's I/O pin.

In order to solve this a relay driver circuit needs to be used, in this case a low side mosfet driver similar to the one from Figure ([ELECTRONICS TUTORIALS, 2018](#)) will be used.

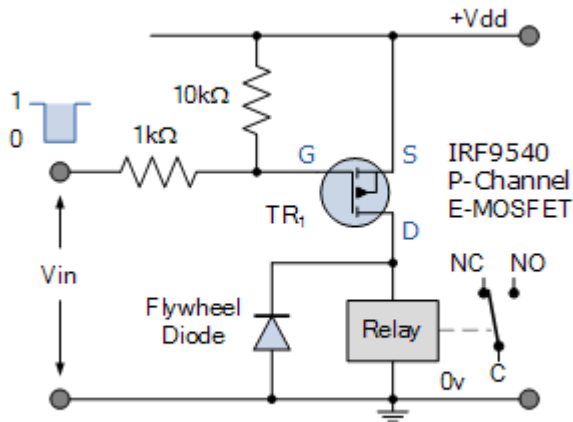


Figura 44 – PMOS low side driver ([ELECTRONICS TUTORIALS, 2018](#))

This is a low-side driver, when the PMOS is submitted to a high logic level (5V) in its gate it will enter on the cutoff region and will not conduct current, hence not activating the relay. On the other hand, when a low logic level (0V) is applied to the device's gate it will enter the saturation region and will conduct current, hence activating the relay (check Section ??).

5.8.1.2 Digital Output Circuit

The digital output circuit will be very similar to the one from Figure 44. The power supply connected to the mosfet will be the 12V source (check Section 5.10.1.2), on the PMOS drain there will be a TVS diode (check Section 2.3.9.2) with a standoff voltage of 12V (SMBJ12A from *Littlefuse* ([LITTLEFUSE, 2015](#))), this TVS will protect the PMOS from reverse current and from overvoltages. Using 12V instead of 5V provides lower current and by Ohm's Law the voltage drop is proportional to the current flowing through a load. So increasing this voltage can ensure that the voltage drop during the connection to the relay will be lower. Figure 45 show the equivalent circuit for the digital output.

The selected PMOS is the NDS332P from *Fairchild* ([FAIRCHILD, 1997](#)), it has a maximum operating continuos current of 1A, maximum gate threshold voltage of 1V, maximum drain-source voltage of 20V and maximum gate source voltage of $\pm 8V$. It is

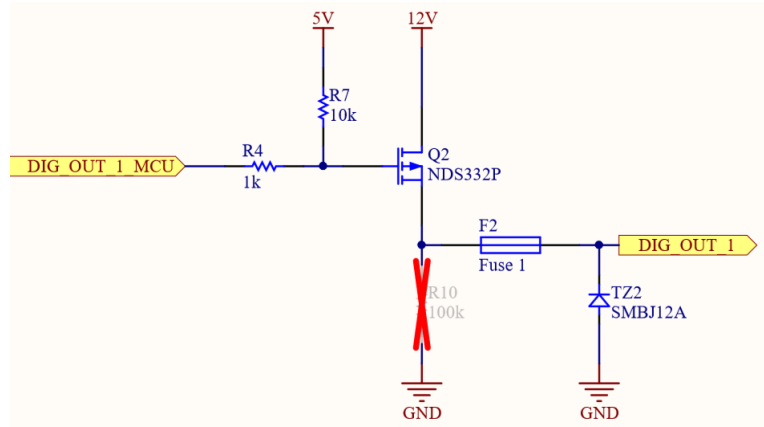


Figura 45 – Digital Output Circuit (GUIMARAES, 2018j)

adequate for this purpose. Resistor R4 is used to limit the magnitude of the current spike that can occur when a driver switches fast and has to charge or discharge a large gate capacitance. Resistor R7 is a pull-up for the gate, it will ensure that the PMOS will be in cutoff region if there is no input for the MCU. Resistor R10 is optional, for activating relays it is not needed, but other loads may require a pull-down, that is why it was placed on the PMOS drain. It was decided to keep any relay out of the board to save space. Moreover, keeping the relay out of the board gives room for using this digital output for other purposes. Fuse F2 is used to limit the current on the TVS in a scenario in which the TVS reaches its clamping voltage.

5.8.2 Digital Inputs

This project does not have any requirement for digital inputs. However, in order to make the project more versatile for the future, it was decided to keep the space on the layout for soldering components to implement digital inputs. Figure 46 show the circuit to interface the digital inputs.

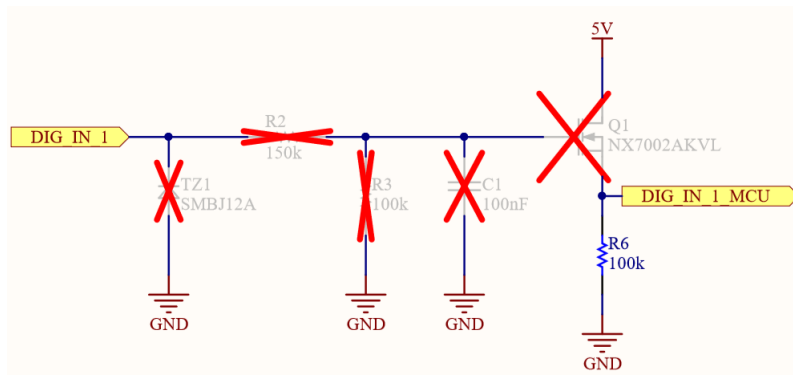


Figura 46 – Digital Input Circuit (GUIMARAES, 2018i)

The chosen NMOS was the NX7002AK from *Nexperia* (NEXPERIA, 2015). This is a extremely versatile NMOS, it has a maximum drain source voltage of 60V, maximum

gate-source voltage of $\pm 20V$ and maximum drain current of $300mA$. This circuit is basically a buffer, it is used just to convert the state of the input signal to the MCU voltage limits.

This circuit is adjustable to different input voltages (V_{IN}), R_2 and R_3 creates a voltage divider and must be chosen according to Equation 5.20.

$$2.1 < \frac{R_3}{R_2 + R_3} \cdot V_{IN} < 5V \quad (5.20)$$

For a $12V$ voltage input as an example, using $R_2 = 150k\Omega$ and $R_3 = 100k\Omega$ will produce a voltage at the gate equal to $4.8V$, meeting the limits from Equation 5.20.

This circuit also has a LPF formed by the combination of R_2 and C_1 , it is used to filter any noise from the input. Equation 5.21 is used to calculate the center frequency of this filter.

$$f_C = \frac{1}{2 \cdot \pi \cdot R_2 \cdot C_1} \quad (5.21)$$

The center frequency f_C must be greater than the maximum input signal frequency to ensure operation.

Finally, TZ1 is a TVS diode, it must be a TVS diode with a standoff voltage equal to the maximum input voltage. The layout was made to fit a SMBJ12CA from *Littlefuse* ([LITTLEFUSE, 2015](#)), this device has the DO-214AB, any device with the same footprint can be soldered on its pads.

5.9 LED driver circuits

A keen aspect of a user operated system is the capability of the system to show useful and relevant feedback data to the user ([LAUREL; MOUNTFORD, 1990](#)). This system will have a high-layer software GUI in order to show processed data to the user as it was defined in Section 4.4 in Item 6. However, some direct hardware feedback is also useful, in this project the main hardware feature to show feedback are LEDs.

The idea is to have LEDs that will indicate in which stage of operation the system is. It was decided to make a separate LED circuit block in order to make changes on LED's types independent from the circuit they are giving feedback. The following sections will show and explain each functionality of the system that will have LED feedback. All LEDs will be directly connect to the power supplies and just their cathodes will be connect to the drivers circuit.

5.9.1 Serial Communication Leds

One important feature of the system is it's serial communication, this is the only way the MCU will communicate with the outside world, as was explained in Section 5.7. In Section 5.7.4 it was said that nets *TX_CON* and *RX_CON* from Figure 43 are open drain input when the system is respectively transmitting and receiving serial data and high-impedance ports when they are not communicating.

The system will have a LED to indicate transmission and another for reception of serial data, the solution to drive this LEDs will be the NTZD3152PT1H from *ON Semiconductor* ([ON SEMICONDUCTOR, 2016b](#)). This is a dual P-Channel mosfet in one IC with very low maximum *Gate Threshold Voltage* ($V_{GS} = -1V$), as the USB/UART feedback pins drains current when communicating, by connecting theses pins to the Gate of these PMOS it will be possible to control when the LEDs will be turned on. Figure 47 show this circuit configuration implemented.

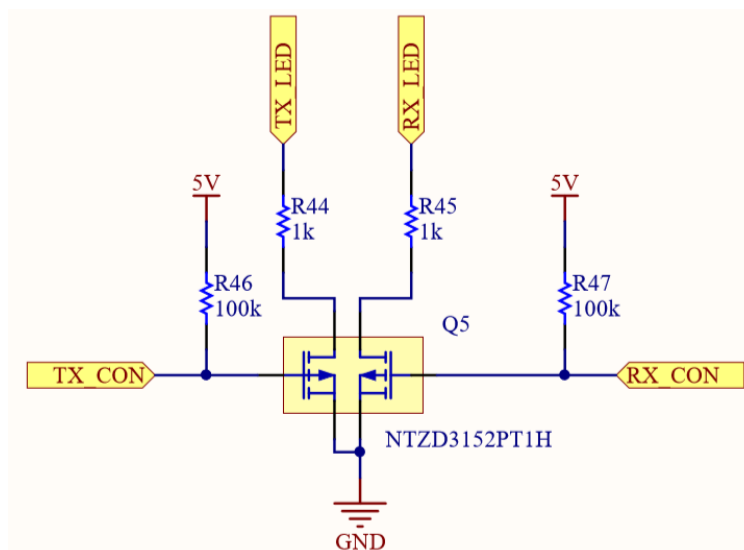


Figura 47 – UART feedback LEDs driver ([GUIMARAES, 2018x](#))

The resistors R44 and R45 are current limiting resistors, their value may vary with the chosen LEDs, so this $1\text{k}\Omega$ value is not necessarily fixed. Resistors R46 and R47 have a relatively bigger resistance of $100\text{k}\Omega$ because they are pull-up resistors, they do not control current on that port, they were used just to guarantee that the voltage on the gate of the PMOS is higher than $1V$ (Gate-Source Threshold Voltage of the transistors according to the NTZD3152PT1H datasheet ([ON SEMICONDUCTOR, 2016b](#))) when the UART/USB IC is turned off (in Section 5.7.2 a possible scenario that the IC is not turned on is presented).

5.9.2 Sensor Disconnection and Acquisition Leds

5.9.2.1 Sensor Disconnection

As it was defined in Item 14 from Section 4.3, the system needs to be able to detect when a sensor is disconnected. Moreover, every sensor in this project has a net that goes to high-logic level (5V, according to Section ssec:the-choosen-mcu) and this signal can be used to activate LEDS to indicate wheter each sensor is connected or not.

5.9.2.2 Acquisition

The major funcition of this project is to make a acquisition system, so the major activity from the MCU is acquiring data. So, to give some feedback to the user a LED was reserved just for the MCU to indicate if the system is acquiring data or not. The control of this LED is controlled directly from the MCU, so if any extra functionality is desired to be implement, no hardware change will need to be carried out, just code.

5.9.2.3 Sensor Disconnection and Acquisition LED driver

As the sensor disconnection LEDs and the acquisition LED are all activated when high-logic level is present on their respective activation nets, the same solution can be applied. The choosen alternative to drive this LEDs is the TPL7407LAPWR from *Texas Instruments* ([TEXAS INSTRUMENTS, 2017](#)), it is a low-side driver than has a high-logic voltage level of 1.5V and a low-level voltage of 0.9V. The driver drains current when a high logic level is present at each channels activation port. This driver has seven channels and can drain up to 600mA per channel, making it more than ideal to drive LEDs. As this maximum drain current is quite high, if other devices such as relays and sirens can be connected instead of the LEDs without changing the hardware project, just changing the current limiting resistors. Figure 48 shows the circuit to drive theese LEDs, resistors R30 to R36 are the current limiting resistors mentioned above and resistors R37 to R43 pull-down resistors used just to guarantee that the logic level will remain low (driver not draining current) if there is no definitive voltage input. The capacitor C10 is just a decoupling capacitor for the IC power supply recommended by the datasheet ([TEXAS INSTRUMENTS, 2017](#)).

5.9.3 Power Supplies Voltage LEDs

This is by far the simplest LED circuit, it is just current limiting resistors connected in series to the LEDs as Figure 49 shows.

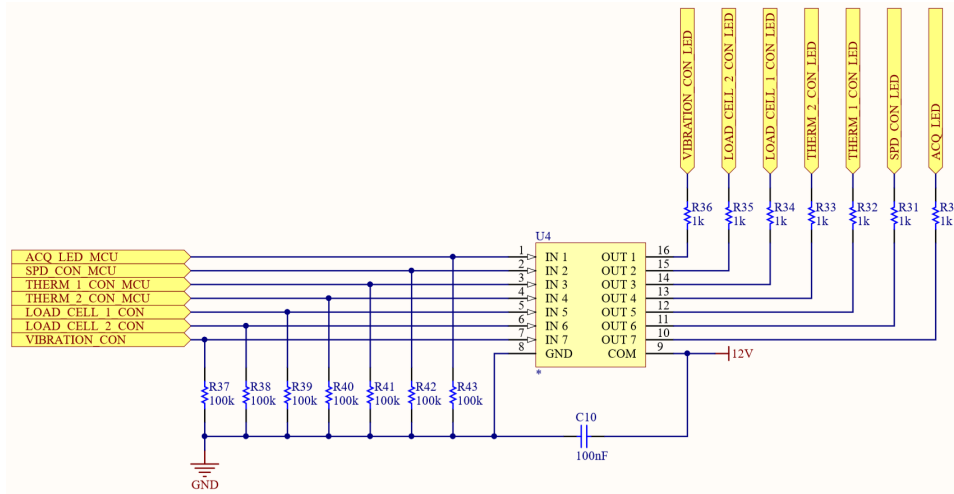


Figura 48 – Sensor Disconnection and Acquisition LED driver circuit ([GUIMARAES, 2018t](#))

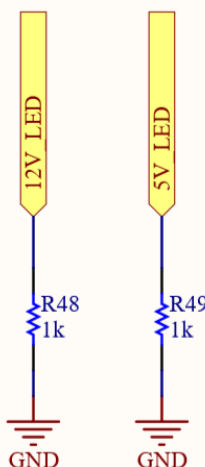


Figura 49 – Power Supplies Voltage LEDs Circuit ([GUIMARAES, 2018r](#))

5.10 Voltage Supplies

5.10.1 Power Supplies

In order to avoid any interference of the AC line, this project will work with a DC voltage input and any other necessary voltages will be acquired from this higher input voltage supply. There are many different types of voltage regulators, nowadays the most common DC/DC being switching regulators. They are more efficient than linear regulators and consequently they waste less heat, the downside is the cost (due to their consequently) and that they tend to have some ripple at the output ([SCHWEBER, 2017](#)). However, as this project does not aim radical cost management and as this ripple can be filtered, this type of voltage regulator was chosen for this project.

5.10.1.1 5V Supply

Most of the chosen components for this project were chosen so they would be capable to work with single-supply of 5V. The chosen voltage regulator for the 5V supply was the TL2575-05 from *Texas Instruments* ([TEXAS INSTRUMENTS, 2014](#)), it has a output up to 1A, voltage drop over 2V and typical efficiency of 88%. Figure 50 shows the circuit used for the 5V supply.

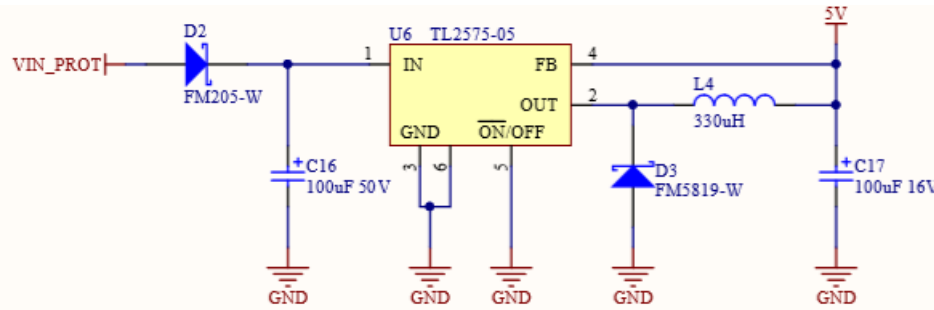


Figura 50 – 5V Power Supply Circuit ([GUIMARAES, 2018e](#))

The diode FM205-W from *Rectron Semiconductor* ([RECTRON SEMICONDUCTOR, 2010a](#)) is used to protect the input of converter from inverse polarity. This diode has a maximum current of 2A, twice the maximum current output of the regulator, so it will not interfere with the input current. Inductor L4 is fundamental for the device to work according to the datasheet. Capacitors C16 and C17 are bypass capacitors recommended by the converter's datasheet. Diode D3 is a catch diode used to protect the converter from flyback currents from the inductor, the datasheet only specifies it should be a Schottky diode with maximum current at least the same as the maximum output current of the converter (1A). The chosen diode is FM5819-W from *Rectron Semiconductor* ([RECTRON SEMICONDUCTOR, 2010b](#)).

According to the datasheet this circuit has an input voltage from 7V to 40V.

5.10.1.2 12V Supply

For the 12V supply the chosen regulator was LM2574-12 from *Texas Instruments* ([TEXAS INSTRUMENTS, 2016](#)), it has a output up to 500mA, voltage drop of 2V, and typical efficiency of 88%. Figure 51 shows the circuit used for the 12V supply.

The diode FM5819-W from *Rectron Semiconductor* ([RECTRON SEMICONDUCTOR, 2010b](#)) is used to protect the input of converter from inverse polarity. This diode has a maximum current of 1A, twice the maximum current output of the regulator, so it will not interfere with the input current. Inductor L5 is fundamental for the device to work according to the datasheet. Capacitors C18 and C19 are bypass capacitors recommended by the converter's datasheet. Diode D5 is a catch diode used to protect the converter from flyback currents from the inductor, the datasheet only specifies it

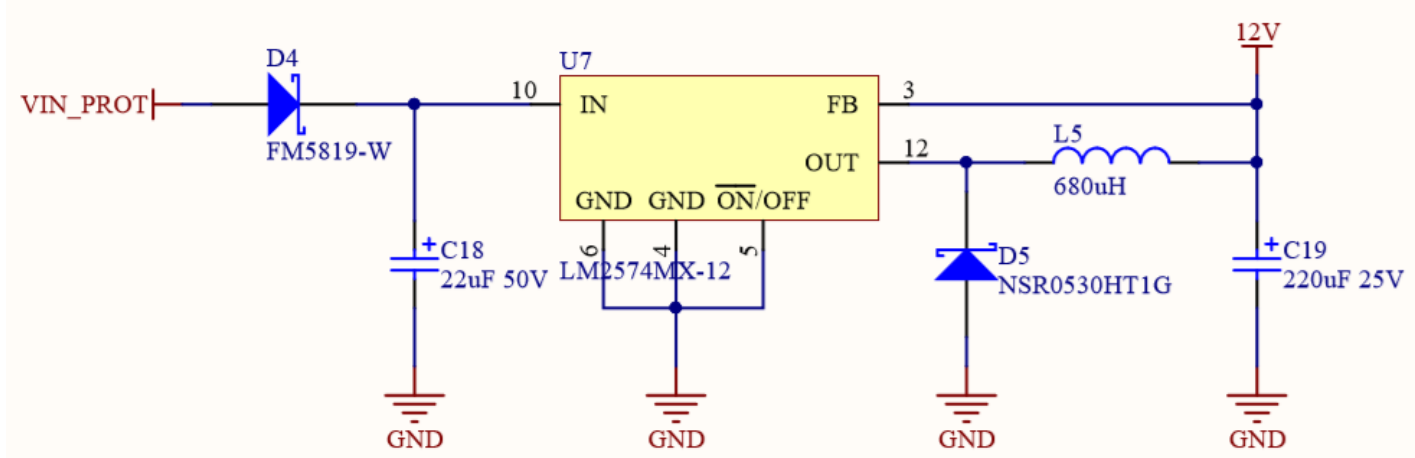


Figura 51 – 12V Power Supply Circuit ([GUIMARAES, 2018b](#))

should be a Schottky diode with maximum current at least the same as the maximum output current of the converter (0.5A). The chosen diode is NSR0530HT1G from *ON Semiconductor* ([ON SEMICONDUCTOR, 2016a](#)).

According to the datasheet, this circuit has an input voltage from 14V to 40V.

5.10.1.3 Voltage Input Protection

The voltage that goes to each of the switching voltage regulators from Sections [5.10.1.2](#) and [5.10.1.1](#) is only protected against inverse polarity but not to overvoltage and overcurrent. Figure [52](#) shows the circuit used to protect the power supplies.

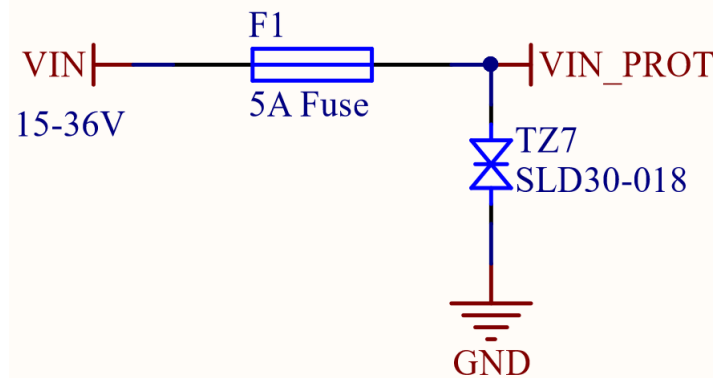


Figura 52 – Voltage Input Protection Circuit ([GUIMARAES, 2018z](#))

TZ7 is a TVS diode used to protect the circuit against overvoltages. The chosen TVS is the SLD24-018, it has a standoff voltage of 24V and a maximum clamping voltage of 38.9 volts (check Section [2.3.9.2.2](#)). Using this TVS limits the input voltage from 14-24V, in the other hand it ensures protection for the voltage regulators. F1 is a fuse with 5A rating, it will not protect the circuit from fast transients, this will be carried out by the TVS. It has the function to open the circuit when the TVS reaches its clamping voltage and protect the TVS.

5.10.2 Voltage References

In this project any power supply that the precision and stability of the output voltage is more concerning than the maximum output current will be called a voltage reference.

5.10.2.1 10V Reference

As it was explained in Section 5.3.2, this voltage reference will be used to excite the load cells sensors of this project. The chosen component for this reference was the LM78L10 from *Microchip* ([HTCKOREA, 2014](#)). According to the datasheet, this voltage reference has a typical tolerance of $\pm 0.2\%$ and has maximum operating output current of 100mA. Load cells have a typical bridge resistance from 350ω to $1k\omega$ ([GMI, 2014](#)). It was defined on this project requirements on Item 9 in Section 4.3 that the system must have two brake pressure acquisition channels. Hence, having two load cells with 350ω bridge resistance and 10V excitation, 68mA of current would be needed, 100mA from the voltage reference would be suitable. Figure 53 shows the reference circuit.

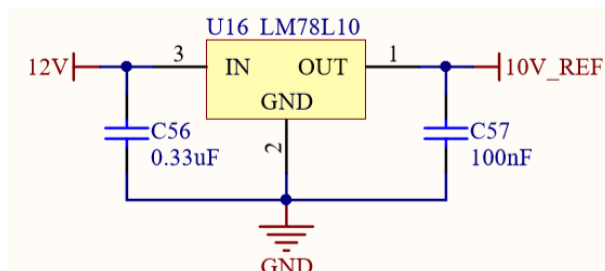


Figura 53 – 10V voltage reference circuit ([GUIMARAES, 2018a](#))

The device's datasheet recommends using two decoupling capacitors, one in the input and other in the output with the given values from Figure 53.

5.10.2.2 4V5 Reference

As said in Section 5.2.4, the sensor detection circuit needs a 4V5 voltage reference for the comparator. This is achieved using the MAX6107EUR+T from *Maxim Integrated* ([MAXIM, 2002](#)). This is a precise 4V5 voltage reference and according to the datasheet it has a tolerance of $\pm 0.4\%$ and a maximum operating output current of 5mA. Figure 54 shows the circuit for the 4V5 voltage reference.

According to the datasheet the only needed extra component is a decoupling capacitor at the output.

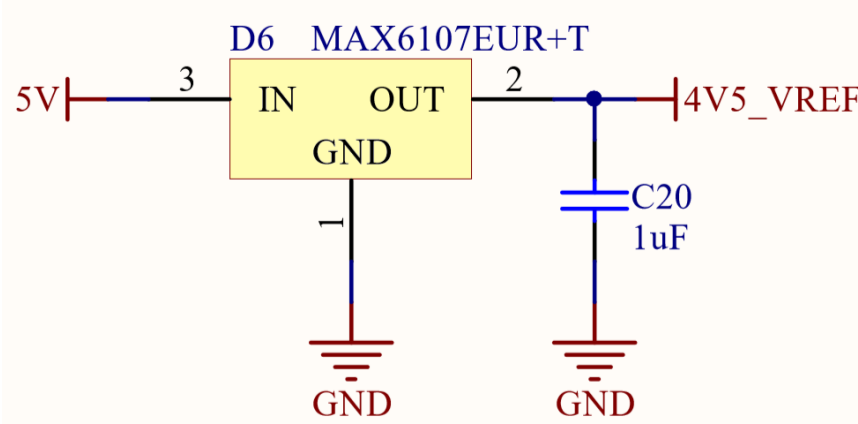


Figura 54 – 4V5 voltage reference circuit (GUIMARAES, 2018d)

5.10.2.3 1V Reference

The 1V reference from the circuit of Section 5.4.1 is achieved using the ADR510ARTZ from *Analog Devices* (ANALOG DEVICES, 2007). This is a 1V precision voltage reference with a tolerance of $\pm 0.35\%$ and maximum operating output current of 10mA. Figure 55 shows the typical circuit using this voltage reference.

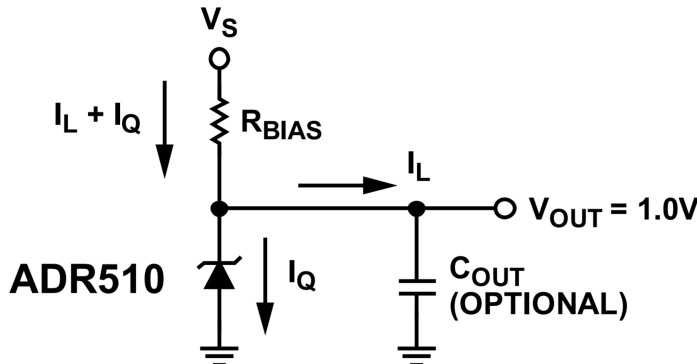


Figura 55 – ADR510 Typical Operating Circuit (ANALOG DEVICES, 2018)

The only external component needed is a bias resistor which can be calculated using ?? (ANALOG DEVICES, 2007).

$$R_{BIAS} = \frac{V_S - V_{OUT}}{I_L - I_Q} \quad (5.22)$$

The used V_S *Voltage Supply* will be the 5V obtained in the circuit from Figure 50 in Section 5.10.1.1. According to the datasheet, the minimum operating voltage (I_Q in this case) is 100uA. Moreover, V_{OUT} is naturally 1V5. The minimum bias current (load current I_L) is of 500nA (according to the IC that used the 1V reference (TEXAS INSTRUMENTS, 2000)). Hence, any value of resistance that guarantees that the current that flows through the regulator is less than 10mA is acceptable.

Using a $1\text{k}\Omega$ resistor a current of 4mA can be achieved. Figure 56 shows the circuit for the 1V reference, the capacitor is just a decoupling capacitor recommended by the datasheet.

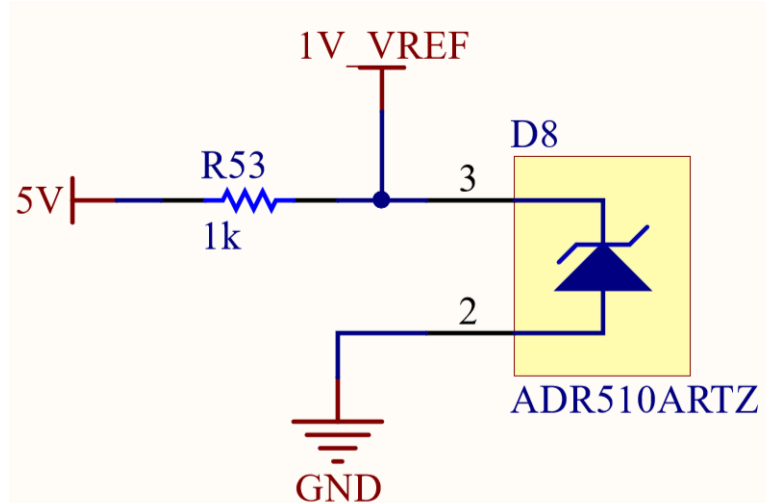


Figura 56 – 1V voltage reference circuit (GUIMARAES, 2018c)

5.11 Printed Circuit Board

5.11.1 PCB Design

The PCB layout for this project was developed using the Altium Designer 17 Software (ALTIUM..., 2017). During the layout design some things were considered to ensure functionality:

- Instead of soldering the connectors directly to the board, empty pads for soldering wires were placed, this way connectors can be chosen later and fixed on the board housing instead of on the board.
- Protection devices such as TVS, Fuses and current limiting resistors were placed very close from the terminal pads in order to prevent cooper tracks to be damaged.
- SMT (Surface Mount Technology) was a priority during design in order to save space on the board.
- Cooper tracks width: The width of every track was chosen according to the electrical signal it is carrying.

Figures 57 and 58 shows respectively the top and the bottom side of the board during design, there are almost no cooperless areas, most of empty spaces were replaced by GND planes in order to make the board corrosion faster and to make a stronger gnd

connection. Other interesting fact is the width of power supply tracks, it is easy to notice they are much more thick than normal signal tracks. The board dimensions are 70mm x 65mm.

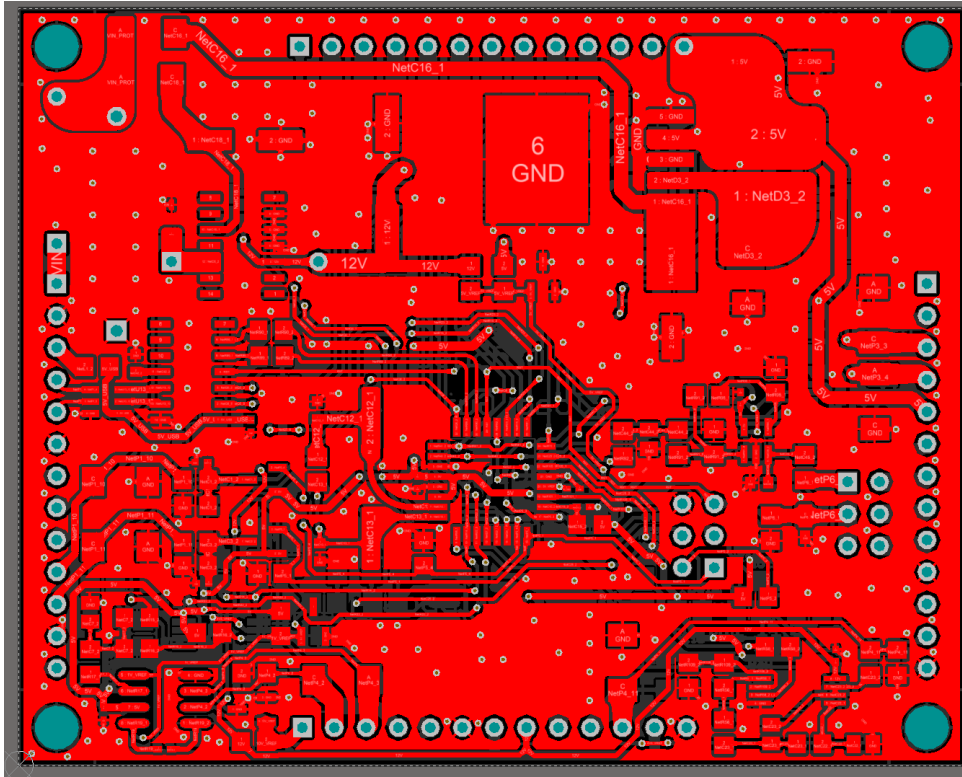


Figura 57 – PCB Top 2D View ([GUIMARAES, 2018p](#))

5.11.2 PCB Assembly

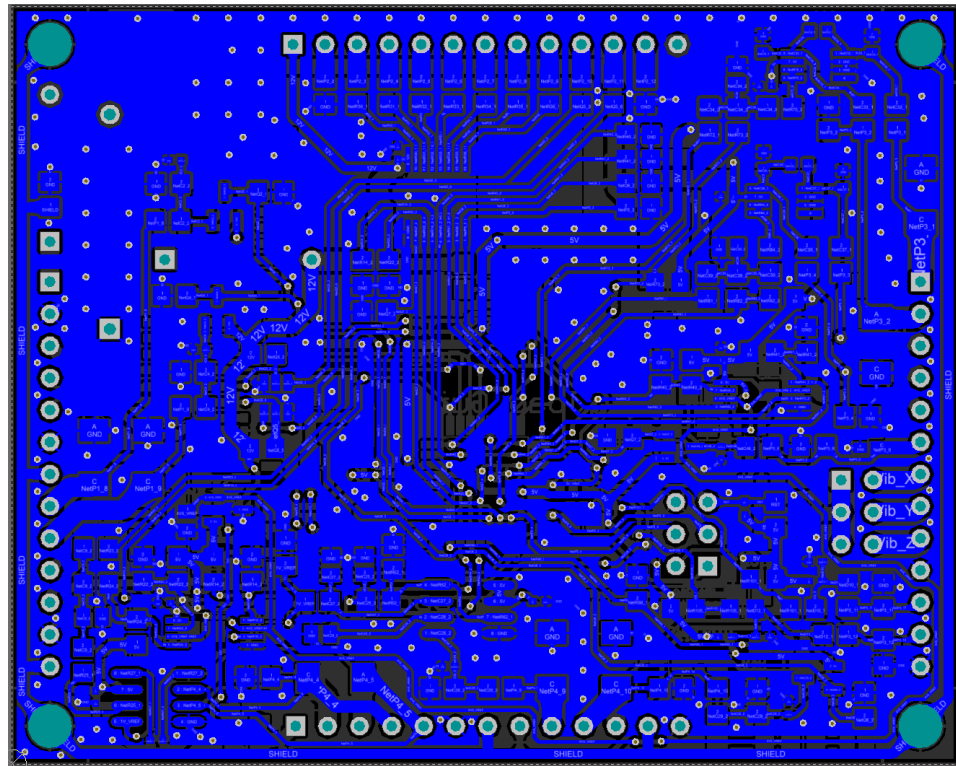


Figura 58 – PCB Bottom 2D View (GUIMARAES, 2018o)

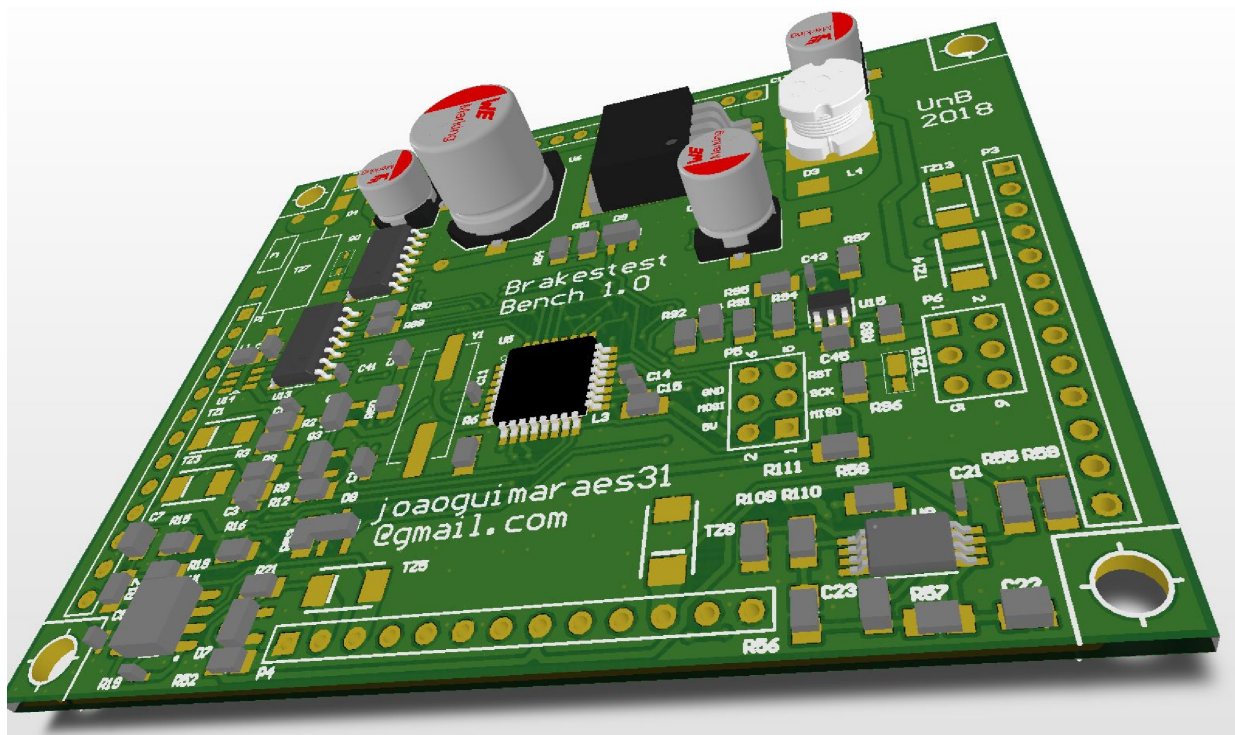


Figura 59 – PCB 3D View (GUIMARAES, 2018n)

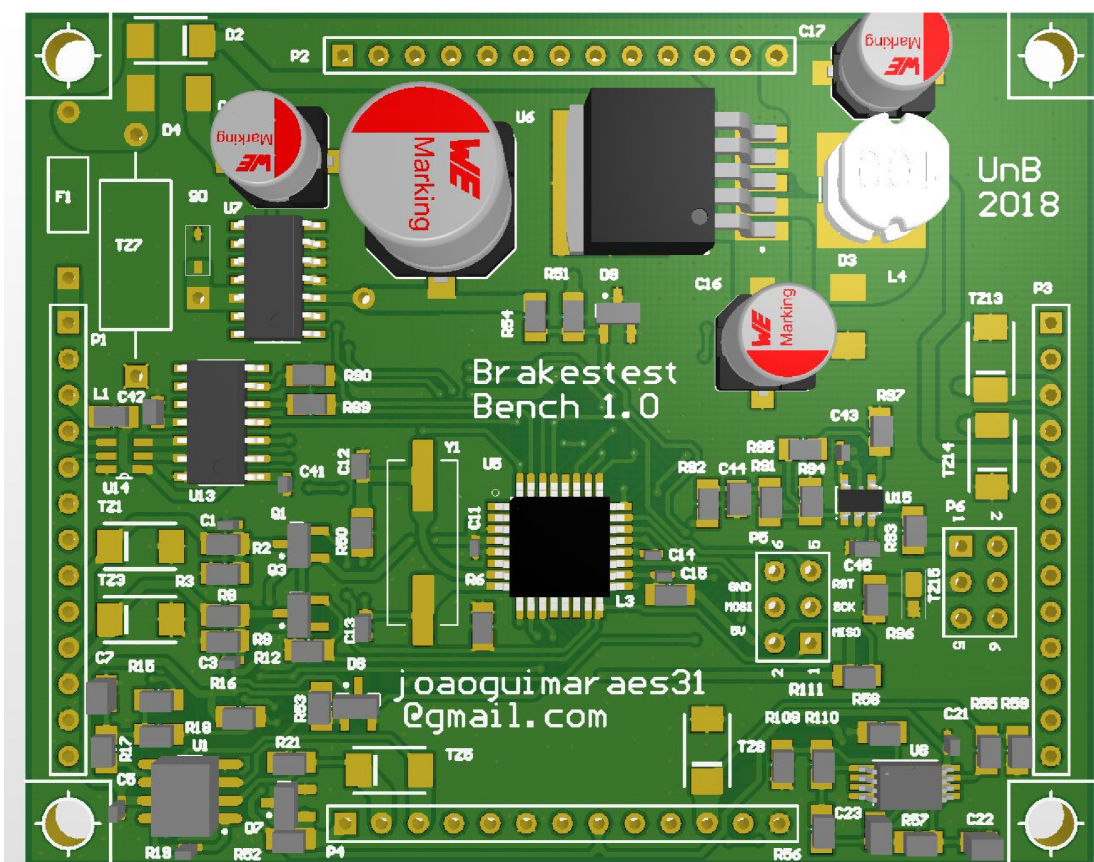


Figura 60 – PCB Top 3D View ([GUIMARAES, 2018q](#))

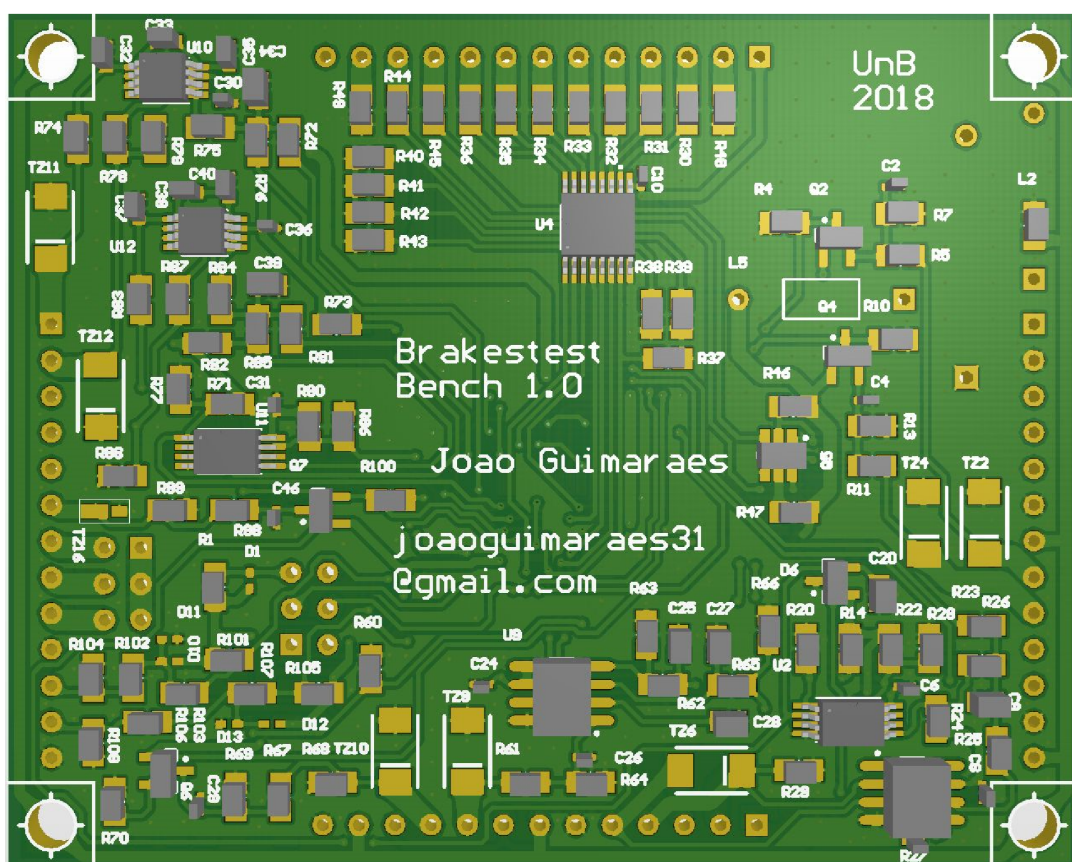


Figura 61 – PCB Bottom 3D View

6 Software Project

This project has two layers of software that communicates with each other, the microcontroller program and a program executing in a computer. There were some functionalities that could be implemented on either layers, as the computer hardware is obviously superior than the microcontroller hardware everything that could be implemented in either layers was implemented in the computer software.

6.1 Microcontroller Code

6.1.1 Microcontroller programming basics

Microcontrollers were traditionally programmed using Assembly language, nowadays we have a different scenario though. With the advancement of compilers, today it is most common to write the code for a microcontroller in C language and let the compiler translate it to a binary assembly format ([MAZIDI; NAIMI; NAIMI, 2010](#)). A convenient reason to use C is that it is one of the most efficient programming languages in terms of execution speed, this happens because it was designed to efficiently map typical machine instructions ([KERNIGHAN; RITCHIE, 2006](#)), so considering real-time constraints and other execution constraints in microcontrollers it is a excellent fit.

A microcontroller code is composed basically of two parts:

- *Setup*: This part of the code is only executed once, as the name may indicate, it is used to set properties, configure timers, inputs and other features of the hardware.
- *Loop*: This part of the code is executed continuously or until some condition is reached.

Other important component of a microcontroller code are interruptions. It is possible to interrupt the standard execution of a program when an event happens, or as it is more common to say, when an event triggers a interruption. This event may be a timer overflow, a event triggered by an input change among other things. Interrupt routines are really useful when working with instrumentation and timers, because using interruptions it is feasible to meet real-time requirements in a project ([MUKARO; CARELSE, 1999](#)).

6.1.2 Microcontroller Code Map

The Figure [62](#) show a functional map of the microcontroller code that can be found entirely in Appendix [A.1](#).

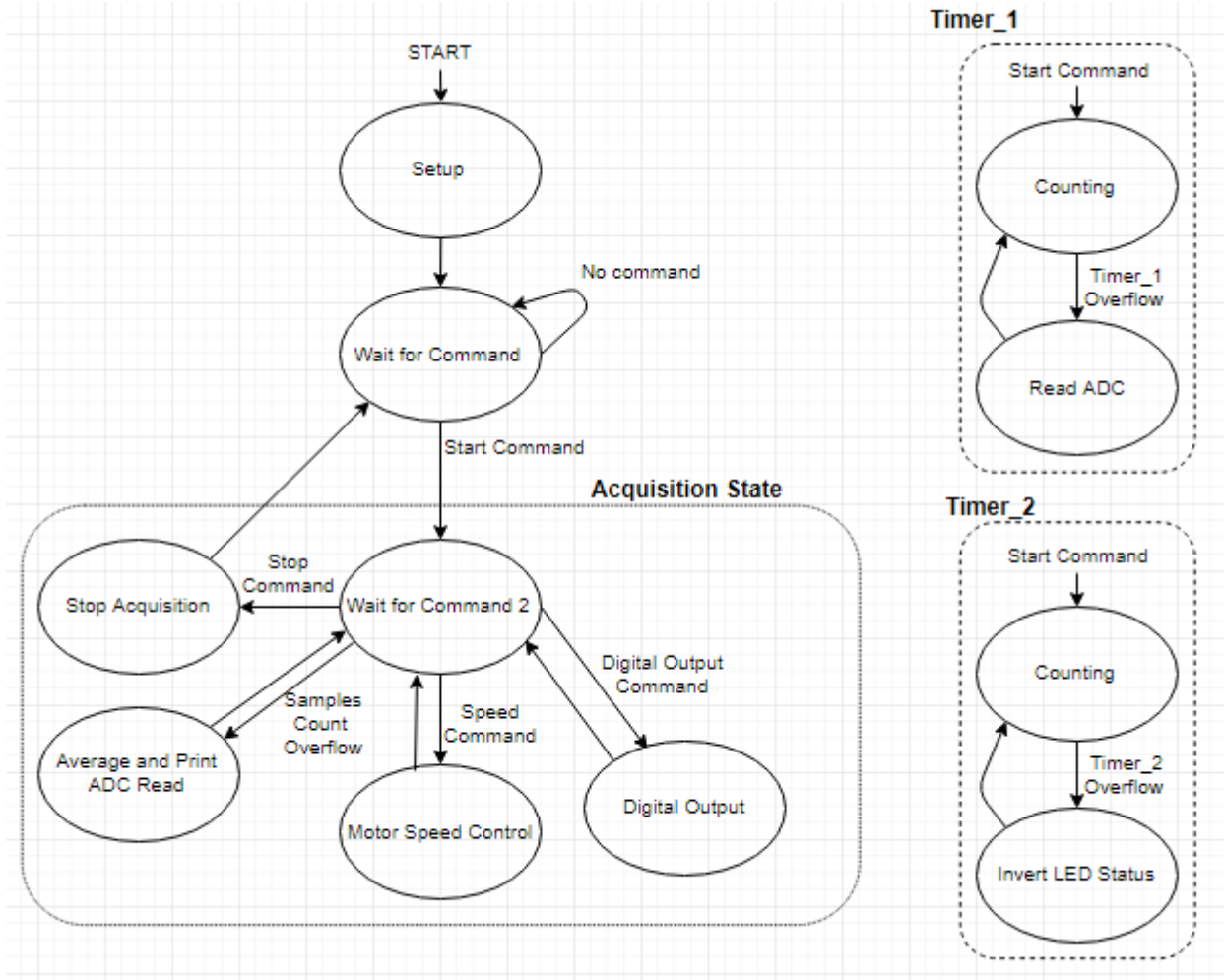


Figura 62 – Microcontroller Code Map (GUIMARAES, 2017b)

As soon as the microcontroller is turned on it enters in the *Setup*, on this part the following things are setted:

- *Timer_1*: Timer_1 max count value is setted and a interruption service routine is appointed.
- *Timer_2*: Same thing done for Timer_1 is done for Timer_2.
- *Serial Port*: The serial port baud rate is defined and the serial port is opened.
- *Port definitions*: The I/O ports are defined as inputs (high impedance) or as outputs (low impedance).

After setting up the code enters in a state in which it waits for a *Start Command* from the computer. This command starts Timer_1 and makes the code enter the *Acquisition State*. Everytime Timer_1 finishes its count a ISR will be triggered, all the analog inputs will be read (sampled) and stored followed by the timer restarting its counting

process. The *Start Command* also starts Timer_2, this timer operates the same way as Timer_1, the difference is that its ISR will only toggle the acquisition LED state.

In the acquisition state, if a *Digital Output Command* is received the code will decrypt this command (this is actually a group of possible commands) and set the digital outputs according to the decrypted message.

A received *Speed Command* instruction will make the code behave in a similar way than *Digital Output Command*, code will decrypt the command (it also is a group of possible commands) and output a corresponding PWM value in the analog output port in order to control the electric motor speed.

During all the *Acquisition State*, everytime Timer_1 ISR does a presetted number of reads, the code makes an average of thoose reads and will send them through the serial port to the computer. After that the code will reset the number of read samples and start to count samples again. Another useful feature is that during all the *Acquisition State* the code is also continuosly reading the microcontroller digital inputs, this inputs are used to detect if a sensor is not connected, if any of the sensors is considered to be disconnected instead of sending the analog reading from the respective sensor input, the code will send a “-1” value to the computer. This way the computer software that the one responsible for treating this event and take the appropriate action.

The code will exit the *Acquisition State* if the computer sends a *Stop Command*. This will also set all digital outputs to a low logic level and will disable both timers interruption service routines. The code will go back to the *Wait for Command* state and wait for a *Start Command* to restart acquisition.

This code architecture was designed in order to make the microcontroller code as simples as possible in order to make execution faster to avoid jeopardizing the real-time constrain. The same code is used during brake tests, during acquisition and any other process. As mentioned before, all the heavy data processing is done by the computer software.

6.2 Computer Software

References

- ADAFRUIT. *Adafruit ADXL335 - 5V ready*. 2016. Cited in page 71.
- ALTER, D. M. *Using PWM Output as a Digital-to-Analog Converter on a TMS320F280x Digital Signal Controller*. [S.l.], 2008. Cited 2 times in page 42 and 75.
- ALTIUM Designer 17. 2017. Disponível em: <<https://www.altium.com/s>>. Cited in page 91.
- ANALOG DEVICES. *ADR510: 1.0 V Precision Low Noise Shunt Voltage Reference*. [S.l.], 2007. Cited in page 90.
- ANALOG DEVICES. *AD8495: Precision Thermocouple Amplifiers with Cold Junction Compensation*. [S.l.], 2010. Cited 3 times in page 60, 61, and 62.
- ANALOG DEVICES. *1ADR510 Typical Operating Circuit*. 2018. Cited 2 times in page 14 and 90.
- ANDREWS, R. *Caution! Your ADC may be only as good as its power supply*. 2015. Disponível em: <https://e2e.ti.com/blogs_/archives/b/precisionhub/archive/2015/05/22/caution-your-adc-may-be-only-as-good-as-its-power-supply>. Cited in page 59.
- ARDUINO. *Arduino REV3 Schematic*. 2010. Cited 2 times in page 59 and 80.
- AUTODESK. *What Differential Signaling Is All About*. 2017. Disponível em: <<https://www.autodesk.com/products/eagle/blog/wp-content/uploads/2017/06/07c0be30313.gif>>. Cited 2 times in page 13 and 44.
- BARTZ, M.; ZHAKSILIKOV, M.; OGAMI, K. Y. *Data driven method and system for monitoring hardware resource usage for programming an electronic device*. [S.l.]: Google Patents, 2004. US Patent 6,785,881. Cited in page 40.
- BOJORGE, N. *Curva de Variação da F.E.M dos Termopares*. 2014. Disponível em: <http://www.termopares.com.br/teoria_sensores_temperatura_termopares_curvas_variacao_fem/curvas.gif>. Cited 2 times in page 13 and 34.
- BRYANT, J. et al. Protecting instrumentation amplifiers. *Sensors*, p. 6, 2000. Cited in page 60.
- BURGESS, K. *PWM to DC Voltage Conversion*. [S.l.], 2015. Cited in page 77.
- CARPARTS. *A Short Course on Brakes*. 2018. Disponível em: <<https://www.carparts.com.br/brakes.htm>>. Cited in page 29.
- CNW. *Volkswagen Gol 1.0 Ficha Técnica*. 2017. Disponível em: <<http://www.carrosnaweb.com.br/fichadetalhe.asp?codigo=1528>>. Cited in page 25.
- CNW. *Volkswagen Gol Plus 1.0 Ficha Técnica*. 2017. Disponível em: <<http://www.carrosnaweb.com.br/fichadetalhe.asp?codigo=431>>. Cited in page 25.

COUNTS, L.; KITCHEN, C. A designer's guide to instrumentation amplifiers. In: _____. 3. ed. [S.l.]: Analog Devices, 2006. cap. 2, p. 3. Adapted. Cited 3 times in page 38, 61, and 62.

DESCONHECIDO. *Typical instrumentation amplifier schematic*. 2016. Disponível em: <https://upload.wikimedia.org/wikipedia/commons/thumb/e/ed/Op-Amp_Instrumentation_Amplifier.svg/400px-Op-Amp_Instrumentation_Amplifier.svg.png>. Cited 2 times in page 13 and 38.

DEVICES, A. *AD8223: Single-Supply, Low Cost Instrumentation Amplifier*. 2008. Cited 3 times in page 13, 64, and 65.

DEVICES, A. Adxl335: Small, low power, 3-axis \pm 3 g accelerometer. *ADXL335 Data Sheet Rev B, Jan*, p. 52, 2010. Cited 2 times in page 70 and 71.

DEVICES, A. *AD8495 Functional Block Diagram*. 2011. Cited 2 times in page 13 and 60.

DEVICES, A. *16-LFCSP Footprint*. 2016. Cited 2 times in page 13 and 71.

DILLON, B. N.; GRIFFEN, N. C.; WEIHS, M. E. *Load cell*. [S.l.]: Google Patents, 1989. US Patent 4,815,547. Cited in page 35.

DORF, R. C.; SVOBODA, J. A. *Introduction to Electrical Circuits*. 8. ed. [S.l.]: LTC, 2014. Cited in page 76.

DUFF, M.; TOWEY, J. *Two Ways to Measure Temperature Using Thermocouples Feature Simplicity, Accuracy, and Flexibility*. [S.l.], 2010. Cited 3 times in page 60, 61, and 62.

ECIL. *Medição com Termopares*. 2016. Disponível em: <<http://www.ecil.com.br/imagens/seedback2.jpg>>. Cited 2 times in page 13 and 34.

EETIMES. *The Serial Port: Never Say Die*. 2013. Disponível em: <https://www.eetimes.com/author.asp?section_id=36&doc_id=1319282>. Cited in page 78.

ELECTRONICS TUTORIALS. *P-channel MOSFET Relay Switch Circuit*. 2018. Disponível em: <<https://www.electronics-tutorials.ws/articles/switch8.gif>>. Cited 2 times in page 14 and 81.

EQUINOX TECH. *ISP Target System Header Selection for AVR and AT89S FLASH Microcontrollers*. Cited 2 times in page 40 and 41.

EQUINOX TECH. *Typical Connections for ISP Programming*. 2018. Cited 2 times in page 13 and 41.

FAIRCHILD. *NDS332P: P-Channel Logic Level Enhancement Mode Field Effect Transistor*. [S.l.], 1997. Cited in page 81.

FERNANDES, J. C. *Segurança nas Vibrações sobre o Corpo Humano*. [S.l.], 2000. 11 p. Cited in page 36.

GARDINALLI, G. J. Comparação do desempenho de frenagem simulada x experimental de um veículo de passeio com freios hidráulicos e abs. *Trabalho de Conclusão de Curso apresentado à Escola Politécnica da Universidade de São Paulo para obtenção do título de Mestre em Engenharia Automotiva*, 2005. Cited in page 25.

GARFINKEL, S. L. Usb deserves more support. *Boston Globe Online*, 1995. Cited in page 43.

GMI. *SIL 2 Load Cell/Strain Gauge Bridge Isolating Converter DIN-Rail Model D1064S*. 2014. Disponível em: <<http://www.gminternational.com/get.php?w=dts&id=DTS0239&pid=>>>. Cited in page 89.

GONZALEZ, C. *What are Human Machine Interfaces and Why Are They Becoming More Important?* 2015. Disponível em: <<http://www.machinedesign.com/iot/what-are-human-machine-interfaces-and-why-are-they-becoming-more-important>>. Cited in page 43.

GOODYEAR. *Brake Calipers: The Top 3 Things You Need to Know*. 2018. Disponível em: <<https://www.goodyearautoservice.com/en-US/brakes/calipers>>. Cited 2 times in page 29 and 31.

GUIMARAES, J. *Brake Test Bench Hardware Project*. 2017. Cited 2 times in page 13 and 55.

GUIMARAES, J. *Brake Test Bench Microcontroller Code Map*. 2017. Cited 2 times in page 14 and 98.

GUIMARAES, J. *Project Problem Depuration*. 2017. Cited 2 times in page 13 and 51.

GUIMARAES, J. *10V voltage reference circuit*. 2018. Cited 2 times in page 14 and 89.

GUIMARAES, J. *12V Power Supply Circuit*. 2018. Cited 2 times in page 14 and 88.

GUIMARAES, J. *1V voltage reference circuit*. 2018. Cited 2 times in page 14 and 91.

GUIMARAES, J. *4V5 voltage reference circuit*. 2018. Cited 2 times in page 14 and 90.

GUIMARAES, J. *5V Power Supply Circuit*. 2018. Cited 2 times in page 14 and 87.

GUIMARAES, J. *Accelerometer Sensor Detection Circuit*. 2018. Cited 2 times in page 14 and 73.

GUIMARAES, J. *Accelerometer Signal Conditioning Circuit*. 2018. Cited 2 times in page 14 and 72.

GUIMARAES, J. *Conditioning Circuit for the Load Cell*. 2018. Cited 2 times in page 13 and 65.

GUIMARAES, J. *Digital Input Circuit*. 2018. Cited 2 times in page 14 and 82.

GUIMARAES, J. *Digital Output Circuit*. 2018. Cited 2 times in page 14 and 82.

GUIMARAES, J. *Load Cell Complete Circuit and Protection Circuit*. 2018. Cited 2 times in page 13 and 66.

- GUIMARAES, J. *MCU Complete Complementary Circuit*. 2018. Cited 2 times in page 13 and 57.
- GUIMARAES, J. *Overvoltage Detection Circuit*. 2018. Cited 2 times in page 13 and 62.
- GUIMARAES, J. *PCB 3D View*. 2018. Cited 2 times in page 14 and 93.
- GUIMARAES, J. *PCB Bottom 2D View*. 2018. Cited 2 times in page 14 and 93.
- GUIMARAES, J. *PCB Top 2D View*. 2018. Cited 2 times in page 14 and 92.
- GUIMARAES, J. *PCB Top 3D View*. 2018. Cited 2 times in page 14 and 94.
- GUIMARAES, J. *Power Supplies Voltage LEDs Circuit*. 2018. Cited 2 times in page 14 and 86.
- GUIMARAES, J. *RFI Standard Filter*. 2018. Cited 2 times in page 13 and 61.
- GUIMARAES, J. *Sensor Disconnection and Acquisition LED driver circuit*. 2018. Cited 2 times in page 14 and 86.
- GUIMARAES, J. *Speed Acquisition Channel Circuit*. 2018. Cited 2 times in page 13 and 69.
- GUIMARAES, J. *Speed Sensor Detection Channel Circuit*. 2018. Cited 2 times in page 13 and 70.
- GUIMARAES, J. *Thermocouple Complete Conditioning and Protection Circuit*. 2018. Cited 2 times in page 13 and 63.
- GUIMARAES, J. *UART feedback LEDs driver*. 2018. Cited 2 times in page 14 and 84.
- GUIMARAES, J. *USB/UART Converter Circuit*. 2018. Cited 2 times in page 14 and 80.
- GUIMARAES, J. *Voltage Input Protection Circuit*. 2018. Cited 2 times in page 14 and 88.
- GUMS, J. *Types of Temperature Sensors*. 2018. Disponível em: <<https://www.digikey.com/en/blog/types-of-temperature-sensors>>. Cited in page 33.
- HALDERMAN, J. D.; MITCHELL, C. D. *Automotive brake systems*. [S.l.]: Prentice Hall, 2016. Cited in page 25.
- HERNANDES, D. *Relembre todos os carros que já lideraram as vendas no Brasil em 60 anos de história*. 2017. Disponível em: <<https://www.flatout.com.br/relembre-todos-os-carros-que-ja-lideraram-as-vendas-no-brasil-em-60-anos-de-historia/>>. Cited in page 25.
- HOLMES, D. G.; LIPO, T. A. *Pulse width modulation for power converters: principles and practice*. [S.l.]: John Wiley & Sons, 2003. v. 18. Cited in page 42.
- HTCKOREA. *3-Terminal 0.1A POSITIVE VOLTAGE REGULATOR*. [S.l.], 2014. Cited in page 89.

- INC.(NORWOOD, M. A. D. *Operational Amplifiers Selection Guide 2011-2012: Detachable Charts Inside for Quick Product Selection & Design Equations*. [S.l.]: Analog Devices, 2011. Cited in page 38.
- INSTRUMENTS, N. *Definition of Strain*. 2016. Disponível em: <<http://www.ni.com/cms/images/devzone/tut/a/83a1fe69763.gif>>. Cited 2 times in page 13 and 35.
- INSTRUMENTS, N. *Wheatstone Bridge Circuit*. 2016. Disponível em: <<http://www.ni.com/cms/images/devzone/tut/a/a28b553b1069.gif>>. Cited 2 times in page 13 and 36.
- INSTRUMENTS, T. *INA 118*. 2000. Cited 2 times in page 13 and 39.
- INSTRUMENTS, T. *INA118 Precision, Low Power Instrumentation Amplifier*. [S.l.], 2000. 29 p. Cited in page 38.
- JAMES, C. Fundamentals of linear electronics: Integrated and discrete. *Fundamentals of linear electronics: integrated and discrete*. Cengage Learning, 2001. Cited in page 42.
- JR, K. N. Equivalence principle for massive bodies. ii. theory. *Physical Review*, APS, v. 169, n. 5, p. 1017, 1968. Cited in page 36.
- KAWAGUCHI, H. Comparaçao da análise de conforto de frenagem subjetiva x objetiva de um veículo de passeio. São Paulo, Brazil, p. 101, 2005. Cited in page 26.
- KEIM, R. *Low-Pass Filter a PWM Signal into an Analog Voltage*. 2016. Disponível em: <<https://www.allaboutcircuits.com/technical-articles/low-pass-filter-a-pwm-signal-into-an-analog-voltage/>>. Cited in page 75.
- KERNIGHAN, B. W.; RITCHIE, D. M. *The C programming language*. [S.l.: s.n.], 2006. Cited in page 97.
- KINNAIRD, C. *Differential signaling best practices*. 2012. Disponível em: <<https://www.ecnmag.com/article/2012/12/differential-signaling-best-practices>>. Cited in page 43.
- KINZIE, P. A.; RUBIN, L. G. Thermocouple temperature measurement. *Physics Today*, v. 26, p. 52, 1973. Cited in page 34.
- LAUREL, B.; MOUNTFORD, S. J. *The art of human-computer interface design*. [S.l.]: Addison-Wesley Longman Publishing Co., Inc., 1990. Cited in page 83.
- LEPKOWSKI, J.; LEPKOWSKI, W. Evaluating tvs protection circuits with spice. *Power Electronics Technology*, PRIMEDIA, v. 32, n. 1, p. 44, 2006. Cited in page 78.
- LIMPERT, R. *Brake design and safety*. [S.l.: s.n.], 1999. Cited in page 29.
- LITTELFUSE. *SMBJ Series Datasheet*. 2017. Cited in page 63.
- LITTLEFUSE. *Transient Voltage Suppression Diodes, SMBJ Series*. [S.l.], 2015. Cited 2 times in page 81 and 83.
- LITTLEFUSE. *Why does USB 2.0 need Circuit Protection?* [S.l.], 2010. Cited in page 79.

- LITTLELFUSE. *ESD Test Wave*. 2015. Cited 2 times in page 13 and 45.
- LITTLELFUSE. *Transient Voltage Suppressors (TVS Diode) Applications Overview*. [S.l.], 2015. Cited 2 times in page 44 and 45.
- MATHIVANAN, N. *PC-based instrumentation: concepts and practice*. [S.l.]: PHI Learning Pvt. Ltd., 2007. Cited in page 44.
- MAXIM. *MAX6107:Low-Cost, Micropower, Low-Dropout, High-Output-Current, SOT23 Voltage Regulator*. [S.l.], 2002. Cited in page 89.
- MAZIDI, M. A.; NAIMI, S.; NAIMI, S. *AVR Microcontroller and Embedded Systems: Using Assembly and C*. 1st. ed. Upper Saddle River, NJ, USA: Prentice Hall Press, 2010. ISBN 0138003319, 9780138003319. Cited in page 97.
- METIVIER, R. *Method for Converting a PWM Output to an Analog Output When Using Hall-Effect Sensor ICs*. [S.l.], 2013. Cited 2 times in page 75 and 76.
- METTINGVANRIJN, A.; PEPER, A.; GRIMBERGEN, C. Amplifiers for bioelectric events: a design with a minimal number of parts. *Medical and Biological Engineering and Computing*, Springer, v. 32, n. 3, p. 305–310, 1994. Cited in page 37.
- MICROCHIP. *MCP6001: 1 MHz, Low-Power Op Amp*. [S.l.], 2009. Cited in page 72.
- MICROCHIP. *MCP2221 Breakout Module*. 2010. Cited 2 times in page 14 and 79.
- MICROCHIP. *USB 2.0 to I2C/UART Protocol Converter with GPIO*. [S.l.], 2016. Cited in page 78.
- MICROCHIP. *Microchp ATmega328PB datasheet*. [S.l.]: ed, 2018. Cited 6 times in page 13, 40, 55, 56, 59, and 81.
- MICROCHIP TECHNOLOGY INC. *In-Circuit Serial Programming ICSP Guide*. [S.l.], 2003. Cited in page 40.
- MUKARO, R.; CARELSE, X. F. A microcontroller-based data acquisition system for solar radiation and environmental monitoring. *IEEE transactions on instrumentation and measurement*, IEEE, v. 48, n. 6, p. 1232–1238, 1999. Cited in page 97.
- NATIONAL INSTRUMENTS. *O Que é Aquisição de Dados?* 2018. Disponível em: <<https://www.ni.com/data-acquisition/what-is/pt/>>. Cited in page 39.
- NEWTON, R. *Brake Temperatures*. 2016. Disponível em: <<http://cartechstuff.blogspot.com.br/2016/04/brake-temperatures.html>>. Cited in page 32.
- NEXPERIA. *60 V, single N-channel Trench MOSFET*. [S.l.], 2015. Cited in page 82.
- NICE, K. *How Disc Brakes Work*. 2017. Disponível em: <<https://s.hswstatic.com/gif/disc-brake3.jpg>>. Cited 2 times in page 13 and 29.
- O'MAHONY, J. J.; GELFAND, M.; MERRICK, E. B. *Pressure sensor disconnect detection for a blood treatment device*. [S.l.]: Google Patents, 2011. US Patent 7,886,611. Cited in page 62.

- ON SEMICONDUCTOR. *USB Filter with ESD Protection*. [S.l.], 2012. Cited in page 79.
- ON SEMICONDUCTOR. *NSR0530H: Schottky Barrier Diode*. [S.l.], 2016. Cited in page 88.
- ON SEMICONDUCTOR. *Small Signal MOSFET, -20 V, -430 mA, Dual P-Channel with ESD Protection*. [S.l.], 2016. Cited in page 84.
- ONSEMI. *STF202-22T1G Circuit*. 2012. Cited 2 times in page 14 and 80.
- OSHANA, R. Introduction to jtag. *Embedded systems programming*, <<http://www.embedded.com/showArticle.jhtml>>, 2002. Cited in page 40.
- PALLÁ, R.; WEBSTER, J. G. et al. *Sensors and signal conditioning*. [S.l.]: John Wiley & Sons, 2012. Cited in page 35.
- PATRICK, W. L. The history of the accelerometer: 1920s-1996 - prologue and epilogue. Ft. Worth - Texas, Estados Unidos da América, p. 9, 2007. Cited in page 37.
- PETROLHEAD GARAGE. *CKP sensor signal example*. 2014. Disponível em: <<https://petrolheadgarage.com/wp-content/uploads/2014/10/EDISDiagram.jpg>>. Cited 2 times in page 13 and 33.
- PILTCHE, A. *A Guide to Computer Ports and Adapters*. 2017. Disponível em: <<https://www.laptopmag.com/articles/port-and-adapter-guide>>. Cited in page 43.
- PINKLE, C. *The Why and How of Differential Signaling*. 2016. Disponível em: <<https://www.allaboutcircuits.com/technical-articles/the-why-and-how-of-differential-signaling/>>. Cited in page 43.
- POLLOCK, D. D. *Thermocouples: theory and properties*. [S.l.]: CRC press, 1991. Cited in page 33.
- RECTRON SEMICONDUCTOR. *FM205: Glass Passivated Silicon Rectifier*. [S.l.], 2010. Cited in page 87.
- RECTRON SEMICONDUCTOR. *FM5819: Surface Mount Schottky Barrier Rectifier*. [S.l.], 2010. Cited in page 87.
- REMAN, M. C. *GM Replacement 10456042 Crankshaft Position Sensor*. 2016. Disponível em: <<http://ep.yimg.com/ay/motorcityreman/general-motors-oe-10456042-crankshaft-position-sensor-1.gif>>. Cited 2 times in page 13 and 32.
- RENESAS. *Application Note 1977: Transient Voltage Suppressors: Operation and Features*. [S.l.], 2016. Cited in page 46.
- RENESAS. *Camping action of a bi-directional TVS*. 2016. Cited 2 times in page 13 and 46.
- RENESAS. *Camping action of a uni-directional TVS*. 2016. Cited 2 times in page 13 and 46.

RENESAS. *V X I characteristic of a bi-directional TVS*. 2016. Cited 2 times in page 13 and 47.

RENESAS. *V X I characteristic of a uni-directional TVS*. 2016. Cited 2 times in page 13 and 47.

RESEARCH, M. T. *USB to Serial adapters Wiki*. 2008. Disponível em: <<http://www.usb-serial-adapter.org/>>. Cited in page 78.

ROMERO, N. A. Johnson noise. *power*, v. 2, p. 4. Cited in page 60.

ROUSE, M. *microcontroller*. 2012. Disponível em: <<http://internetofthingsagenda.techtarget.com/definition/microcontroller>>. Cited in page 40.

RZTRONICS. *Duty Cycle*. 2016. Disponível em: <<https://i1.wp.com/rztronics.com/wp-content/uploads/2016/10/pwm.gif?zoom=1.899999976158142&resize=390%2C427>>. Cited 2 times in page 13 and 42.

SAE. *Dynamometer Global Brake Effectiveness*. Rio de Janeiro, Brasil, 2003. 18 p. Cited 3 times in page 30, 31, and 32.

SAE. *SAE*. 2016. Disponível em: <<http://www.sae.org/>>. Cited 3 times in page 25, 27, and 51.

SCHROEDER, T. *Crankshaft position sensor*. [S.l.]: Google Patents, 2002. US Patent 6,346,808. Cited in page 32.

SCHWEBER, B. *Understanding the Advantages and Disadvantages of Linear Regulators*. 2017. Disponível em: <<https://www.digikey.com/en/articles/techzone/2017/sep/understanding-the-advantages-and-disadvantages-of-linear-regulators>>. Cited in page 86.

SONGLE. *Songle Relay*. 2018. Cited in page 80.

SOUZA, S. Xavier-de et al. The benefits of low operating voltage devices to the energy efficiency of parallel systems. *arXiv preprint arXiv:1709.08689*, 2017. Cited in page 45.

SPECIFICATION-REV, U. S. B. 1.0, jan. 15, 1996. *Sec*, v. 9, n. 2, p. 184–185. Cited in page 43.

STANDARD, F. 1037c. telecommunications: Glossary of telecommunication terms. *Institute for Telecommunications Sciences*, v. 7, 1996. Cited in page 41.

TEXAS INSTRUMENTS. *Analysis of the Sallen-Key Architecture*. Dallas, Texas 75265, 1999. Cited 3 times in page 14, 76, and 77.

TEXAS INSTRUMENTS. *LM2907 and LM2917 Frequency to Voltage Converter*. [S.l.], 2000. Cited 3 times in page 66, 67, and 90.

TEXAS INSTRUMENTS. *LM2574x SIMPLE SWITCHER 0.5-A Step-Down Voltage Regulator*. [S.l.], 2016. Cited in page 87.

TEXAS INSTRUMENTS. *TPL7407LA 30-V 7-Channel Low Side Driver*. [S.l.], 2017. Cited in page 85.

- TEXAS INSTRUMETS. *LM2907 Tachometer with Adjustable Zero Speed Voltage Output*. 2018. Cited 2 times in page 13 and 67.
- TEXAS INSTRUMENTS. *TL2575, TL2575HV 1-A Simple Step-Down Switching Voltage Regulators*. [S.l.], 2014. Cited in page 87.
- THOMSEN, A. et al. *Application of a conditionally stable instrumentation amplifier to industrial measurement*. [S.l.]: Google Patents, 2003. US Patent 6,525,589. Cited in page 37.
- TODAS as Medidas de Pneu. 2018. Disponível em: <<https://www.pneusfacil.com.br/comprepneus>>. Cited in page 68.
- UK, M. O. *Compression Accelerometer*. 2016. Disponível em: <[http://www.maintenanceonline.co.uk/maintenanceonline/content_images/figure-2\(1\).jpg](http://www.maintenanceonline.co.uk/maintenanceonline/content_images/figure-2(1).jpg)>. Cited 2 times in page 13 and 37.
- UNKNOWN. *USB2.0 cable*. 2017. Disponível em: <http://pinouts.ru/Slots/USB_pinout.shtml>. Cited 2 times in page 13 and 43.
- WAIT, J. V.; HUELSMAN, L. P.; KORN, G. A. *Introduction to operational amplifier theory and applications*. [S.l.]: McGraw-Hill Companies, 1975. Cited in page 37.
- WALTERS, K. *How To Select Transient Voltage Suppressors*. [S.l.], 2016. Cited in page 46.
- WEG. *CFW-08 Frequency Inverter*. [S.l.], 2009. Cited in page 74.
- WEG. *WEG CFW08 Frequency Inverter*. 2017. Disponível em: <http://ecatalog.weg.net/files/produtos/CFW-08_G.jpg>. Cited 2 times in page 14 and 74.
- WINDOW, A. L.; HOLISTER, G. S. et al. *Strain gauge technology*. [S.l.]: Applied science publishers, 1982. Cited in page 35.

Appendix

APPENDIX A – First Appendix

A.1 Microcontroller Code

```

//Libraries
#include <TimerOne.h>
#include <MsTimer2.h>
#include <math.h>

//HW DEFINITIONS
//Digital ports
///inputs
#define ADC_CON_0 2
#define ADC_CON_1 3
#define ADC_CON_2 4
#define ADC_CON_3 6
#define ADC_CON_4 7
#define ADC_CON_5 8
///outputs
#define DIG_OUT_PORT_0 9
#define DIG_OUT_PORT_1 10
#define RELAY_OUT_0 11
#define RELAY_OUT_1 12
#define ACQ_LED 13

//Analog Ports
#define PWM_OUT 5

//COMMUNICATIONS DEFINITIONS
#define START_ACQ_BYTE 21
#define STOP_ACQ_BYTE 22
#define MASTER_RESET_BYTE 23
#define NULL_DIGITAL_BYTE 96
#define MAX_DIGITAL_BYTE 111
#define NULL_SPEED_BYTE 155

```

```
#define MAX_SPEED_BYTE 255
```

//GENERAL DEFINITIONS

```
#define SET 1  
#define RESET 0  
#define ACQ_LED_BLINK_MS 250  
#define SAMPLE_RATE 10  
#define NUMBER_OF_SAMPLES 100
```

//GLOBAL VARS

```
static boolean acquisitionEnabled=false;
```

```
int samples=RESET;
```

```
short DIGITAL_OUT_PORTS[] = {DIG_OUT_PORT_0, DIG_OUT_PORT_1, RELAY_0, RELAY_1};  
short DIGITAL_IN_PORTS[] = {ADC_CON_0, ADC_CON_1, ADC_CON_2, ADC_CON_3};
```

```
boolean digitalInstruction={RESET,RESET,RESET,RESET};
```

```
static float sensorData[] = {RESET, RESET, RESET, RESET, RESET, RESET};
```

//Function to write to digital ports

```
void digitalOutputControl(){
```

```
for (int i=RESET; i<NUMBER_OF_DIGITAL_PORTS; i++){
```

```
digitalWrite(DIGITAL_OUT_PORTS[i], digitalInst
```

}

}

```
//Function to set all digital outputs to low
```

```
void resetDigOutputs();
```

for (int i=RESET; i<NUMBER_OF_DIGITAL;

$\{ \dots \}$

// Function to configure

```
configureTimer0();
```

```

}

//Function to configure Timer 1 - ACQUISITION
void configureTimer1(){
    Timer1.attachInterrupt(timer1_OISR);
    Timer1.initialize(SAMPLE_RATE);
    Timer1.stop();
}

//Function to configure timer 2 - LED
void configureTimer2() {
    MsTimer2::set(ACQ_LED_BLINK_MS, timer2_OISR);
}

//Timer 1 overflow interruption routine
void timer1_OISR(){
    if (samples<NUMBER_OF_SAMPLES){
        if(enableAcquisition==true){
            //Lendo dado analogico
            sensorData[0]=sensorData[0]+analogRead(A0);
            sensorData[1]=sensorData[1]+analogRead(A1);
            sensorData[2]=sensorData[2]+analogRead(A2);
            sensorData[3]=sensorData[3]+analogRead(A3);
            sensorData[4]=sensorData[4]+analogRead(A4);
            sensorData[5]=sensorData[5]+analogRead(A5);
            samples++;
        }
    }
}

//Timer 1 overflow interruption routine
void timer2_OISR(){
    if(enableAcquisition){
        digitalWrite(ACQ_LED_PIN, digitalRead(ACQ_LED_PIN));
    } else{
        digitalWrite(ACQ_LED_PIN, LOW);
    }
}

```

```
//Function to write adc results in serial port
void printResults(int * result){
    Serial.print(result[0]);
    Serial.print(",");
    Serial.print(result[1]);
    Serial.print(",");
    Serial.print(result[2]);
    Serial.print(",");
    Serial.print(result[3]);
    Serial.print(",");
    Serial.print(result[4]);
    Serial.print(",");
    Serial.print(result[5]);
    Serial.print(".");
}

void IOsetup(){
    pinMode(ACQ_LED_PIN,OUTPUT);

    for (int i=0;i<6;i++){
        if (i<4){
            pinMode(DIGITAL_OUT_PORTS[i],OUTPUT)
        }
        pinMode(DIGITAL_IN_PORTS[i],INPUT);
    }

}

void setup(){
    Serial.begin(9600);
    IOsetup();
    digitalWrite(ACQ_LED_PIN,LOW);

    configureTimer0();
    configureTimer1();
    configureTimer2();
    MsTimer2::start();
}
```

```

void loop (){
    if ( samples>=NUMBER_OF_SAMPLES){
        Timer1. stop ();
        static int resultAcq [ 6 ];

        for (int k=0;k<6;k++){
            resultAcq [ counter ] = (int) roundf (
                sensorData [ counter ] );
            if ( sensorData [ counter ] == RESET )
                break;
        }
        samples=RESET;
        Timer1. restart ();

        printResults ( resultAcq );
    }

    if ( Serial . available ()){

        char byteRead = Serial . read ();

        switch ( byteRead ){

            case START_ACQ_BYTE:{
                if ( ! acquisitionEnabled ){
                    acquisitionEnabled=true ;
                    samples=RESET;
                    Timer1. restart ();
                }
                break ;
            }

            case STOP_ACQ_BYTE:{
                acquisitionStop ();
            }
            break ;

            case MASTER_RESET_BYTE:{
                acquisitionStop ();
                resetDigOutputs ();
            }
        }
    }
}

```

```
break;

default:{  
    if (byteRead>=NULL_SPEED_BYT  
        unsigned char speed_byte = by  
        speed_byte=NULL_SPEED_BYT;  
        int speed=RESET;  
        speed = 1023*speed_byte/(MAX_  
        analogWrite(PWM_OUT,speed );  
  
    }else if ((byteRead>=NULL_DIGITAL_BYT  
        for (int i = 3; i>-1; i--) {  
            digit  
        }  
        digitalOutputControl(  
    }  
    break;  
}  
}
```